TAXONOMY, SYSTEMATICS, AND VENOM COMPONENTS OF NEOBISIID PSEUDOSCORPIONS (PSEUDOSCORPIONES: NEOBISIIDAE)

by

Garrett B. Hughes

A Dissertation Submitted to the Faculty of the

GRADUATE INTERDISCIPLINARY PROGRAM IN ENTOMOLOGY AND INSECT SCIENCE

In Partial Fulfillment of the Requirements

For the Degree of

DOCTOR OF PHILOSOPHY

WITH A MAJOR IN ENTOMOLOGY AND INSECT SCIENCE

In the Graduate College

THE UNIVERSITY OF ARIZONA

2017

THE UNIVERSITY OF ARIZONA
GRADUATE COLLEGE

As members of the Dissertation Committee, we certify that we have read the dissertation prepared by Garrett B. Hughes, titled "Taxonomy, Systematics, and Venom Components of Neobisiid Pseudoscorpions (Pseudoscorpiones: Neobisiidae)" and recommend that it be accepted as fulfilling the dissertation requirement for the Degree of Doctor of Philosophy.

_____Date: 13 July 2017
Wendy Moore

_____Date: 13 July 2017
Michael Sanderson

_____Date: 13 July 2017
Michael Riehle

_____Date: 13 July 2017
Michelle McMahon

Final approval and acceptance of this dissertation is contingent upon the candidate's submission
of the final copies of the dissertation to the Graduate College. I hereby certify that I have read this dissertation prepared under my direction and recommend that it be accepted as fulfilling the dissertation requirement.

_____ Date: 13 July 2017
Dissertation Director:
Wendy Moore

STATEMENT BY AUTHOR

This dissertation has been submitted in partial fulfillment of the requirements for an advanced degree at the University of Arizona and is deposited in the University Library to be made available to borrowers under rules of the Library.

Brief quotations from this dissertation are allowable without special permission, provided that an accurate acknowledgement of the source is made. Requests for permission for extended quotation from or reproduction of this manuscript in whole or in part may be granted by the head of the major department or the Dean of the Graduate College when in his or her judgment the proposed use of the material is in the interests of scholarship. In all other instances, however, permission must be obtained from the author.

SIGNED: Garrett B. Hughes

TABLE OF CONTENTS

ABSTRACT.....5
CHAPTER 1.....6
CHAPTER 2.....9
REFERENCES.....11
APPENDIX A.....13
APPENDIX B.....34
APPENDIX C.....78

ABSTRACT

Pseudoscorpions are a diverse lineage of arachnids with a rich history of taxonomic study. However, they remain one of the lesser-known groups of arachnids and many questions about these enigmatic arthropods remain. The present work revises the taxonomy and systematics of the family Neobisiidae in the Southwest, documenting the existence of several new species and a hitherto unknown clade from the Sky Island region of southeastern Arizona. It also describes the venom of a pseudoscorpion for the first time, through comparative transcriptomic studies.

Seven new species are described and assigned to the genus *Globocreagris*, extending the known range of this genus from California into Arizona, Oregon, and Washington. The monophyly of the subfamily Neobisiinae was tested using two genes (COI and 28S). Molecular phylogenetic analysis of both genes and the pattern of trichobothrial placement on the chelae supports removing *Parobisium* from the subfamily Neobisiinae, and placing it within the subfamily Microcreagrinae, a reassignment here made.

Although it has long been known that most pseudoscorpions possess venom glands in their pincers which they use to subdue their arthropod prey, the components of the venom have never been identified. Using comparative transcriptomics from the pedipalps of *Globocreagris* the first putative venom proteins in pseudoscorpions were identified. Putative venom proteins include astacin-like metalloproteases, chitinases, cysteine-rich secretory proteins, Kunitz-type serine protease inhibitors, phospholipase A2, and scorpion La1-like peptides.

CHAPTER 1.
INTRODUCTION

1.1 An overview of major topics

The present work is focused on expanding the current knowledge about a particular group of organisms. It includes vastly different research questions that are unified by the taxon of study: the pseudoscorpion family Neobisiidae. The following sections provide background into this taxon and the major fields of study included in this work: taxonomy, systematics, and venom research.

1.1.1 Pseudoscorpiones: Neobisiidae

Pseudoscorpions are bizarre and fascinating creatures. Pseudoscorpions have pincer-like pedipalps – or chelae – which bear resemblance to the pedipalps of their cousins, the scorpions. Unlike scorpions, pseudoscorpions do not possess a post-anal telson modified into a venomous sting. Instead, pseudoscorpions of the suborder Iocheirata possess venom in their chelae (Harvey 1992). Like the vast majority of arachnids, pseudoscorpions are predators and they use their chelate palps and associated venom to seize and incapacitate prey (De Andrade & Gnaspini 2002). Pseudoscorpions are one of three orders of arachnids that produce venom for prey capture. While scorpion and spider venom has been well-studied, very little is known about pseudoscorpion venom (von Reumont et al. 2014). To date, only one study has investigated pseudoscorpion venom (Dos Santos & Coutinho-Netto 2006), but pseudoscorpion venom protein sequences are currently unknown.

Pseudoscorpions live cryptic lives and are most often found in the interstices of soil, leaf litter, rocks, and wood. Pseudoscorpions have 3 juvenile instars (termed protonymph, deutonymph and tritonymph) followed by the adult life stage. The life stage of a typical pseudoscorpion is easily discerned by examining the movable finger of the pedipalp chelae which will have 1, 2, 3, or 4 trichobothria depending on if the specimen is a protonymph, deutonymph, tritonymph or adult (Chamberlin 1931). When pseudoscorpions molt, they use silk from their chelicerate mouthparts to construct small, protective chambers within their confined habitat (Kew 1914). Adult females also use this silk to construct brood chambers for the hatching of their eggs (Weygoldt 1969). Pseudoscorpions are predatory and feed on other small arthropods, though some cooperatively forage to take down larger prey (Zeh & Zeh 1990).

Members of the family Neobisiidae are found in caves, leaf litter, and in the soil throughout the Northern Hemisphere. They can be distinguished from other pseudoscorpion families by the following combination of characters: 1) the loss of venom gland in the movable finger of the pedipalp chelae (leaving a single venom gland in the fixed finger), 2) the presence of dentate subterminal tarsal setae, 3) the presence of three or more setae apex of the pedipalpal coxae (formerly called the

manducatory process). There are currently 580 species described from 32 genera and 2 subfamilies (Harvey 2013).

1.1.2 Taxonomy & Systematics

Taxonomy is the field of naming new species, genera, families, etc., and classifying those organisms into a meaningful hierarchical system of relationships. Rules for taxonomy are governed by the International Code of Zoological Nomenclature (http://www.iczn.org/iczn/index.jsp). Our current system for naming uses two-names for each species. This binomial nomenclature originated with Linnaeus and his *Systema Naturae* (1735). Important considerations when naming species include designating a name-bearing holotype specimen which will be permanently deposited in a museum. When species names are assigned, they are accompanied with a written description of the species. With nearly 4,000 described species, pseudoscorpions have a rich taxonomic history. Still, new species are frequently discovered, described and named.

Historically, new species were described when clear morphological differences were discovered. In the last decade, however, new species have sometimes been described only on the basis of molecular data, usually DNA sequences (Yang & Rannala 2010). This is especially true of cryptic species (Bickford et al. 2007). To date, no pseudoscorpions have been described by molecular sequences alone; all have had morphological features that distinguished new species from previously-described species.

When classifying organisms, those that are more closely related through evolutionary descent are grouped first. Thus, the least-inclusive taxa (e.g. genera) are composed of organisms that share a much more recent common ancestor than more-inclusive taxa (e.g. order). Phylogenetics – the field of inferring evolutionary relationships – is an integral tool for systematic classification of organisms. Relationships can be inferred using morphological or molecular data. Molecular phylogenies are much more common, perhaps because they are faster and there is often less confusion about homology of characters, especially for protein-coding genes. Phylogenies are relatively rare for pseudoscorpions, with only a handful of papers that have employed their use for determining evolutionary relationships within the order (Harvey 1992, Wilcox et al. 1997, Harvey & Volschenk 2007, Zeh et al. 2003, Moulds et al. 2007, Murienne et al. 2008, Pfeiler et al. 2008, Van Heerden et al. 2013, Harrison et al. 2014, Cosgrove et al. 2016.).

1.1.3 Venom research

Venoms are mixtures of various chemicals produced by an animal that alter normal biological functions when injected into a host. Venoms are found in a wide array of animals, including arthropods, mollusks, reptiles, and mammals. Although these organisms are very divergent, many have convergently recruited the same types of proteins to their venoms (Fry et al. 2009). Venoms are important to study because

of the potential harm they cause to humans and because the compounds found in the venom can be used in scientific research and medical therapy (Lewis & Garcia 2003).

Venom proteins can be studied by extraction, purification, and high-performance liquid chromatography for direct protein-sequencing (Escoubas 2006), or using next-generation RNA-sequencing to examine the transcripts found in venom glands (Kozlov et al. 2008). After identification, proteins are often characterized, which includes deducing secondary, tertiary, and quaternary structure of the proteins, as well as assessing protein function. For studying lesser-known organisms with no data on venom composition, transcriptomic RNA-sequencing has proven to be a cost-effective way to explore the putative proteins in the venom (von Reumont et al. 2014). For pseudoscorpions, nothing is known of protein sequences.

1.2 Dissertation Format

The format of this dissertation follows the guidelines found in article IV of the University of Arizona Dissertation Formatting Guide, which outlines details for manuscript-based dissertations. The following chapter contains brief descriptions of the manuscripts prepared during the current research. Each manuscript can be found in the appendix of this dissertation. These manuscripts will be submitted to peer-reviewed journals for publication.

CHAPTER 2.
THE CURRENT STUDY

This chapter provides information on the manuscripts prepared during the current study on pseudoscorpions. The titles, authors, and a brief description of the manuscript are provided. The scope of each manuscript descends into less-inclusive taxonomic levels, beginning at the family level, then genus, then information from a single species.

2.1 Title: Maintaining Monophyly of the Subfamily Neobisiinae (Pseudoscorpiones: Neobisiidae)

Authors: Garrett B. Hughes, Wendy Moore

The pseudoscorpion family Neobisiidae contains two subfamilies: Neobisiinae and Microcreagrinae. Historically, these two taxa were distinguished by the shape of the spinneret – elongate in the Microcreagrinae and reduced in the Neobisiinae. Subsequent morphological investigations found this character to be labile and other characters were discovered. We obtained specimens of the neobisiine, *Parobisium charlotteae,* which looked to us to be microcreagrines in every respect except for the reduced galea, including the placement of trichobothria on the pedipalp chelae, the positions of which indicated that this genus belongs in the subfamily Microcreagrinae. To test whether this species belongs in Neobisiinae, we collected DNA sequences for two genes (cytochrome oxidase subunit-1 and 28S ribosomal RNA) from pseudoscorpions throughout the family Neobisiidae and conducted a phylogenetic analysis using maximum likelihood. We also conducted a parametric bootstrap test of significance and found that *Parobisium charlotteae*, and the entire genus *Parobisium*, does not belong to the subfamily Neobisiinae. We therefore revised the taxonomy by moving *Parobisium* out of Neobisiinae and into Microcreagrinae.

2.2 Title: Discovery, phylogeny, and biogeography of a new lineage of *Globocreagris* (Pseudoscorpiones: Neobisiidae) from the Arizona Sky Islands

Authors: Garrett B. Hughes, Wendy Moore

We discovered a new lineage of pseudoscorpions belonging to the genus *Globocreagris* in the Arizona Sky Islands. This lineage of neobisiids lives at high elevations in the pine and mixed-conifer biomes of the mountains. Until this study, members of the genus *Globocreagris* were only known from California. We created a molecular phylogeny of Neobisiidae using two genes (cytochrome oxidase subunit-1 and 28S ribosomal RNA) to demonstrate that these Sky Island pseudoscorpions were more closely-related to *Globocreagris nigrescens* from California than they were to other neobisiids found in mountains in Arizona. Examining slide-mounted material from museum collections, we expanded the

known range of *Globocreagris* to include Oregon, Washington, and Arizona, in addition to its previously known area of California.

One hypothesis for biogeography of organisms in the Arizona Sky Island region is that they speciated during the Pleistocene interglacial cycles. We conducted a molecular dating analysis to explore whether this scenario was likely for this new lineage of pseudoscorpions. Using a conservatively fast rate of molecular evolution, we found that the members of this species had diverged before the Pleistocene glacial cycles.

Finally, we described 7 new species of *Globocreagris*: *G. pinalensis*, *G. huachucaensis*, *G. santaritaensis*, *G. santacatalinaensis*, *G. rinconensis*, *G. pinalenoensis*, and *G. chiricahuaensis*.

2.3 Title: The First Putative Venom Sequences from a Pseudoscorpion (Pseudoscorpiones: Neobisiidae)

Authors: Garrett B. Hughes, Wendy Moore

Pseudoscorpions have long been known to possess venom in their pedipalp pincers (chelae), but no study has identified the components of their venom. Using next-generation RNA-sequencing technology, we explored the venom composition of *Globocreagris pinalenoensis*. We collected 50 specimens and removed their pedipalps. We dissected out the venom glands and also collected the patella and femur of each pedipalp into a separate sample. The RNA in these two samples were sequenced, assembled, translated into open reading frames, and annotated with an automated pipeline that reported most similar known sequences, gene ontology predictions, and protein family information. We conservatively filtered the assembled sequences by only considering putative proteins that were at least 5-times more highly expressed in the venom samples compared to the patella-femur samples. We manually examined these for candidate venom proteins. We discovered the following putative venom proteins in the pseudoscorpion venom gland: chitinases, cysteine-rich secretory proteins, Kunitz-type serine protease inhibitors, phospholipase A2, and scorpion La1-like peptides.

REFERENCES.

Bickford, D., D.J. Lohman, N.S. Sodhi, P.K.L. Ng, R. Meier, K. Winker, K.K. Ingram, I. Das. 2007. Cryptic species as a window on diversity and conservation. *Trends in Ecology & Evolution*, 22(3): 148–155.

Chamberlin, J.C. 1931. The arachnid order Chelonethida. Stanford University Press, Stanford, California.

Cosgrove, J.G., I. Agnarsson, M.S. Harvey, & G.J. Binford. 2016. Pseudoscorpion diversity and distribution in the West Indies: sequence data confirm single island endemism for some clades, but not others. *Journal of Arachnology*, 44(3): 257–271.

De Andrade, R. & Gnaspini, P. (2002). Feeding *in Maxchernes iporangae* (Pseudoscorpiones, Chernetidae) in captivity. *Journal of Arachnology* 30: 613-617.

Dos Santos, W.F. & Coutinho-Netto, J. (2006). Effects of Paratemnus elongates pseudoscorpion venom in the uptake and binding of the L-glutamate and GABA from rat cerebral cortex. *Journal of Biochemical and Molecular Toxicology*, 20: 27-34.

Fry, B.G., K. Roelants, D.E. Champagne, H. Scheib, J.D.A. Tyndall, G.F. King, T.J. Nevalainen, J.A. Norman, R.J. Lewis, R.S. Norton, C. Renjifo, & R.C. Rodríguez de la Vega. 2009. The toxicogenomic multiverse: convergent recruitment of proteins into animal venoms. *Annual Review of Genomics and Human Genetics*, 10: 483–511.

Escoubas, P. 2006. Mass spectrometry in toxinology: a 21st-century technology for the study of biopolymers from venom. *Toxicon*, 47: 609–613.

Harrison, S.E., M.T. Guzik, M.S. Harvey, & A.D. Austin. 2014. Molecular phylogenetic analysis of Western Australian troglobitic chthoniid pseudoscorpions (Pseudoscorpiones: Chthoniidae) points to multiple independent subterranean clades. *Invertebrate Systematics*, 28(4): 386–400.

Harvey, M.S. (1992). The phylogeny and classification of the Pseudoscorpionida (Chelicerata: Arachnida). *Invertebrate Taxonomy* 6: 1373–1435.

Harvey, M.S. & E.S. Volschenk. 2007. Systematics of the Gondwanan pseudoscorpion family Hyidae (Pseudoscorpiones: Neobisiioidea): new data and a revised phylogenetic hypothesis. *Invertebrate Systematics*, 21(4): 365–406.

Harvey, M.S. (2013). Pseudoscorpions of the World, version 3.0. Western Australian Museum, Perth. http://www.museum.wa.gov.au/catalogues/pseudoscorpions

Kew, H.W. 1914. On the nests of Pseudoscorpiones: with historical notes on the spinning-organs and observations on the building and spinning of the nests. *Proceedings of the Zoological Society of London*, 1914: 93–11.

Kozlov, S., A. Malyavka, B. McCutchen, A. Lu, E. Schepers, R. Herrmann, & E. Grishin. 2005. A novel strategy for the identification of toxinlike structures in spider venom. *PROTEINS: Structure, Function, and Bioinformatics*, 59: 131–140.

Lewis, R.J. & M.L. Garcia. 2003. Therapeutic potential of venoms. *Nature Reviews Drug Discovery*, 2: 790–802.

Moulds, T.A., Murphy, N., Adams, M., Reardon, T., Harvey, M.S., Jennings, J. & Austin, A.D. (2007). Phylogeography of cave pseudoscorpions in southern Australia. *Journal of Biogeography* 34: 951–962.

Murienne, J., Harvey, M.S. & Giribet, G. (2008). First molecular phylogeny of the major clades of Pseudoscopriones (Arthropoda: Chelicerata). *Molecular Phylogenetics and Evolution*, 49 (3): 170–184.

Pfeiler, E., Bitler, B.G., Castrezana, S., Matzkin, L.M. & Markow, T.A. (2008). Genetic diversification and demographic history of the cactophilic pseudoscorpion *Dinocheirus arizonensis* from the Sonoran Desert. *Molecular Phylogenetics and Evolution*, 52 (1): 133–141.

von Reumont, B.M., L.I. Campbell, S. Richter, L. Hering, D. Sykes, J. Hetmank, R.A. Jenner, & C. Bleidorn. 2014. A polychaete's powerful punch: venom gland transcriptomics of *Glycera* reveals a complex cocktail of toxin homologs. *Genome Biology and Evolution*, 6(9): 2406–2423.

Weygoldt, P. (1969). *The biology of pseudoscorpions*. Harvard University Press: Cambridge, Massachusetts.

Wilcox, T.P., L. Hugg, J.A. Zeh, & D.W. Zeh. 1997. Mitochondrial DNA sequencing reveals extreme genetic differentiation in a cryptic species complex of Neotropical pseudoscorpions. *Molecular Phylogenetics and Evolution*, 7(2): 208–216.

Yang, Z. & B. Rannala. 2010. Bayesian species delimitation using multilocus sequence data. *PNAS*, 107(20): 9264–9269.

Zeh, J.A., Zeh, D.W. & Bonilla, M.M. (2003). Phylogeography of the harlequin beetle-riding pseudoscorpion and the rise of the Isthmus of Panama. *Molecular Ecology* 12: 2759–2769.

APPENDIX A.

MAINTAINING MONOPHYLY OF THE SUBFAMILY NEOBISIINAE (PSEUDOSCORPIONES: NEOBISIIDAE)

Garrett B. Hughes and Wendy Moore

Department of Entomology, University of Arizona, Tucson, AZ, 85721, USA; Email: gbhughes@email.arizona.edu

Formatted for the Journal of Arachnology.

Abstract.— Pseudoscorpions use their galea (spinnerets) to spin silken chambers. The form of the galea has been used to differentiate subfamilies within the family Neobisiidae (elongate and membranous in Microcreagrinae; reduced and sclerotic in Neobisiinae). However, the presence of reduced galea in some members of Microcreagrinae sets a precedent for variation within these subfamilies. Another character used to diagnose the subfamilies is the sub-basal position of trichobothria *ist* in Microcreagrinae compared to its distal position in Neobisiinae, but this character is also found in the neobisiine genus *Parobisium*. The inconsistency of these characters calls into question the monophyly of the subfamilies and/or the characters used to diagnose them. We inferred the phylogeny of Neobisiidae with the goal of testing whether the subfamilies are monophyletic and to investigate how many times each of the subfamilial characters have evolved. We found that both families were paraphyletic. In the case of Neobisiinae, moving the genus *Parobisium* out of the subfamily results in a monophyletic Neobisiinae and character consistency with the position of trichobothria *ist*. We therefore remove *Parobisium* from Neobisiinae. With this most recent molecular phylogeny, we find that there have been at least three independent reductions of the galea in Neobisiidae.

Keywords.— Galea, molecular systematics

Pseudoscorpions are found throughout most of the world. They often dwell in the interstices of cryptic habitats like soil, leaf litter, tree bark, and caves. Pseudoscorpions occasionally spin silken chambers in these hidden areas using the galea, or spinneret, present on the movable finger of each chelicera. These structures connect to silk glands in the cephalothorax (Chamberlin 1931). Most pseudoscorpions spin silken chambers for molting or for hatching new brood, but some also create silken chambers for periods of quiescence, such as hibernation or aestivation (Kew 1914). Other pseudoscorpions have more specialized uses for silken chambers. For example, *Lasiochernes pilosus* (Ellingsen, 1910) uses silken chambers as a retreat to which it returns after foraging, and therefore leaves an opening through which it exits and enters (Weygoldt 1969). *Halobisium occidentale* Beier, 1931 lives in the mud of marshes and estuaries and uses the silken chambers to create a dry space to live in (Carlton 2007). Despite the presence of diverse forms of galea, silken chambers produced by pseudoscorpions appear to be very similar (Kew 1914).

Members of the family Neobisiidae are found in caves, leaf litter, and in the soil throughout the Northern Hemisphere. There are currently two subfamilies: Neobisiinae and Microcreagrinae. These subfamilies are distinguished by two characters: the galea shape and chela trichobothrial patterns. The Microcreagrinae have elongate galeae (Fig. 1a, b) and trichobothrium *ist* is sub-basal (Fig. 2c); the Neobisiinae have reduced galeae (Fig. 1c, d) and trichobothrium *ist* is distal (Fig. 2a) (Harvey 1992). However, these characters are not wholly consistent between the two subfamilies. There are several microcreagrines that also have a reduced galea, including *Roncocreagris iglesiasae* Zaragoza, 2003, *R. murphyorum* Judson, 1992, and the *R. galeonuda* group species, *R.*

galeonuda (Beier, 1955), *R. clavata* (Beier, 1955), and *R. robusitor* (Beier, 1959). As has been noted by previous authors (Zaragoza 2008), the presence of this character state outside of Neobisiinae calls into question its stability and utility as a defining character of the subfamily and therefore the monophyly of both subfamilies as presently constituted. Within the Neobisiinae, the genus *Parobisium* (Chamberlin, 1930) is diagnosed by a sub-basal *ist* – the same character used to diagnose Microcreagrinae (Fig. 2b). The inconsistency of these characters calls into question the monophyly of subfamilies that have been defined by them.

We investigated the monophyly of the subfamilies using molecular phylogenetics. We also explored how many times the subfamilial character states evolved in Neobisiidae.

METHODS

Neobisiid specimens were freshly collected by GBH, donated by other collectors, or obtained from species housed at the Museum of Comparative Zoology (MCZ) at Harvard. Sequences of non-neobisiid taxa for the molecular phylogeny were primarily obtained from the NCBI GenBank database. In total, we analyzed COI and 28S from140 specimens of neobisiids and 19 outgroup taxa (Table 1).

DNA extractions were performed with the QIAGEN DNEasy kit following the standard ATL buffer protocol for extraction from tissues. Before placing specimens in a Proteinase K solution, we removed the pedipalps and punctured the pleural membrane of the abdomen to allow the protein-degrading solution access to the internal soft tissues.

Voucher specimens for this project were deposited in the University of Arizona Insect Collection (UAIC), the Museum of Comparative Zoology (MCZ) and the French National Museum of Natural History (MNHN) as indicated in Table 1.

DNA was amplified using Eppendorf Mastercycler model 5333 or Eppendorf Mastercycler gradient model 5331 (Eppendorf, Hamburg, Germany). Primers used for cytochrome oxidase subunit 1 (COI) were the forward primer LCO1490 (GCATAGTTCACCATCTTTC) and the reverse primer HCO2198 (TAAACTTCAGGGTGACCAAAAAATCA). Primers for 28S ribosomal DNA (28S) included the forward primers LS30F (ACCCCCTRAATTTAAGCATAT) and LS58F (GGGAGGAAAAGAAACTAAC), and the reverse primers LS1126R (TCGGAAGGAACCAGCTACTA) and LS1066R (CGACCGATTTGCACGTCAG). For all genes, the PCR protocol included an initial temperature of 94°C for 2 minutes, followed by 35 cycles of denaturing at 94°C for 30 seconds, annealing at 50-55°C for 30 seconds, and extension at 72°C for 60-95 seconds. Sequencing was performed at the University of Arizona Sequencing Core on an Applied Biosystems 3730XL DNA Analyzer.

We aligned sequences with MAFFT v.7.310 (Katoh & Standley 2013) within Mesquite (Maddison & Maddison 2016). The 28S sequences were aligned under the E-INS-I setting and COI was aligned under default settings.

We conducted phylogenetic analyses using RAxML v8.2.4 (Stamatakis 2014) through Mesquite's Zephyr package (Maddison & Maddison 2015). We analyzed genes separately and in combination. We included COI codon positions 1 and 2 and 28S resulting in 3 total partitions for the combined COI-28S analysis. We implemented a

GTR+gamma+invariant model of evolution for all 3 partitions as suggested by jModeltest 2 (Darriba et al. 2012) on the CIPRES Science Gateway V 3.3. For each analysis RAxML kept the best tree of 500 replicate searches. We also conducted 500 bootstrap replicates, with 2 searches each, on the combined dataset using the same 3 data partitions.

RESULTS

Parobisium charlotteae fell outside the Neobisiinae clade in all analyses (Fig. 3, results from single gene analyses not shown, but trees are available from the authors upon request). The remaining Neobisiinae formed a well-supported clade (bootstrap support 94; Fig. 3).

Our phylogeny shows 3 independent evolutions of reduced galeae. The movement of trichobothria *ist* from sub-basal to distal happened only once.

DISCUSSION

Neither Neobisiinae nor Microcreagrinae were recovered as monophyletic in our phylogenetic analysis. The type genus of Microcreagrinae is *Microcreagris,* whose type species is *Microcreagris gigas* (Balzan 1892). The type specimen was missing for decades and was rediscovered relatively recently (Ćurčić 2001). With the type missing for so long, and the original description being so generic, it is unclear at this time which species truly belong to *Microcreagris*. *Microcreagris* is reported to be restricted to China

and Afghanistan (Ćurčić 1981), and on that basis, several new genera of microcreagrines were erected in the 1980s (Ćurčić 1978, 1981, 1982, 1984, 1989). Unfortunately, many of these genera are unsatisfactorily diagnosed, leading to issues with placing newly-discovered microcreagrines from North America (Harvey & Muchmore 2010). Intense molecular and morphological investigations of microcreagrines with more complete taxonomic sampling than the present study will be necessary to untangle the taxonomic status of Microcreagrinae.

The genus Neobisiinae was not recovered as monophyletic, but this was only due to the placement of *Parobsium charlotteae*. The genus *Parobisium* shares the same diagnostic trait as Microcreagrinae: the sub-basal placement of trichobothria *ist* (Chamberlin 1930; Harvey 1992). According to our phylogeny, this character likely evolved only once, but it seems that the apomorphic state is actually the distal placement of *ist*. If this is the case, Microcreagrinae is only distinguished on the basis of two plesiomorphies: the elongate galea and sub-basal *ist*. Although we only have molecular data for *P. charlotteae*, the morphological similarity of *P. charlotteae* to the descriptions of its congeneric species gives us confidence in moving the entire genus out of Neobisiinae. Despite the taxonomic confusion surrounding Microcreagrinae, we believe it is beneficial to disassociate *Parobisium* from Neobisiinae. We hereby move *Parobisium* to the subfamily Microcreagrinae on the basis of the molecular evidence and trichobothrial positions.

Family Neobisiidae Chamberlin, 1930

Subfamily Microcreagrinae Balzan, 1892

This new discovery now presents us with an interesting scenario in which to study the evolution of galea form and function within neobisiids. There are now at least 3 independent reductions of the galea within Neobisiidae. Although Kew (1914) noted that the behaviors used to build silk chambers are universally the same across different forms of galea, the many variations on galea morphology across pseudoscorpions is surely tied in some way to each species' behavior. Indeed, sexual dimorphism of the galea has been found in pseudoscorpions (Harvey 1995). One of us (GBH) has observed that males may have galea that are slightly smaller with less prominent branching (compare Fig. 1A and 1B). Such a trend could be expected in species that do not build chambers for quiescent periods, such as aestivation or hibernation. These species would primarily build chambers for molting and for brood. Since adult males do not construct molting chambers or brood chambers, it is unsurprising to see a minor reduction of the galea in males of some species. If such minor differences occur between sexes of a single species, then it would not be surprising to find a significant ecological explanation for the cause of the drastic reduction of the galea in Neobisiinae, *Roncocreagris* species group, and *Parobisium*. To date however, such ecological explanations remain elusive. Additional future studies investigating how galea form differs at the microscopic level across neobisiid taxa may reveal new characters defining natural groups within the family.

ACKNOWLEDGEMENTS

Our greatest thanks go to Neil Marchington who provided the specimens of *P. charlotteae*. We are also deeply grateful to Mark Harvey for mentoring GBH during the early stages of this project. We thank the following for collecting and donating other specimens: Marshal Hedin and his lab, Gonzalo Giribet, Alan Yanahan, Angela Hoover, Jeff Eble, Jillian Cowles, and Tim Cota. We thank the following for additional assistance in the lab and field: Reilly McManus, Jason Schaller, Antonio Gomez, James Robertson, Paul Marek, Marty Meyer, and other members of the Moore lab. This work is in partial fulfillment of GBH's PhD degree in the Graduate Interdisciplinary Program in Entomology and Insect Science at the University of Arizona. The following collecting permits from the U.S. National Parks Service were obtained for collection of specimens used in this study: GOGA-2013-SCI-0007, GRBA-2013-SCI-0014, and SAGU-2011-SCI-0004. This project received funding support from the following grants and institutions: East Asia and Pacific Summer Institute (EAPSI) award 1209343 from the National Science Foundation; Ernst Mayr Travel Grant in Animal Systematics from the Harvard Museum of Comparative Zoology; Entomology and Insect Science Graduate Student Research Support Award from the University of Arizona Center for Insect Science; National Science Foundation award 1206382 to WM.

LITERATURE CITED

Balzan L. 1892. Voyage de M. E. Simon au Vénezuéla (Decembre 1887-Avril 1888), 16 mém, Arachnidees, Chernetes (Pseudoscorpiones). Annales de la société entomologi1ue de France 60:497-552.

Beier. M. 1931. Neue pseudoscorpione der U. O. Neobisiinea. Mitteilungen aus dem Zoologischen Museum in Berlin 17:299-318.

Beier, M. 1955. Neue Beiträge zur Kenntnis der iberischen Pseudoscorpioniden-Fauna. Eos, Madrid 31:87-122.

Beier, M. 1959. Ergänzungen zur iberischen Pseudoscorpioniden-Fauna. Eos, Madrid 35:113-131.

Carlton, J.T. 2007. The Light and Smith manual: Intertidal invertebrates from Central California to Oregon. University of California Press.

Chamberlin, J.C. 1930. A synoptic classification of the false scorpions or chela-spinners, with a report on a cosmopolitan collection of the same. Part II. The Diplosphyronida (Arachnida-Chelonethida). Annals and Magazine of Natural History 10:1-48, 585-620.

Chamberlin, J.C. 1931. The arachnid order Chelonethida. Stanford University Press, Stanford, California.

Chamberlin, J.C. 1962. New and little-known false scorpions, principally from caves, belonging to the families Chthoniidae and Neobisiidae (Arachnida, Chelonethida). Bulletin of the American Museum of Natural History 123:299-352.

Ćurčić, B.P.M. 1978. Tuberocreagris, a new genus of pseudoscorpions from the United States (Arachnida, Pseudoscorpiones, Neobisiidae). Fragmenta Balcanica Musei Macedonici Scientarium Naturalium 10:111-121.

Ćurčić, B.P.M. 1981. A revision of some North American, Pseudoscorpions (Neobisiidae, Pseudoscorpiones). Glasnik Muzeja Srpske Zemlje, Beograd (B) 36:101-107.

Ćurčić, B.P.M. 1982. *Americocreagris*, a new genus of pseudoscorpions from the United States. Bulletin de l'Académie Serbe des Sciences et des Arts, Classe des Sciences Naturelles et Mathématiques 80:47-50.

Ćurčić, B.P.M. 1984. A revision of some North American species of *Microcreagris* Balzan, 1982, (Arachnida: Pseudoscorpiones: Neobisiidae). Bulletin of the British Arachnological Society 6:149-166.

Ćurčić, B.P.M. 1989. Further revision of some North American false scorpions originally assigned to Microcreagris Balzan, (Pseudoscorpiones, Neobisiidae). Journal of Arachnology 17:351-362.

Ćurčić, B.P.M. 2001. Further report on the identity of *Microcreagris gigas* Balzan (Neobisiidae, Pseudoscorpiones). Archive of Biological Science Belgarde 53:91-98.

Darriba, D., G.L. Taboada, R. Doallo, & D. Posada. 2012. jModelTest 2: more models, new heuristics and parallel computing. Nature Methods 9:772.

Ellingsen, E. 1910. Die pseudoskorpione des Berliner Museums. Mitteilungen aus dem Zoologischen Museum in Berlin 3:357-423.

Harvey, M.S. 1992. The phylogeny and classification of the Pseudoscorpionida (Chelicerata: Arachnida). Invertebrate Taxonomy 6:1373-1435.

Harvey, M.S. 1995. *Barbaraella* gen. nov. and *Cacoxylus* Beier (Pseudoscorpionida: Chernetidae), two remarkable sexually dimorphic pseudoscorpions from Australia. Records of the Western Australian Museum 52:199-208.

Harvey, M.S. & W.B. Muchmore. 2010. Two new cavernicolous species of the pseudoscorpion genus *Cryptocreagris* from Colorado (Pseudoscorpiones: Neobisiidae). Subterranean Biology 7:55-64.

Judson, M.L.I. 1992. *Roncocreagvis murphyovum* n. sp. and *Occitanobisium nanum* (Beier) n. comb. (Neobisiidae) from Iberia, with notes on the sternal glands of pseudoscorpions (Chelonethi). Bulletin of the British Arachnological Society 9:26-30.

Katoh, K. & D.M. Standley. 2013. MAFFT multiple sequence alignment software version 7: improvements in performance and usability. Molecular Biology and Evolution 30:772-780.

Kew, H.W. 1914. On the nests of Pseudoscorpiones: with historical notes on the spinning-organs and observations on the building and spinning of the nests. Proceedings of the Zoological Society of London 1914:93-11.

Maddison, W. P. & D.R. Maddison. 2016. Mesquite: a modular system for evolutionary analysis. Version 3.10 http://mesquiteproject.org

Maddison, D.R. & W.P. Maddison. 2015. Zephyr: a Mesquite package for interacting with external phylogeny inference programs. Version 1.1. https://mesquitezephyr.wikispaces.com

Miller, M.A., W. Pfeiffer & T. Schwartz 2010. “Creating the CIPRES Science Gateway for inference of large phylogenetic trees" in Proceedings of the Gateway Computing Environments Workshop (GCE), 14 Nov. 2010, New Orleans, LA, pp 1-8.

Murienne, J., M.S. Harvey & G. Giribet. 2008. First molecular phylogeny of the major clades of Pseudoscorpiones (Arthropoda: Chelicerata). Molecular Phylogenetics and Evolution 49:170-184.

Stamatakis, A. 2014. RAxML Version 8: A tool for phylogenetic analysis and post-analysis of large phylogenies. bioinformatics 30:1312-1313.

Weygoldt, P. 1969. The Biology of Pseudoscorpions. Harvard University Press, Cambridge, Massachusetts.

Zaragoza, J.A. 2003. *Roncocreagris iglesiasae*, nueva especie cavernicola de Asturias Arachnida, Pseudoscorpiones, Neobisiidae). Revista Ibérica de Aracnología 7:89-94.

Zaragoza, J.A. 2008. On the status of the subspecies of *Roncocreagris galeonuda* (Pseudoscorpiones: Neobisiidae): importance of the chelal microsetae pattern. Remarks on the genus *Roncocreagris* Mahnert. Revista Ibérica de Aracnología 15:35-46.

Table 1. Taxon sampling table indicating specimen voucher numbers, GenBank accession numbers, and primers used for each specimen used in this study. MCZ numbers are lot numbers rather than specimen numbers. All others are unique specimen numbers. WB – Whole Body; C- Chelae

Figure 1a-d.

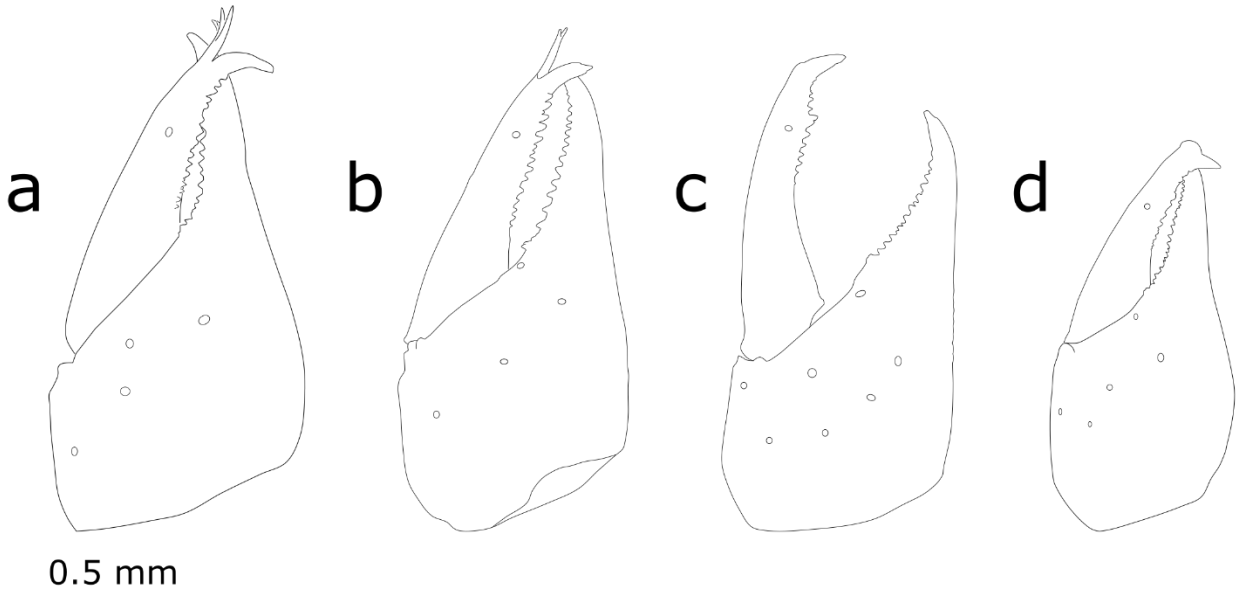

Figure 2a-c.

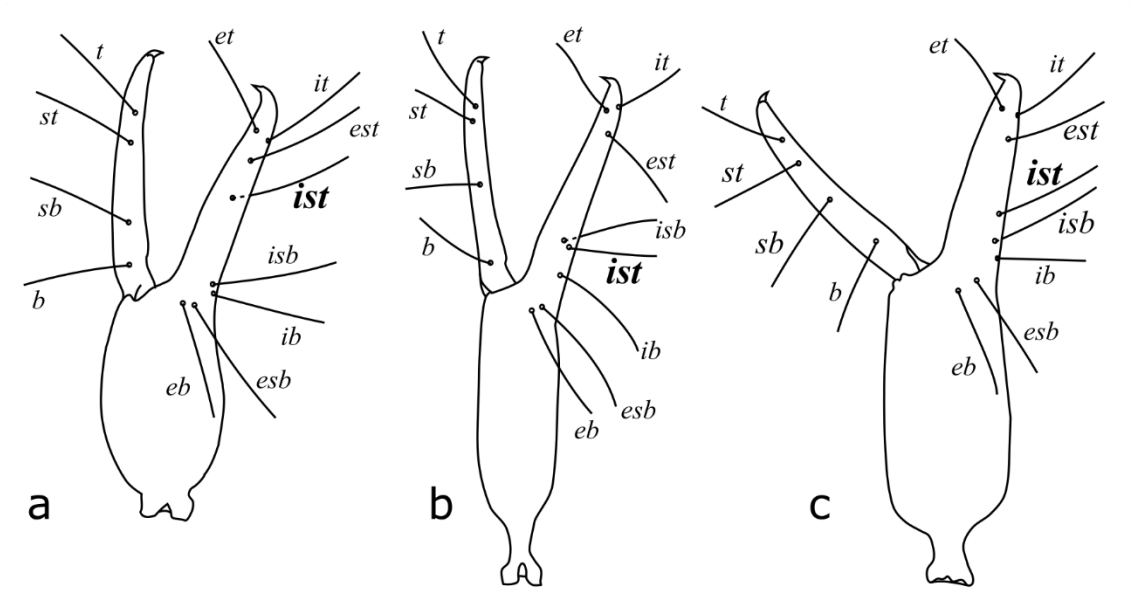
t
et
it
st
est
sb
ist
isb
b
ib
eb
esb
a
t
et
it
st
est
sb
isb
b
ist
ib
esb
eb
b
et
it
t
est
st
ist
isb
sb
ib
b
esb
eb
c

Figure 3.

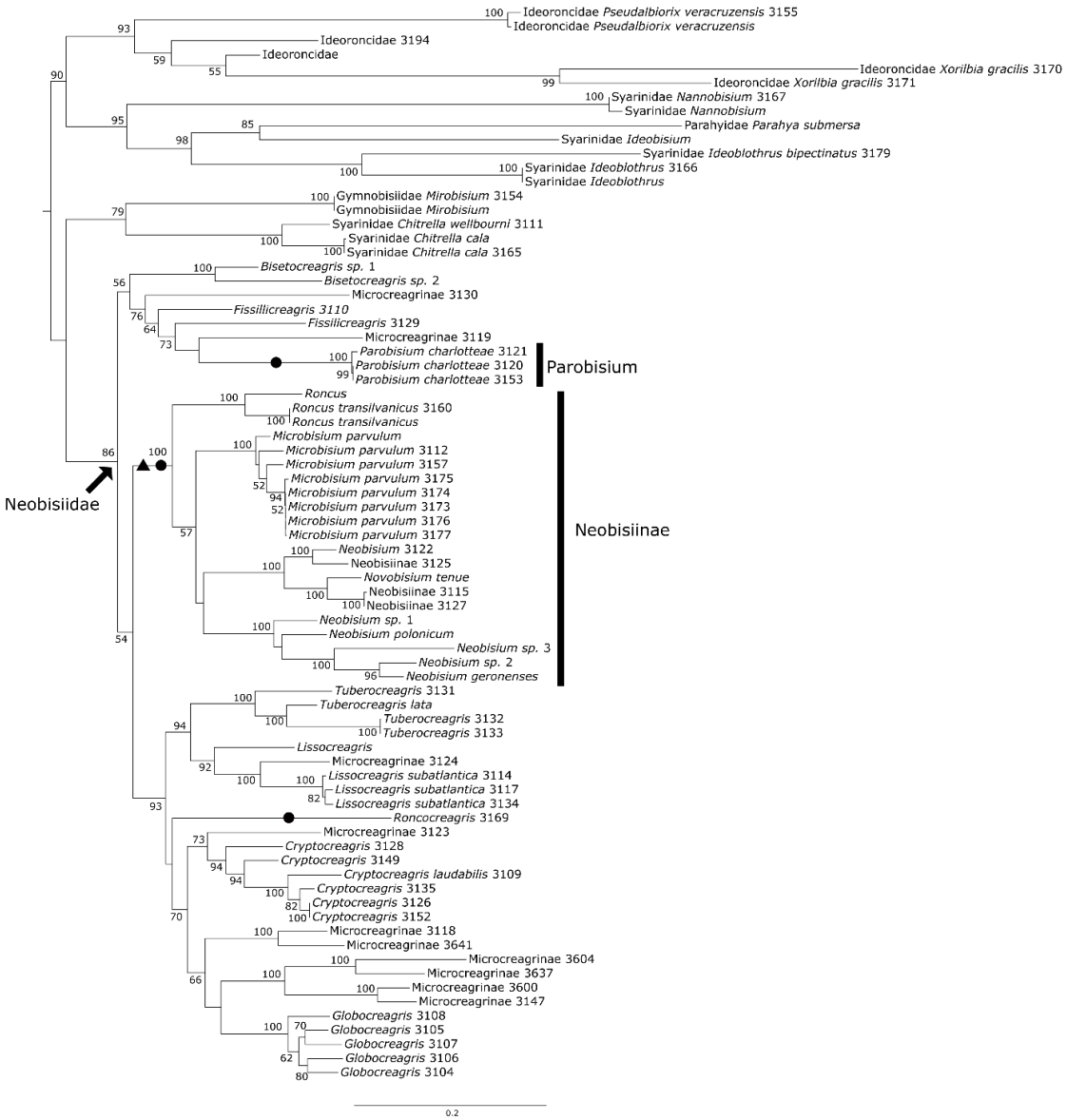
Ideoroncidae Pseudalbiorix veracruzensis 3155
Ideoroncidae Pseudalbiorix veracruzensis
Ideoroncidae 3194
Ideoroncidae
Ideoroncidae Xorilbia gracilis 3170
Ideoroncidae Xorilbia gracilis 3171
Syarinidae Nannobisium 3167
Syarinidae Nannobisium
Parahyidae Parahya submersa
Syarinidae Ideobisium
Syarinidae Ideoblothrus bipectinatus 3179
Syarinidae Ideoblothrus 3166
Syarinidae Ideoblothrus
Gymnobisiidae Mirobisium 3154
Gymnobisiidae Mirobisium
Syarinidae Chitrella wellbourni 3111
Syarinidae Chitrella cala
Syarinidae Chitrella cala 3165
Bisetocreagris sp. 1
Bisetocreagris sp. 2
Microcreagrinae 3130
Fissilicreagris 3110
Fissilicreagris 3129
Microcreagrinae 3119
Parobisium charlotteae 3121
Parobisium charlotteae 3120
Parobisium charlotteae 3153
Parobisium
Roncus
Roncus transilvanicus 3160
Roncus transilvanicus
Microbisium parvulum
Microbisium parvulum 3112
Microbisium parvulum 3157
Microbisium parvulum 3175
Microbisium parvulum 3174
Microbisium parvulum 3173
Microbisium parvulum 3176
Microbisium parvulum 3177
Neobisium 3122
Neobisiinae 3125
Novobisium tenue
Neobisiinae 3115
Neobisiinae 3127
Neobisium sp. 1
Neobisium polonicum
Neobisium sp. 3
Neobisium sp. 2
Neobisium geronenses
Neobisiinae
Neobisiidae
Tuberocreagris 3131
Tuberocreagris lata
Tuberocreagris 3132
Tuberocreagris 3133
Lissocreagris
Microcreagrinae 3124
Lissocreagris subatlantica 3114
Lissocreagris subatlantica 3117
Lissocreagris subatlantica 3134
Roncocreagris 3169
Microcreagrinae 3123
Cryptocreagris 3128
Cryptocreagris 3149
Cryptocreagris laudabilis 3109
Cryptocreagris 3135
Cryptocreagris 3126
Cryptocreagris 3152
Microcreagrinae 3118
Microcreagrinae 3641
Microcreagrinae 3604
Microcreagrinae 3637
Microcreagrinae 3600
Microcreagrinae 3147
Globocreagris 3108
Globocreagris 3105
Globocreagris 3107
Globocreagris 3106
Globocreagris 3104
0.2

Figure 1a–d. Chelicera of 4 members of Neobisiidae illustrating differences in galea morphology on the movable fingers: a. *Cryptocreagris sp.*, female (Microcreagrinae); b. *Cryptocreagris sp.*, male (Microcreagrinae); c. *Parobisium charlotteae*, male; d. an unidentified neobisiid, male (Neobisiinae).

Figure 2a-c. External aspect of pedipalp chelae, especially calling attention to the position of trichobothrium *ist*: a. *Neobisium carolinense*, b. *Parobisium charlotteae*, c. *Americocreagris Columbiana*. Illustrations adapted from Chamberlin (1962).

Figure 3. Molecular phylogeny of members of Neobisiidae inferred from COI and 28S sequences using maximum likelihood. Node values indicate bootstrap support. *Parobisium* is not contained within the rest of the subfamily Neobisiinae. All other taxa belong to the subfamily Microcreagrinae. Evolution of characters used to diagnose neobisiid subfamilies are denoted as on tree branches: a triangle shows the shift of trichobothrium *ist* from sub-basal to distal; a circle shows the reduction of the galea. Arrow indicates the most recent common ancestor of Neobisiidae.

DNA Number	Body Part	Taxon/ geographic origin	Specimen/lot number	GenBank accession number COI	GenBank accession number 28S	COI Forward Primer	COI Reverse Primer	28S Forward Primer	28S Reverse Primer
Ideoroncidae									
3194	WB	Ideoroncidae USA: AZ	UAIC1113067	MF124552	NA	HCO1490	HCO2198	NA	NA
		Ideoroncidae	MNHN-JAD70	JN018183.1	NA	NA	NA	NA	NA
3155	C	*Pseudalbiorix veracruzensis* Mexico: Oaxaca	MCZ 130499	NA	MF124381	HCO1490	HCO2198	LS30F	LS1126R
		Pseudalbiorix veracruzensis	MCZ 130499	EU559567.1	EU559474.1	NA	NA	NA	NA
3171	C	*Xorilbia gracilis* Brazil	MCZ 36800	MF124532	MF124395	HCO1490	HCO2198	LS30F	LS1126R
3170	C	*Xorilbia gracilis* Guyana	MCZ 36676	NA	MF124394	HCO1490	HCO2198	LS30F	LS1126R
Gymnobisiidae									
3154	C	*Mirobisium sp.* USA: MD	MCZ 130497	MF124518	MF124380	HCO1490	HCO2198	LS30F	LS1126R
		Mirobisium sp.	JM-2008	EU559547.1	EU559473.1	NA	NA	NA	NA
Syarinidae									
3165	C	*Chitrella cala* USA: CA	MCZ 130522	MF124527	MF124389	HCO1490	HCO2198	LS30F	LS1126R
		Chitrella cala	MCZ 130522	EU559551.1	EU559479.1	NA	NA	NA	NA
3111	WB	*Chitrella wellbourni* USA: CA	UAIC1113007	MF124481	MF124342	HCO1490	HCO2198	LS30F	LS1126R
3179	C	*Ideoblothrus bipectinatus* Papua New Guinea	MCZ 45816	MF124537	MF124401	HCO1490	HCO2198	LS30F	LS1126R
		Ideoblothrus sp.	MCZ 130524	EU559562.1	EU559480.1	NA	NA	NA	NA
3166	C	*Ideblothrus sp.* Colombia	MCZ 130524	MF124390	MF124528	HCO1490	HCO2198	LS30F	LS1126R
		Ideobisium sp.	NA	EU559549.1	EU559458.1	NA	NA	NA	NA
3167	C	*Nannobisium sp.* Equatorial Guinea	MCZ 130525	MF124529	MF124391	HCO1490	HCO2198	LS30F	LS1126R
		Nannobisium sp.	MCZ 130525	EU559561.1	EU559481.1	NA	NA	NA	NA
Parahyidae									
		Parahya submersa	MCZ 130517	EU559548.1	EU559478.1	NA	NA	NA	NA
Neobisiidae									
		Bisetocreagris sp. 1	MNHN-JAC35	JN018181.1	JN018395.1	NA	NA	NA	NA
		Bisetocreagris sp. 2	MNHN-JAD69	JN018182.1	JN018396.1	NA	NA	NA	NA
3109	WB	*Cryptocreagris laudabilis* USA: NM	UAIC1113005	MF124479	NA	HCO1490	HCO2198	NA	NA
3126	WB	*Cryptocreagris sp.* USA: NM	UAIC1113022	MF124495	MF124356	HCO1490	HCO2198	LS30F	LS1126R
3135	WB	*Cryptocreagris sp.* USA: NM	UAIC1113031	MF124504	NA	HCO1490	HCO2198	NA	NA
3152	WB	*Cryptocreagris sp.* USA: NM	UAIC1113048	MF124516	MF124378	HCO1490	HCO2198	LS30F	LS1126R
3149	WB	*Cryptocreagris sp.* USA: NV	UAIC1113045	MF124513	MF124375	HCO1490	HCO2198	LS30F	LS1126R
3129	WB	*Fissilicreagris sp.* USA: CA, Humboldt Co.	UAIC1113025	MF124498	MF124359	HCO1490	HCO2198	LS30F	LS1066R
3108	WB	*Globocreagris* USA: AZ, Pinaleño Mts.	UAIC1113004	MF124478	MF124340	HCO1490	HCO2198	LS30F	LS1126R
3105	WB	*Globocreagris* USA: AZ, Rincon Mts.	UAIC1113001	MF124475	MF124337	HCO1490	HCO2198	LS30F	LS1126R
3104	WB	*Globocreagris* USA: AZ, Santa Catalina Mts.	UAIC1113000	MF124474	MF124336	HCO1490	HCO2198	LS30F	LS1126R
3106	WB	*Globocreagris* USA: AZ, Santa Catalina Mts.	UAIC1113002	MF124476	MF124338	HCO1490	HCO2198	LS30F	LS1126R
3107	WB	*Globocreagris* USA: AZ, Santa Rita Mts.	UAIC1113003	MF124477	MF124339	HCO1490	HCO2198	LS30F	LS1126R
		Lissocreagris sp.	MCZ 130501	NA	EU559450.1	NA	NA	NA	NA
3117	WB	*Lissocreagris subatlantica* USA: TN	UAIC1113013	MF124486	MF124347	HCO1490	HCO2198	LS30F	LS1126R
3134	WB	*Lissocreagris subatlantica* USA: NC	UAIC1113030	MF124503	MF124364	HCO1490	HCO2198	LS30F	LS1126R
3114	WB	*Lissocreagris subatlantica* USA: TN	UAIC1113010	MF124484	MF124345	HCO1490	HCO2198	LS30F	LS1126R
		Microbisium parvulum	MCZ 130502	NA	EU559476.1	NA	NA	NA	NA
3173	C	*Microbisium parvulum* Mexico	MCZ 37164	NA	MF124396	HCO1490	HCO2198	LS30F	LS1126R
3174	C	*Microbisium parvulum* Mexico	MCZ 37883	NA	MF124397	HCO1490	HCO2198	LS30F	LS1126R

3175	WB	*Microbisium parvulum* Mexico	MCZ 37879	MF124533	MF124398	HCO1490	HCO2198	LS30F	LS1126R
3176	C	*Microbisium parvulum* Mexico	MCZ 37883	MF124534	MF124399	HCO1490	HCO2198	LS30F	LS1126R
3177	WB	*Microbisium parvulum* Mexico	MCZ 37886	MF124535	MF124400	HCO1490	HCO2198	LS30F	LS1126R
3157	C	*Microbisium parvulum* USA: MD	MCZ 130502	MF124520	MF124383	HCO1490	HCO2198	LS30F	LS1126R
3112	WB	*Microbisium parvulum* USA: UT	UAIC1113008	MF124482	MF124343	HCO1490	HCO2198	LS30F	LS1126R
3600	WB	Microcreagrinae USA: AZ, Black Hills	UAIC1113073	MF124558	MF124421	HCO1490	HCO2198	LS30F	LS1126R
3604	WB	Microcreagrinae USA: AZ, Bradshaw Mts.	UAIC1113077	MF124562	MF124425	HCO1490	HCO2198	LS30F	LS1126R
3637	WB	Microcreagrinae USA: AZ, Superstition Mts.	UAIC1113110	MF124587	MF124458	HCO1490	HCO2198	LS30F	LS1126R
3147	WB	Microcreagrinae USA: AZ, Sabino Canyon	UAIC1113043	MF124511	MF124373	HCO1490	COHua2R	LS30F	LS1126R
3110	WB	Microcreagrinae USA: CA	UAIC1113006	MF124480	MF124341	HCO1490	HCO2198	LS30F	LS1066R
3641	WB	Microcreagrinae USA: CA	UAIC1113114	MF124591	MF124462	HCO1490	HCO2198	LS58F	LS1066R
3128	WB	Microcreagrinae USA: CA, Calaveras Co.	UAIC1113024	MF124497	MF124358	HCO1490	HCO2198	LS30F	LS1066R
3130	WB	Microcreagrinae USA: CA, Calaveras Co.	UAIC1113026	MF124499	MF124360	HCO1490	HCO2198	LS30F	LS1126R
3118	WB	Microcreagrinae USA: CA, San Benito	UAIC1113014	MF124487	MF124348	HCO1490	HCO2198	LS30F	LS1126R
3119	WB	Microcreagrinae USA: CA, San Mateo	UAIC1113015	MF124488	MF124349	HCO1490	HCO2198	LS30F	LS1066R
3124	WB	Microcreagrinae USA: TN	UAIC1113020	MF124493	MF124354	HCO1490	HCO2198	LS30F	LS1126R
3127	WB	Neobisiinae USA: TN	UAIC1113023	MF124496	MF124357	HCO1490	HCO2198	LS30F	LS1126R
3115	WB	Neobisiinae USA: TN	UAIC1113011	MF124485	MF124346	HCO1490	HCO2198	LS30F	LS1066R
3125	WB	Neobisiinae USA: VA	UAIC1113021	MF124494	MF124355	HCO1490	HCO2198	LS30F	LS1066R
		Neobisium geronenses	MNHN-JAC22	JN018184.1	JN018398.1	NA	NA	NA	NA
		Neobisium polonicum	MCZ 130503	NA	EU559457.1	NA	NA	NA	NA
		Neobisium sp. 1	MNHN-JAA9	NA	NA	NA	NA	NA	NA
		Neobisium sp. 2	MNHN-JAC-14	JN018208.1	NA	NA	NA	NA	NA
		Neobisium sp. 3	MNHN-JAC15	JN018209.1	NA	NA	NA	NA	NA
3122	WB	*Neobisium sp.* USA: NC	UAIC1113018	MF124491	MF124352	HCO1490	HCO2198	LS30F	LS1066R
		Novobisium tenue	MCZ 130504	NA	EU559452.1	NA	NA	NA	NA
3120	WB	*Parobisium charlotteae* USA: OR	UAIC1113016	MF124489	MF124350	HCO1490	HCO2198	LS30F	LS1066R
3121	WB	*Parobisium charlotteae* USA: OR	UAIC1113017	MF124490	MF124351	HCO1490	HCO2198	LS30F	LS1066R
3123	WB	*Parobisium charlotteae* USA: OR	UAIC1113019	MF124492	MF124353	HCO1490	HCO2198	LS30F	LS1126R
3153	WB	*Parobisium charlotteae* USA: OR	UAIC1113049	MF124517	MF124379	HCO1490	HCO2198	LS30F	LS1126R
3169	C	*Roncocreagris sp.* Spain	MCZ 130546	MF124531	MF124393	HCO1490	HCO2198	LS30F	LS1126R
		Roncus pugnax	NA	NA	AF124962.1	NA	NA	NA	NA
		Roncus sp.	MNHN-JAC28	JN018186.1	JN018400.1	NA	NA	NA	NA
		Roncus transsilvanicus	MCZ 130505	NA	EU559477.1	NA	NA	NA	NA
3160	C	*Roncus transsilvanicus* Slovakia	MCZ 130505	MF124523	MF124385	HCO1490	HCO2198	LS30F	LS1126R
		Tuberocreagris lata	MCZ 130508	NA	EU559451.1	NA	NA	NA	NA
3132	WB	*Tuberocreagris sp.* USA: VA, Lee Co.	UAIC1113028	MF124501	MF124362	HCO1490	HCO2198	LS30F	LS1126R
3133	WB	*Tuberocreagris sp.* USA: VA, Lee Co.	UAIC1113029	MF124502	MF124363	HCO1490	HCO2198	LS30F	LS1126R
3131	WB	*Tuberocreagris sp.* USA: VA, Washington Co.	UAIC1113027	MF124500	MF124361	HCO1490	HCO2198	LS30F	LS1126R

APPENDIX B.

DISCOVERY, PHYLOGENY, AND BIOGEOGRAPHY OF A NEW ASSEMBLAGE OF *GLOBOCREAGRIS* (PSEUDOSCORPIONES: NEOBISIIDAE) FROM THE ARIZONA SKY ISLANDS

Garrett B. Hughes and Wendy Moore

Department of Entomology, University of Arizona, Tucson, AZ, 85721, USA; Email: gbhughes@email.arizona.edu

ABSTRACT

Seven new pseudoscorpion species in the genus *Globocreagris* are described. Each is endemic to coniferous forest of a different mountain range among the southern Arizona Sky Islands. Through our own collecting efforts and our study of museum material, we extend the range of *Globocreagris*, known previously from California only, to include Arizona, Oregon, and Washington. Results of divergence time estimation indicate that the genus arrived in the Sky Island region at least 7.5 million years ago and species have likely been isolated from one another since before the beginning of Pleistocene glaciation cycles.

INTRODUCTION

Pseudoscorpions are small arachnids found throughout the world. They can be found on all continents except Antarctica (Harvey 2013). They occupy a variety of cryptic habitats, including soil, leaf-litter, caves, trees, nests, beehives, rotting cacti, and intertidal zones (Weygoldt 1969). They primarily occupy areas with high humidity and tiny spaces to crawl through, though some species are adapted to arid environments. Pseudoscorpions prey on small arthropods like springtails, beetles, flies, booklice, and various larvae (Weygoldt 1969). They use their chelate, pincer-like pedipalps the grasp and subdue their prey (De Andrade & Gnaspini 2002). Many pseudoscorpions possess venom glands in their chelae used to envenomate their prey. Some pseudoscorpions also use their chelae to grab hold of more mobile animals, especially flying ones, as a form of transportation—a behavior called phoresy. Pseudoscorpion phoresy has been reported in the families Atemnidae, Cheiridiidae, Cheliferidae, Chernetidae, Chthoniidae, and Syarinidae (Muchmore 1971). They may utilize beetles, moths, wasps, flies (Muchmore 1971) and even mammals (Francke & Villegas-Guzmán 2006) or birds (Worth 1971) as their phoretic hosts.

The pseudoscorpion family Neobisiidae is mostly composed of species that live in soil and leaf litter of forests or in caves. They are distinguished from other families by the presence of 3 or more setae on the manducatory process of the pedipalp coxae, and by the loss of a venom gland in the movable finger, leaving them with one venom gland in the fixed finger (Harvey 1992). Neobisiids are not known to have any behaviors that aid in dispersal such as phoresy. Their low dispersal ability means they should show much more population structure than phoretic pseudoscorpions and may even have more endemic species. Unfortunately, the taxonomy of North American Neobisiidae, especially for taxa within the subfamily Microcreagrinae, is currently unstable, with about a dozen described genera, many of which have poor diagnoses and include only a few species. Previous workers have also acknowledged the poor state of microcreagrine taxonomy and have had difficulty assigning new species to existing genera (Buddle 2010, Harvey & Muchmore 2010). The current taxonomic situation makes it difficult to place species in genera on the basis of morphology alone.

We recently discovered a new lineage of neobisiid in the Sky Island region of southern Arizona. We tentatively assigned these specimens to the genus *Globocreagris* Ćurčić, 1984 on the basis of the enlarged, globular, lateral genital sacs. However, given the geographic distance between the new Arizona lineage and *Globocreagris* from

California, we sought molecular data to support this designation. We obtained a single specimen of *Globocreagris nigrescens* (Chamberlin, 1952) from southern California. We include it in our molecular phylogenetic analysis to test our hypothesis that the new Arizona Sky Island pseudoscorpions belong to *Globocreagris*.

The Sky Island region of southern Arizona and northwestern Mexico consists of approximately 57 mountain ranges that span the low desert gap between the Rocky Mountains and Colorado Plateau, and the Sierra Madre Occidental of Mexico. These mountains are part of the Basin and Range Province, formed by tectonic extensions beginning around 30 million years ago (Ferrari et al 2013) and which resulted in the stark elevation contrasts seen today. Basin and Range tectonics appears to have ended (or greatly slowed) around 7 million years ago (Colgan et al. 2006), though the elevational differences between mountains and valleys were probably established well before then.

Today, mixed conifer forests occur only at the tops of the highest Sky Island ranges. These forests harbor a unique set of plants (Brusca et al. 2013) and animals (Meyer et al. 2015) relative to those found at lower elevations in the same mountain ranges. Given the isolated nature of these habitats, many researchers have questioned how these taxa came to exist in these mountain-top forests. One possibility is that taxa migrated into the region, following the expansion of forests during cooler glacial periods. The past 2.6 million years (the Pleistocene Epoch) have been characterized by cycles of glacial and inter-glacial periods (Broecker & Denton 1990). As temperatures cooled during the glacial periods, the plants and animals that are now restricted to the tops of the mountains may have been able to migrate along corridors, allowing access to previously uninhabited mountains. Subsequent interglacial periods resulted in warmer temperatures that caused the cooler adapted flora and fauna to retreat back up the mountains, thus isolating populations. Pleistocene divergence of Sky Island taxa has been hypothesized for spiders (Ayoub & Riechert 2004), birds (McCormack et al. 2008), rattlesnakes (Bryson et al. 2011), and garter snakes (Wood et al. 2011).

It is also possible that some taxa occupied higher-elevation habitats long before the Pleistocene glacial cycles began. These lineages may have diverged before the Pleistocene, as seen in montane scorpions (Bryson et al. 2013). In this scenario, widespread taxa may have lived in the highlands of this region before the tectonic expansion that formed the Basin and Range Province. As the valleys formed (and warmed), these taxa may have been isolated to high-elevation peaks and lacked the ability to disperse to other mountains.

We used divergence time estimation using molecular clocks to determine which of these scenarios most likely resulted in the distribution patterns of *Globocreagris* seen today.

MATERIALS & METHODS

Collection, Extraction, Sequencing, and Specimen Preparation

We collected 85 pseudoscorpion specimens from the following mountain ranges in Arizona: Santa Catalina, Santa Rita, Rincon, Huachuca, Chiricahua, Pinaleño, Pinal, Superstition, Bradshaw, and Black Hills. We found pseudoscorpions by sifting leaf litter and duff along with the top 5 centimeters of moist soil, or by flipping rocks, branches, and other debris in areas with moist soil and checking the underside of the debris. Most

specimens were collected at high elevations in the pine and mixed conifer zones of the mountain ranges, however some were found in low elevation riparian areas, such as Sabino Canyon near the base of the Santa Catalina Mountains. Including these specimens and other outgroup specimens, we had a total of 136 specimens.

We extracted DNA from whole-body specimens or from pedipalps (Table 1). For whole-body extractions, we removed both pedipalps at the trochanter–femur joint. We removed the chela of one pedipalp from the patella. We made an incision in the other pedipalp at the patella–chela joint and another incision in one side of the abdominal pleural membrane to facilitate infiltration of digestion chemicals into the tissues. For non-whole-body specimens, we removed a single pedipalp from the specimen and made an incision in the patella–chela joint as above. Pseudoscorpions are typically preserved as cleared, disarticulated, slide-mounted specimens for long-term storage in collections so this procedure facilitated extraction of DNA and preparation of morphological voucher specimens. After disarticulating the specimen, we followed the standard ATL buffer tissue protocol from the DNEasy Blood & Tissue extraction kit (QIAGEN). DNA extractions are stored at -80°C in the Moore lab at the University of Arizona. Voucher specimens are deposited in the University of Arizona Insect Collection (UAIC1113000-UAIC1113113).

We amplified partial gene fragments of cytochrome oxidase c subunit I (COI) and the large ribosomal subunit DNA (28S) using an Eppendorf Mastercycler thermal cycler (Hamburg, Germany). The primers and sequence numbers for each specimen are listed in Table 1. PCR products were sequenced at the University of Arizona Genetics Core on an 3730X Applied Biosystems Automatic Sequencer. COI PCR products from DNA3116, DNA3142-3146, and DNA3614-3619 were sent to Eton Bioscience Inc. (San Diego, CA) for sequencing.

We aligned DNA sequences using Opal (Wheeler & Kececioglu 2007) implemented through the Opalescent package (Wheeler & Maddison 2012) in Mesquite (Maddison & Maddison 2016), followed by manual adjustment of the output alignment. Manual adjustment of COI was facilitated by calculating codon positions for all of the nucleotides in the alignment and coloring the nucleotides by amino acid. The alignment revealed stop codons and single-base deletions in *Globocreagris nigrescens* from California and the specimens from the Huachuca mountains, indicating that these sequences may be nuclear mitochondrial segments (numts).

Phylogenetic inference

We inferred phylogenies using RAxML v.8.2.8 (Stamatakis 2014) through the Cipres portal v.3.3 (www.phylo.org) using datasets of COI only, 28S only, and combined COI and 28S. We used PartitionFinder (Lanfear et al. 2012) to determine partitions for the molecular data. Accordingly, we split COI into 3 partitions and set 28S as a single partition and applied a general time-reversible model of evolution with a gamma distribution of rates among sites (GTR+Gamma) among each partition. Although PartitionFinder recommended we include a parameter for invariant sites in our model, we omitted this from the analysis because Stamatakis (2014) recommends against using invariant sites in RAxML analyses. We conducted a maximum likelihood tree search with 500 independent starting trees. We conducted rapid bootstrap analyses under a GTRGAMMA model (see Stamatakis 2014) and allowed RAxML to halt the

bootstrapping automatically, resulting in 360 bootstrap replicates. We used RAxML to draw the bootstrap partitions onto the best tree.

Divergence Dating

Divergence times are commonly estimated through the use of molecular clocks, which can be calibrated with fossils (see Wood et al. 2011, Bryson et al. 2011) or with dated geographic events (when specimen distributions within clades in the phylogeny correspond to a variance event of a known age) (see Bryson et al. 2013). However, for our question, there is no suitable geographic event and fossil specimens are either unknown or do not include the apomorphic characters needed to be placed within a clade on the phylogeny. In order to investigate whether the Sky Island neobsiids diverged before or during the Pleistocene glaciation events, we used several different published rates of molecular evolution to explore minimum and maximum estimates for the age of *Globocreagris* and the species within the region. (see McCormack et al. 2008).

We conducted two divergence time estimation analyses using BEAST 2.4.2 (Bouckaert et al. 2014) through the CIPRES portal v.3.3 (www.phylo.org). Lacking reliable calibration for our clock, we chose to explore divergence dates with clock rates reported in the literature. Scorpions in the Sky Island region appear to have diversified before the Pleistocene glacial-interglacial cycles (Bryson et al. 2013), so we chose to investigate whether pseudoscorpions would show a similar pattern under a fast rate of molecular evolution. If a fast divergence rate results in pre-Pleistocene divergence, we can be confident that sky island neobisiids diversified before the glacial-interglacial cycles, regardless of their actual rate of divergence.

The COI region of arthropods is often said to evolve at an average rate of 2.3% divergence per million years (Brower 1994). For arachnids, that rate can be as slow as 0.5% (Clouse & Wheeler 2014) or as fast as 2.7% (Gantenbein & Largiadèr 2003) divergence per million years. For arthropods, the fastest known rate of divergence of COI is 17.212% in Coleoptera (Pons et al. 2010).

We conducted two divergence dating analyses in BEAST under a relaxed lognormal molecular clock using the fastest reported arachnid substitution rate of 0.0135, which corresponds to a COI divergence rate of 2.7% per million years, and the fastest arthropod rate of 17.212%, which corresponds to a substitution rate of 0.08606. We performed the divergence analyses only on the COI region and removed all end gaps before the analysis. We also removed sequences we thought to be nuclear mitochondrial DNA segments (numts). We did not partition the data by codon position because our substitution rate is the average rate across the gene. We used jModelTest 2.1.10 (Darriba et al. 2012, Guindon & Gascuel 2003) on the CIPRES portal v.3.3. to find the best substitution model for our single-partition dataset. One of the best models was an HKY model (Hasegawa 1985), which we incorporated into BEAST using the kappa and proportion invariant sites parameters from jModelTest. We set a Yule model of species birth for the analysis. We set the MCMC chain length to 40,000,000 and sampled every 5,000th tree, resulting in 8,000 trees. We conducted each analysis twice with random starting seeds and used Tracer v1.6 (Rambaut et al. 2014) to confirm convergence of the chains and adequate effective sample sizes of the parameters. For each rate, we used LogCombiner to combine the trees recorded during the two runs and compiled those trees into one tree using TreeAnnotator (Bouckaert et al. 2014).

RESULTS

We encountered what appear to be nuclear copies of COI in several specimens. We identified these pseudogenes by examining the translated sequences and looking for stop codons introduced by insertions or deletions. In the case of the Huachuca specimens, we created a new reverse primer to exclude insertions that caused the frame shift. Unfortunately, we were unable to recover a functional sequence of COI (no stop codons) for the Huachuca specimens or from from *G. nigrescens*.

Phylogenetic Inference

Globocreagris nigrescens consistently nested within the Sky Island clade in our phylogeny (Figure 2). The main diagnostic features of *Globocreagris* are enlarged, globular, sclerotic lateral genital sacs in the male, which also lacks paired dorsal sacs; a pair of glandular setae (also called discal setae) displaced to the middle of the sternite on segments VI-VII (Figure 5); 4-6 setae on the manducatory process; and robust appendages (Muchmore 1994). Surprisingly, we did not find *Globocreagris* in the more northerly mountains along the Mogollon Rim. Instead, we found a different clade of Neobisiidae. These possess lateral genital sacs in the male that are not heavily sclerotized and are small and narrow (Figure 3). Although they are not *Globocreagris*, they form a monophyletic lineage sister to *Globocreagris.*

We also examined slide-mounted pseudoscorpions from California, Oregon, and Washington (Table S1). We found many that share the morphological characteristics of *Globocreagris*, especially the lateral genital sacs of the male, so we here expand the known range of *Globocreagris* from only California to include Oregon, Washington, and Arizona (Figure 4).

Divergence Dating

When observed in Tracer v1.6 (Rambaut et al. 2014), all BEAST runs had effective sample sizes well above 500 and the two runs under each rate converged. The divergence analyses in BEAST resulted in a monophyletic clade of Sky Island *Globocreagris*. Under the fastest COI rate known for arachnids, the most recent common ancestor of these species occurred between 7.5–10 million years ago (Figure 5), which is before the beginning of the Pleistocene, 2.6 million years ago. Individual lineages were no younger than 4 million years old. Under the fastest COI rate known for any arthropod, the most recent common ancestor of the Sky Island *Globocreagris* occurred between 1.15-1.6 million years ago, which is during the Pleistocene glacial cycles.

DISCUSSION

Due to the presence of pseudogenes in our phylogeny (*G. nigrescens* and specimens from the Huachuca Mountains), we are unable to draw definite conclusions about relationships of these species to other species within *Globocreagris*. However, the similarity of these pseudogenes to other species in the Arizona sky islands, in conjunction with the male lateral genital sac morphology, leads us to conclude that the newly discovered sky island pseudoscorpions belong to the genus *Globocreagris*. The southern

Arizonan Sky Islands harbor a new complex of *Globocreagris* species, but it is unclear whether the Arizona specimens represent a single monophyletic lineage, owing to the uncertainty surrounding the placement of the California specimen (Figure 2) and the lack of samples from the Sky Islands of northern Sonora, Mexico. However, the strong support values for each clade from different mountain ranges lead us to conclude that each mountain range contains its own distinct species. We base this determination on the phylogenetic species concept (Mishler & Brandon 1987). Furthermore, several of these species are supported by another phylogenetic species concept (Wheeler & Platnick 2000) on the basis of the molecular apomorphies outlined in the diagnosis section of each new species below.

We were surprised to see a connection between the Sky Island neobisiids and the species from California because of the large distance between these two areas, but a recent study on harvestmen (*Siltacina sura* species group) has shown a similar pattern of relationships (DiDomenico & Hedin 2016). Both the harvestmen and pseudoscorpions are unable to cross the Sonoran Desert between the Arizona Sky Islands and southern California. Unlike the Sky Island *Globocreagris* species, these harvestmen are found at much lower elevations (DiDomenico & Hedin 2016). *Globocreagris* species in Arizona typically inhabit high-elevation mixed conifer forests. However, *G. nigrescens* is known from packrat middens in Francis Simes Hastings Natural History Reservation near Monterey, California (Chamberlin 1952). This reserve has some oak woodland habitat, a few pines, grasslands, chaparral, and riparian habitats (Griffin 1990); there is no mixed conifer habitat similar to what is found in the Arizona Sky Islands. Additionally, other non-*Globocreagirs* neobisiids from Arizona are found at low elevations, such as the one from Sabino Canyon in the Santa Catalina Mountains. Despite the low elevations of these localities, both include a riparian habitat. It may be that high-humidity habitats are more important to these neobisiids than particularly high elevation. Future studies using habitat niche modeling may assist in determining why *Globocreagris* appears to inhabit such dramatically different elevations and provide guidance on finding other members of this genus.

We used BEAST to explore the divergence dates of the sky island *Globocreagris* under two rates of molecular evolution. We predicted that if a fast rate of molecular evolution indicated that the new species diverged from one another before the start of the Pleistocene, roughly 2.6 million years ago, then their divergence was not influenced by Pleistocene glacial cycles. We used ~~t~~two rates: one that was the fastest mitochondrial rate we could find for arthropods (0.08606 substitutions/site/million years, Pons et al. 2010), and one that was the fastest rate for arachnids (0.0135 substitutions/site/million years, Gantenbein & Largiadèr 2003). We found that the fastest arthropod rate resulted in species diverging within the Pleistocene while the fastest arachnid rate resulted in all species diverging before the Pleistocene. Which rate more accurately represents pseudoscorpion evolution? Pseudoscorpions have been reported to have amino acid divergence between 3-6 times greater than scorpions (Young & Hebert 2015), though this doesn't necessarily translate to faster rates of evolution at the species level. Additionally, the fast rate for beetles is unusually high, even for beetles (Andújar et al. 2012). Given that the fastest arachnid rate is more in line with other reported rates (Figure 6), we believe it is not unlikely that Sky Island *Globocreagris* species diverged before the Pleistocene, similar to *Vaejovis* scorpions (Bryson et al. 2013), and that their speciation was not influenced by

Pleistocene glaciation cycles. However, a properly calibrated molecular clock analysis needs to be conducted before this conclusion can be accepted.

TAXONOMIC TREATMENT

Measurements

Measurements are given in mm for all specimens. Numbers separated by slashes represent the length followed by the width, following Chamberlin 1952. Terminology is adopted from Harvey (1992). Chela total length includes the pedicel while the chela hand length does not.

Abbreviations

USA = United States of America
CAS = California Academy of Sciences
EMEC = University of California, Berkeley, Essig Museum of Entomology Collection
BMEC = University of California, Davis, Bohart Museum of Entomology Collection
UAIC = University of Arizona Insect Collection
Co. = county
M = male
F = female
T = tritonymph
D = deutonymph
P = protonymph
N = nymph

Globocreagris huachucaensis, sp. nov.

Figures 3A, 7, 8G, 9B

Material examined

Types: holotype male, U.S.A.: ARIZONA: Cochise County, Coronado National Forest, Huachuca Mountains, Carr Peak, under natural debris in aspen stand, 12 October 2014, 2799 m elevation, N 31.41305°, W 110.30579°, G.B. Hughes & A.D. Yanahan (UAIC 1113087). 2 paratype M, and 8 paratype F collected with holotype (UAIC 1113038-1113042, UAIC 1113088-1113092).

Etymology

This species is named after its type locality of the Huachuca Mountains in southeastern Arizona.

Diagnosis

Because we only recovered pseudogenes from this species, we do not know which of the sequence differences would be found in the actual COI sequence and which are unique to the pseudogenes. However, we report the differences here for comparison and hope that future work will provide diagnostic molecular characters for this species.

G. huachucaensis specimens exclusively share the following nucleotides at the listed positions in the COI alignment: A at position 5, T at position 49, T at 50, G at 54, A at 57, C at 79, A at 86, T at 98, A at 107, A at 136, A at 182, T at 220, C at 226, A at 266, G at 287, A at 314, T at 337, T at 349, C at 353, G at 370, C at 442, G at 467, C at 470, T at 472, G at 481, G at 493, A at 532, A at 595, G at 602, A at 620, T at 621, and A at 625. They also have insertions in the following positions: 62-64, 164-175, 194-199, 540-441, 560-562, 578-580, and 596-598. There is a single deletion at 130 and a deletion at 203-208. In the 28S alignment, this species exclusively has a G at position 239, T at 611, A at 612, T at 613, and C at 665.

Description

Chelicera: Chelicera with 7 setae on hand and 1 subdistal seta on movable finger. Galea is double bifid (one major fork with each branch forking separately for a total of 4 terminals). Rallum composed of 7-8 blades; the basal-most blade less than half the length of the others and not pinnate while other blades are pinnate. Serrulae of normal shape for Neobisiidae, with squared tips on serrula exterior and tooth-like tips on at least the distal half of serrula interior.

Pedipalps: Pedipalps dark red with only extremely minute granules visible over all surfaces at high magnification. Manducatory process with 4-5 setae. Fingers approximately 50% longer than hand. Nodus ramosus terminates less than the vendens' length from the base of the venom tooth. On movable finger, *b* and *sb* in basal third, *st* and *t* in distal half. Distance between *b-sb* and *st-t* approximately the same, distance between *sb-st* much larger.

Cephalothorax: Cephalothorax brownish-red. Carapace with 24-28 setae. Eyes well-developed and reflect light in uncleared specimens. Epistome well-developed.

Legs: Pale creamy yellow to grey. Femur-patella suture of Leg IV perpendicular to axis of the combined segment; patella roughly 15-20% longer than femur. Subterminal tarsal setae bifid and dentate. Arolium undivided and shorter than tarsal claws.

Abdomen: Sclerites dark grey, pleural membrane pale grey. Tergites uniseriate. Sternites biseriate on VI-VII, though glandular setae displaced slightly anteriad on VIII-X.

Genitalia: Anterior genital operculum (sternite II) of male with a dense cluster of 22-29 setae. Posterior genital operculum (sternite III) has 8-15 intermediary setae roughly divided into two groups on either side of the midline, in addition to a posterior row of setae. Internally, there are 3 setae on either side of the midline in the genital atrium formed by segment II. Lateral genital sacs are large, sclerotic, and globose. Median genital sac short, barley reaching sternite V.

Anterior genital operculum (sternite II) of female with two paired rows or clusters of setae consisting of 2-7 setae each. The internal female genitalia are not visible in the specimens available.

Male—Measurements given for holotype male, followed by paratype male in parentheses. Body length 2.85 (3.27). Carapace 0.84/0.74 (0.94/0.78); carapace ocular breadth 0.73 (0.82). Chelicera 0.46/0.28 (0.55/0.32); cheliceral movable finger 0.26 (0.44). Pedipalp: trochanter 0.5/0.29 (0.59/0.3); femur 0.98/0.26 (1.16/0.3); patella 0.83/0.35 (0.92/0.38); chela 1.57/0.46 (1.81/0.52); chela depth 0.45 (0.52); chela hand

0.71 (0.81); movable finger 0.82 (0.99). Leg I: femur 0.41/0.10 (0.50/0.12); patella 0.3/0.11 (0.35/0.14); tibia 0.45/0.09 (0.51/0.12); metatarsus 0.23/0.07 (0.24/0.08); tarsus 0.33/0.06 (0.35/0.09). Leg IV: femur 0.42/0.23 (0.45/0.28); patella 0.44/0.23 (0.54/0.28); tibia 0.76/0.90 (0.86/0.14); metatarsus 0.26/0.08 (0.29/0.11); tarsus 0.43/0.10 (0.46/0.09). Female—Measurements given for 3617 with ranges given in parentheses for all paratype females. Body length 3.15 (2.66-3.15). Carapace 0.90/0.81 (0.9-1.03/0.69-0.91); ocular breadth 0.78 (0.70-0.86). Chelicera 0.47/0.31 (0.46-0.54/0.26-0.35); cheliceral movable finger 0.43 (0.37-0.46). Pedipalp: trochanter 0.56/0.29 (0.45-0.63/0.23-0.31); femur 1.06/0.28 (0.92-1.19/0.22-0.30); patella 0.88/0.39 (0.73-0.98/0.32-0.42); chela 1.72/0.52 (1.43-1.83/0.41-0.56); chela depth 0.49 (0.39-0.56); chela hand 0.74 (0.6-0.84); movable finger 0.96 (0.81-0.98). Leg I: femur 0.44/0.12 (0.37-0.51/0.11/0.14); patella 0.31/0.14 (0.18-0.36/0.11-0.15); tibia 0.43/0.09 (0.39-0.52/0.09-0.11); metatarsus 0.20/0.09 (0.19-0.31/0.07-0.10); tarsus 0.34/0.08 (0.31-0.35/0.07-0.08). Leg IV: femur 0.42/0.24 (0.32-0.47/0.21/0.28); patella 0.50/0.24 (0.44-0.56/0.21-0.28); tibia 0.81/0.13 (0.64-0.88/0.1-0.15); metatarsus 0.28/0.1 (0.19-0.31/0.09-0.12); tarsus 0.44/0.09 (0.36-0.48/0.09-0.11).

Globocreagris pinalenoensis, sp. nov.
Figures 1, 8F, 9C
Material examined
Types: holotype M, U.S.A.: ARIZONA: Graham County, Coronado National Forest, Pinaleño Mountains, Mount Graham, Cunningnham Loop Trail #316, 13-14 September 2014, 2700 m elevation, N 32.68011°, W 109.891162°, G.B. Hughes, A.D. Yanahan, & A.M. Hoover (UAIC 1113032). 1 paratype F collected with male (UAIC 1113033). 4 paratype F collected with same data except collected from Grant Hill Loop trail, N 32.66823°, W 109.88026°, 2764 m elevation (UAIC 1113034-1113037). 1 paratype F, U.S.A.: ARIZONA: Graham County, Pinaleño Mountains, N 32°41.546", W 109°53.988", 2743 m elevation, 10 October 21012, J. Ebel (UAIC 1113004). 1 paratype F, U.S.A.: ARIZONA: Graham County, Pinaleño Mountains, Grant Hill Loop Trail trailhead, sifted from soil about 0-1 inch under the ground, ground covered in pine needles with lots of decaying logs, 20-Aug-2011, G.B. Hughes (UAIC 1113009).

Etymology
This species is named after its type locality of the Pinaleño Mountains in southeastern Arizona.

Diagnosis
G. pinalenoensis specimens exclusively share the following nucleotides at the listed positions in the COI alignment: A at position 83, and C at 279.

Description
Chelicera: Cheliceral hand with 7 setae, movable finger with 1. Galea double bifid (one major fork with each branch forking separately for a total of 4 terminals). Rallum composed of 10 baldes in male, all blades at least partially pinnate, the basal-most 2 about 2/3 the height of the other blades. Other specimens have 7-10 blades. When fewer blades are present, basal-most blade tends to lack pinnations. Serrulae of normal shape

for Neobisiidae, with squared tips on serrula exterior and tooth-like tips on at least the distal half of serrula interior.

Pedipalps: Pedipalps dark red with only extremely minute granules visible over all surfaces at high magnification. Manducatory process with 3-5 setae. Fingers no more than 25% longer than hand. Nodus ramosus terminates less than the vendens' length from the base of the venom tooth. On movable finger, *t* is about 3/4 from base of finger. Trichobothria *t* is about half a trichobothrial pit's length closer to *st* than *b* is from *sb*. Distance between *st* and *sb* is about one and a half trichobothrial pit's length more separated than *b* and *sb*. On fixed finger, *eb* occurs where finger meets hand. Trichobothria *eb*, *ib*, *isb*, and *ist*, are in basal 1/4 of fixed finger. Trichobothria *est* is just in the 3rd quarter of the fixed finger from the base. Trichobothria *it* and *et* are in the distalmost quarter of the fixed finger.

Cephalothorax: Cephalothorax brownish-red. Carapace with 25 setae. Eyes are well-developed and reflect light in uncleared specimens. Epistome angular and well-developed.

Legs: Pale creamy yellow to grey. Suture between Femur IV and Patella IV roughly perpendicular to the axis of the combined segment, the patella roughly 13-20% longer than femur. Subterminal tarsal setae bifd and dentate. Arolium undivided and shorter than tarsal claws.

Abdomen: Sclerites dark grey, pleural membranes pale grey. Tergites uniseriate. Glandular setae anteriorly displaced on VI-X, but most prominently on VI-VII.

Genitalia: Anterior genital operculum (sternite II) of male with 33 setae. Posterior genital operculum (sternite III) with 12 intermediarey setae in addition to the posterior row of setae. Internally, there are 3 setae on either side of the midline in the genital atrium formed by segment II. Lateral genital sacs are large, sclerotic, and globose. Median genital sac not visible. Anterior genital operculum of female with a row of 3 setae (occasionally 4, the fourth not always in line), parallel with the margin of the segment, on either side of the midline. Internal genitalia of the female were not observed in the specimens available.

Measurements

Male—Measurements for holotype male. Body length 3.59. Carapace 1.04/0.96; ocular breadth 0.85. Chelicera 0.55/0.31; movable finger 0.44. Pedipalp: trochanter 0.57/0.33; femur 1.16/0.33; patella 0.96/0.45; chela 1.72/0.61; chela depth 0.60; chela hand 0.84; movable finger 0.93. Leg I: femur 0.44/0.15; patella 0.35/0.14; tibia 0.53/0.10; metatarsus 0.23/0.08; tarsus 0.35/0.06. Leg IV: femur 0.44/0.26; patella 0.56/0.26; tibia 0.93/0.15; metatarsus 0.29/0.10; tarsus 0.45/0.08.

Female—Measurements given for paratype female from the same locality as the paratype male [3137] followed by the range of paratype female measurements in parentheses. Body length 4.18 (2.44-4.18). Carapace 1.04 (0.96-1.07); ocular breadth 0.91 (0,81-0.91). Chelicera 0.57/0.34 (0.54-0.59/0.32-0.36); movable finger 0.47 (0.43-0.47). Pedipalp: trochanter 0.61/0.33 (0.58-0.66/0.3-0.33); femur 1.15/0.35 (1.12-1.22/0.30-0.35); patella 0.96/0.46 (0.92-1.04/0.39-0.46); chela 1.77/0.65 (1.77-1.96/0.56-0.65); chela depth 0.66 (0.53-0.66); chela hand 0.81 (0.78-0.83); movable finger 0.96 (0.96-1.08). Leg I: femur 0.47/0.14 (0.47-0.57/0.13-0.14); patella 0.31/0.15 (0.31-0.35/0.13-0.14); tibia 0.52/0.11 (0.52-0.56/0.1-0.11); metatarsus 0.2/0.09 (0.2-0.22/0.07-0.1); tarsus 0.37/0.09 (0.35-

0.37/0.08-0.09). Leg IV: femur 0.49/0.28 (0.4-0.52/0.27-0.29); patella 0.58/0.28 (0.56-0.59/0.27-0.29); tibia 0.95/0.15 (0.93-1.01/0.14-0.16); metatarsus 0.29/0.11 (0.28-0.32/0.09-0.12); tarsus 0.47/0.11 (0.46-0.52/0.09-0.11).

Globocreagris chiricahuaensis, sp. nov.
Figures 8A, 9A
Material examined
Types: holotype M, U.S.A.: ARIZONA: Cochise County, Chiricahua Mountains, Coronado National Forest, Fly's Peak, 2957 m elevation, N 31.87302°, W 109.28364°, sifted from dirt in sides of pits left in soil from rolling large rocks, 1 July 2015, G.B. Hughes & A.D. Yanahan (UAIC 1113068).
Other material: 3 T collected with the holotype (UAIC 113050, UAIC 1113051, UAIC 1113052).

Etymology
This species is named after its type locality of the Chiricahua Mountains in southeastern Arizona.

Diagnosis
G. chiricahuaensis specimens exclusively share the following nucleotides at the listed positions in the COI alignment: A at position 256 and C at position 460. In the 28S alignment, this species exclusively has a G at 146.

Description
Chelicera: Cheliceral hand with 7 setae, movable finger with 1 subdistal seta. Galea double bifid.
Rallum: Composed of 7 blades, the basal-most blade less than half as long as the others. The other 6 blades have comb-like bristles on the anterior edge of the blades. The distal-most blade has a wider base and is slightly separated from the other blades as is typical for neobisiids.
Serrulae of normal shape for Neobisiidae, with squared tips on serrula exterior and tooth-like tips on at least the distal half of serrula interior.

Pedipalps: Pedipalps orange-red with only extremely minute granules visible over all surfaces at high magnification. Manducatory process with 4 setae. Fingers about 15% longer than hand. Nodus ramosus terminates less than the vendens' length from the base of the venom tooth. On movable finger, *t* is about 3/4 from base of finger. Trichobothria *t* is about half a trichobothrial pit's length closer to *st* than *b* is from *sb*. Distance between *st* and *sb* is about one and a half trichobothrial pit's length more separated than *b* and *sb*. On fixed finger, *eb* and *esb* are on distal part of chela hand. Trichobothria *ib*, *isb*, and *ist*, are in basal 1/4 of fixed finger. Trichobothria *est* is just in the 3rd quarter of the fixed finger from the base. Trichobothria *it* and *et* are in the distalmost quarter of the fixed finger.

Cephalothorax: Cephalothorax orange-red. Carapace with 25 setae. Eyes are well-developed and reflect light in uncleared specimens. Epistome angular and well-developed.

Legs: Legs pale yellow-grey. Suture between Femur IV and patella IV roughly perpendicular to the axis of the combined segment, the patella roughly 25%longer than femur. Subterminal tarsal setae bifid, with terminal branches dentate. Arolia undivided, shorter than tarsal claws.

Abdomen: Sclerites grey, pleural membranes pale grey. Tergites uniseriate. Glandular setae displaced slightly anteriad on V, VIII, and IX; prominently anteriad on VI and VII.

Genitalia: Anterior genital operculum (sternite II) of male with 37 setae, posterior genital operculum (sternite III) with 7 anterior and 4 intermediate setae in addition to the posterior row of setae. Internally, there are 3 setae on either side of the midline in the genital atrium formed by segment II. Lateral genital sacs are large, sclerotic, and globose. Adult female unknown.

Measurements

Male—Measurements given for holotype male. Body length 2.76. Carapace 0.9/0.74; ocular breadth 0.75. Chelicera 0.47/0.29; movable finger 0.37. Pedipalp: trochanter 0.51/0.26; femur 0.98/0.29; patella 0.77/0.35; chela length 1.56; chela depth 0.39; chela hand 0.68; movable finger 1.08. Leg I: femur 0.43/0.13; patella 0.3/0.14; tibia 0.43/0.09; metatarsus 0.19/0.1; tarsus 0.31/0.08. Leg IV: femur 0.4/0.22; patella 0.5/0.22; tibia 0.79/0.14; metatarsus 0.24/0.1; tarsus 0.41/0.09.

The holotype appears lightly sclerotized, similar to tritonymphs of most neobisiids. The holotype has no chela width reported because the sides of the chela have collapsed inward, leading us to believe that the holotype may have been a teneral adult.

Globocreagris santaritaensis, sp. nov.

Figures 8E, 9D

Material examined

Types: holotype M, U.S.A.: ARIZONA: Santa Cruz County, Coronado National Forest, Santa Rita Mountains, Bellous Springs, 5 September 2011, 2500 m elevation, J. Ebel (UAIC 1113003). Paratype F, U.S.A.: ARIZONA: Pima County, Santa Rita Experimental Range, Santa Rita Mountains, 17 January 2015, J. Cowels (UAIC 1113047).

Other material: 7 T, U.S.A.: ARIZONA: Santa Cruz Co., Santa Rita Mountains, Coronado National Forest, Mt. Wrightson, below summit, under rocks in shade of pine/oak, 2816 m elevation, N 31.69565°, W 110.84715°, 8 July 2015, G.B. Hughes & A.D. Yanahan (UAIC 1113103-1113109. 10 T, U.S.A. ARIZONA: Santa Cruz County, Santa Rita Mountains, Mt. Hopkins, under rocks by observatory lodging and picnic area, 2539 m, N 31.69059°, W 110. 88.455°, 13 July 2015, G.B. Hughes & A.D. Yanahan (UAIC 1113093-1113102).

Etymology

This species is named after its type locality of the Santa Rita Mountains in southeastern Arizona.

Diagnosis

G. santaritaensis specimens exclusively share the following nucleotides in the 28S alignment: A at position 139, A at position 146, and A at 151. They also have a single base insertion at position 149 of the 28S alignment.

Description

Chelicera: Chelicera with 7 setae present on dorsum of hand and 1 seta present on movable finger. Galea double bifid (one major fork with each branch forking separately for a total of 4 terminals). Rallum composed of 8 blades, the basal-most blade bare and less than half as long as the others; the other 7 blades with comb-like bristles on the anterior edge of the blades; the distal-most blade with a wider base and is slightly separated from the other blades as is typical for neobisiids. Serrulae of normal shape for Neobisiidae, with squared tips on serrula exterior and tooth-like tips on at least the distal half of serrula interior.

Pedipalps: Pedipalps dark red with only extremely minute granules visible over all surfaces at high magnification. Manducatory process with 4-5 setae. Fingers roughly twice as long as the hand in males and roughly 25% longer than the hand in females. Nodus ramosus terminates less than the vendens' length from the base of the venom tooth. On the movable finger of the male, trichobothria *b* and *sb* are closer to one another than are *st* and *t*. The gap between *sb* and *st* is about equal to the sum of the distance of *b-sb* and *st-t*. In the female, the distances between *b-sb* and *st-t* are about the same. As with the male, there is a large gap between the basal and terminal setae. On fixed finger, *eb* and *esb* are located where the finger meets the hand. Trichobothria *ib*, *isb*, and *ist*, are in basal third of fixed finger. Trichobothria *est*, *et*, and *it* are in the distal third of the finger.

Cephalothorax: Carapace brownish-red. Carapace with 24-27 setae. Eyes are well-developed and reflect light in uncleared specimens. Epistome angular and prominent.

Legs: Legs pale cream-grey. Suture between femur IV and patella IV roughly perpendicular to the axis of the combined segment, the patella roughly 15-22% longer than femur. Subterminal tarsal setae bifid and dentate. Arolia undivided and shorter than tarsal claws.

Abdomen: Abdominal sclerites dark grey; membranes grey. Tergites uniseriate. In the female, uniseriate except in segments VI-X in which two glandular setae are displaced anteriad. In the male, only segments VI-VII biseriate, though VIII-X have glandular setae slightly out of line with the posterior row of setae. Sternite IV of male with anterior cleft.

Genitalia: Anterior genital operculum (sternite II) of male with 11 setae. Posterior genital operculum (sternite III) with 7 intermediate setae in addition to the posterior row of setae. Lateral genital sacs large, sclerotic, and globose. Median genital sac reaching to midpoint of sternite VI. Two groups of 2 setae found internally.Anterior genital operculum (sternite II) of female with two groups of 3 setae on either side of the midline. Internal genitalia not visible in specimens available.

Measurements

Measurements are given for the holotype male followed by the paratype female in parentheses. Body length 3.33 (5.25). Carapace 1.04/0.92 (1.48/1.07); ocular breadth 0.90 (1.08). Chelicera 0.58/0.33 (0.70/0.41); movable finger 0.44 (0.58). Pedipalp: trochanter

0.63/0.33 (0.81/0.39); femur 1.26/0.31 (1.54/0.40); patella 1.0/0.41(1.31/0.54); chela 2.06/0.54 (2.30/0.78); chela depth 0.41 (0.78); chela hand 0.87 (1.07); movable finger 1.13 (1.13). Leg I: femur 0.54/0.13 (0.69/0.16); patella 0.39/0.15 (0.47/0.18); tibia 0.60/0.10 (0.74/0.12); metatarsus 0.25/0.0.9 (0.28/ 0.10); tarsus 0.41/0.07 (0.48/0.09). Leg IV: femur 0.52/0.26 (0.62/0.31); patella 0.60/0.26 (0.76/0.31); tibia 1.04/0.15 (1.32/0.15); metatarsus 0.32/0.10 (0.39/0.11); tarsus 0.53/0.09 (0.59/0.11).

Globocreagris santacatalinaensis, sp. nov.
Figures 8B, 9F
Material examined
Types: holotype M, U.S.A.: ARIZONA: Pima County, Coronado National Forest, Santa Catalina Mountains, Mt. Lemmon, Sunset Trailhead, pine litter at base of tree, 2369 m, N32°25'36.9", W110°44'29.6", 28 September 2012, G.B. Hughes (UAIC 1113002). Paratype F collected with holotype male (UAIC 1113062).
Other material: 3 T collected with holotype and paratype (UAIC 1113059-1113061). 1 tritonymph, U.S.A.: ARIZONA: Pima County, Coronado National Forest, Santa Catalina Mountains, Marshall Gulch Trail, N32°25'40.4", W110°45'20.1", 4 August 2012, coll. G.B. Hughes (UAIC 1113000). 1 T, U.S.A.: ARIZONA: Pima County, Coronado National Forest, Santa Catalina Mts., Mt. Lemmon, Bigelow Rd., N32.41767°, W110.72416°, 1 August 2014, G.B. Hughes (UAIC 1113063).

Etymology
This species is named after its type locality of the Santa Catalina Mountains in southeastern Arizona.

Diagnosis
G. santacatalinaensis specimens exclusively share the following nucleotides at the listed positions in the COI alignment: A at position 94 and G at position350.

Description
Chelicera: Chelicera with 7 setae present on dorsum of hand and 1 seta present on movable finger. Galea double bifid (one major fork with each branch forking separately for a total of 4 terminals). Rallum composed of 7 blades, basal-most blade lacks a comb of spines and is less than half the length of most other blades. The other 6 blades have a pectinate comb on the anterior margin. The distal-most blade has a wider base and is slightly separated from the other blades as is typical for neobisiids. Serrulae of normal shape for Neobisiidae, with squared tips on serrula exterior and tooth-like tips on at least the distal half of serrula interior.

Pedipalps: Pedipalps dark red to orange brown. Pedipalps virtually smooth with minute, nearly imperceptible granules. Manducatory process with 4-5 setae (4 in the holotype male and 5 in the paratype female). Fingers in the male are about 1.5 times as long as the hand, while in the female the fingers are only slightly longer than the hand. Nodus ramosus terminates less than the vendens' length from the base of the venom tooth. On movable finger, *t* is about 3/4 from base of finger. Trichobothria *t* is about half a trichobothrial pit's length closer to *st* than *b* is from *sb*. Distance between *st* and *sb* is about one and a half trichobothrial pit's length more separated than *b* and *sb*. On fixed

finger, *eb* and *esb* are on basal-most part of finger. Trichobothria *ib*, *isb*, and *ist*, are in basal third of fixed finger. Trichobothria *it*, *et*, and *est* are in the distal third of the fixed finger.

Cephalothorax: Cephalothroax reddish brown to orange-brown. Carapace with 25 setae. Eyes are well-developed and reflect light in uncleared specimens. Epistome acutely pointed.

Legs: Legs pale yellowish-grey. Suture between Femur IV and Patella IV roughly perpendicular to the axis of the combined segment, the patella roughly 25% longer than femur.

Subterminal seta structure: Subterminal tarsal setae bifid, with terminal branches dentate.

Arolia relative size and whether complete or divided: Arolim undivided and shorter than tarsal claws.

Abdomen: Abdomen grey. Tergites more or less uniseriate. Sternites subtly biseriate on segments VIII-X and strongly biseriate on VI-VII.

Genitalia: Anterior genital operculum (sternite II) of male with 26 setae; posterior genital operculum (sternite III) with 10 intermediate setae in addition to the posterior row of setae. The lateral genital sacs are large, sclerotic, and globose. The median genital sac is not visible. There are two groups of 3 setae internally. Anterior genital operculum (sternite II) of female with 2 setae on the right of the midline and 3 setae on the left. The internal genitalia of the female are not visible in the paratype.

Measurements

Measurements are given for the holotype male followed by the paratype female in parentheses. Body length 2.38 (2.74). Carapace 0.88/0.70 (0.98/0.88); ocular breadth 0.72 (0.85). Chelicera 0.51/0.26 (0.57/0.32); movable finger 0.39 (0.43). Pedipalp: trochanter 0.53/0.26 (0.60/0.31); femur 1.02/0.27 (1.08/0.31); patella 0.86/0.35 (0.94/0.41); chela 1.65/0.46 (1.78/0.57); chela depth 0.44 (0.58); chela hand 0.60 (0.84); movable finger 0.89 (0.96). Leg I: 0.44/0.13 (0.43/0.14); patella 0.35/0.13 (0.37/0.15); tibia 0.49/0.09 (0.56/0.12); metatarsus 0.21/0.07 (0.20/0.09); tarsus 0.33/0.06 (0.35/0.08). Leg IV: femur 0.38/0.24 (0.45/0.28); patella 0.48/0.24 (0.56/0.28); tibia 0.81/0.14 (0.92/0.15); metatarsus 0.29/0.09 (0.30/0.11); tarsus 0.42/0.09 (0.46/0.10).

Globocreagris rinconensis, sp. nov.

Figures 8C, 9E

Material examined

Types: holotype M, U.S.A.: ARIZONA: Saguaro National Park, Rincon Mts., North Slope Trail, pit fall traps, 2464.3 m elevation, N 32.22313°, W 110.55060°, 28 Aug-20 Sep 2011, J. Eble (UAIC 1113064). 1 paratype F collected from the same pitfall transect as holotype male, 2458.5 m elevation, N 32.22096°, W 110.55421° (UAIC 1113065). *Other material*: 1 T collected with paratype female (1113066). 1 T, U.S.A.: ARIZONA: Saguaro National Park, Rincon Mountains, vicinity of Manning Camp, on steep slope with deep litter, 28 August 2011, coll. G.B. Hughes (UAIC 1113001).

Etymology

This species is named after its type locality of the Rincon mountains in southeastern Arizona.

Diagnosis

G. rinconensis specimens exclusively share the following nucleotides at the listed positions in the COI alignment: G at position 40, G at position 241, and G at 556. In the 28S alignment, this species exclusively has an A at 327 and a T at 647.

Description

Chelicera: Chelicera with 7 setae present on dorsum of cheliceral hand and 1 seta present on movable finger. Galea double bifid (one major fork with each branch forking separately for a total of 4 terminals). Rallum composed of 8 blades, basal-most blade lacks a comb of spines and is less than half the length of most other blades. The next blade is slightly taller but does have spines on the anterior edge, as do the other 6 blades. The distal-most blade has a wider base and is slightly separated from the other blades as is typical for neobisiids. Serrulae of normal shape for Neobisiidae, with squared tips on serrula exterior and tooth-like tips on at least the distal half of serrula interior.

Pedipalps: Pedipalps dark red. Pedipalp articles with granulations over the entire articles but very low so as to be almost imperceptible. Manducatory process with 3-5 setae. Fingers about 25% longer than the chela hand. Nodus ramosus terminates almost immediately. On movable finger, trichobothria *b* and *sb* are in the basal quarter of the finger while *st* and *t* are in the distal half. The distance between *b* and *sb* is approximately 4-5 trichobothrial pits and is the same distance between *st* and *t*. There is a great distance between the pairs *b*-*sb* and *st*-*t*. On the fixed finger, *eb* and *esb* are placed where the finger meets the hand, while *ib*, *isb*, and *ist* are on the basal quarter of the finger. Trichobothria *est*, *et*, and *it* are in the distal third of the fixed finger.

Cephalothorax: Cephalothorax brownish-red. Carapace with 26 setae. Eyes well-developed and reflect light in uncleared specimens. Epistome angular and well-developed.

Legs: Legs pale grey. Suture between Femur IV and Patella IV roughly perpendicular to the axis of the combined segment, the patella roughly 20% longer than femur. Subterminal tarsal setae bifid, with terminal branches dentate. Arolia undivided and shorter than tarsal claws.

Abdomen: Abdominal sclerites dark grey, membranes pale grey. Abdominal tergites more or less uniseriate, with some setae placed slightly anteriad to others. Sternites VI and VII have 2 setae displaced anteriad of the posterior row. Sternites V and VIII-X have the same setae only slightly moved forward, but not such that they appear to be in a different row.

Genitalia: Anterior genital operculum (sternite II) of the male with 36 setae. Posterior genital operculum (sternite III) with 14 intermediary setae in addition to the posterior row. The lateral genital sacs are large, sclerotic, and globose. The median genital sac almost reaches the posterior margin of the fourth sternite. There are two groups of 4 setae internally. The anterior genital operculum (sternite II) of the female with two groups of three setae, each group straddling the midline. The internal genitalia of the female are not visible in the paratype.

Measurements

Measurements are given for the holotype male followed by the paratype female in parentheses. Body length 3.04 (3.17). Carapace 1.00/0.83 (1.07/0.91); ocular breadth 0.85 (0.86). Chelicera 0.59.0.33 (0.59/0.31); movable finger 0.45 (0.48). Pedipalp; trochanter 0.63/0.31 (0.63/0.31); femur 1.18/0.30 (1.18/0.31); patella 1.01/0.41 (1.00/0.42); chela 1.89/0.55 (1.86/0.60); chela depth 0.52 (0.56); chela hand 0.81 (0.78); movable finger 1.00 (1.00). Leg I: femur 0.57/0.14 (0.49/0.13); patella 0.40/0.15 (0.37/0.14); tibia 0.57/0.11 (0.56/0.11); metatarsus 0.23/0.08 (0.24/0.09); tarsus 0.40/0.08 (0.40/0.90). Leg IV: femur 0.50/0.28 (0.48/0.27); patella 0.60/0.28 (0.58/0.27); tibia 0.94/0.15 (0.98/0.14); metatarsus 0.31/0.10 (0.32/0.11); tarsus 0.51/0.10 (0.49/0.09).

Globocreagris pinalensis, sp. nov.
Figures 8D, 9G
Material examined
Types: holotype F, U.S.A.: ARIZONA: Gila Co., Tonto National Forest, Pinal Mountains, Upper Pinal Campground, under rocks beneath aspens and pines, N 33.28372°, W 110.82298°, 2353 m elevation, 28-29 May 2013, G.B. Hughes & A.D. Yanahan (UAIC 1113054). 4 paratype F collected with the holotype (UAIC 1113053, UAIC 1113055-1113057).
Other material: 1 tritonymph collected with holotype.

Etymology
This species was named after the type locality of the Pinal mountains in southeastern Arizona.

Diagnosis
G. pinalensis specimens exclusively share the following nucleotides at the listed positions in the COI alignment: G at position 154, G at 178, T at 259, T at 370, and T at 514.

Description

Chelicera: Chelicera with 7 setae present on dorsum of cheliceral hand and1 seta present on movable finger. Galea double bifid, with 1 major fork and each branch containing another smaller fork. Rallum with 7-10 blades. In the holotype, there are 10 blades, the basal-most blade approximately 1/4 the length of the other blades. The next 2 blades are about half the length of the remaining 7. The shortest blade has a serrate anterior edge but lacks the comb-like teeth of the other 9 blades. In other specimens, the shortest blade is about half the length of the other blades and has a serrate edge. For all specimens, the distal-most blade is on a wide, triangular base, separated from the other blades as is typical for Neobisiidae. Serrulae of normal shape for Neobisiidae, with squared tips on serrula exterior and tooth-like tips on at least the distal half of serrula interior.

Pedipalps: Pedipalps dark red, with very minute granulations over all articles at very high magnification. Manducatory process with 4-5 setae. Fingers only slightly longer than chela hand.
Venom apparatus: Nodus ramosus terminates almost immediately. On movable finger, *b* and *sb* are in the basal quarter of the finger while *st* and *t* are in the distal half. The distance between *b* and *sb* is approximately the same as the distance between *st* and *t*.

There is a greater distance between the pairs *b-sb* and *st-t*. On the fixed finger, *eb* and *esb* are placed where the finger meets the hand, while *ib*, *isb*, and *ist* are on the basal quarter of the finger. Trichobothria *est*, *et*, and *it* are in the distal half of the fixed finger.

Cephalothorax: Cephalothorax brownish-red. Carapace with 24-26 setae. Eyes well-developed and reflect light in uncleared specimens. Epistome angular and pointed.

Legs: Legs pale grey. Suture between Femur IV and Patella IV roughly perpendicular to the axis of the combined segment, the patella approximately 18-25% longer than the femur.

Subterminal tarsal setae bifid, with terminal branches dentate. Arolia undivided and shorter than tarsal claws.

Abdomen: Abdominal sclerites dark grey. Pleural membranes pale grey. Tergites uniseriate. Sternites biseriate on VI-VIII in some specimens, VI-VII in others; more or less uniseriate on all other sternites, except glandular setae slightly displaced anteriad on segments IX, X and VIII in specimens where VII is not biseriate. Sternite 4 with an anterior notch.

Genitalia: Setae of female genital operculae: Anterior genital operculum with two rows of three setae roughly parallel with the sternite margins. In some specimens, additional setae may be present, bringing the total number of setae to 7 per cluster, though the row of three is maintained in all specimens. Internal genitalia of the female not visible in the available specimens. The male is unknown.

Measurements

Measurements for holotype female given, followed by the range of measurements for all female types in parentheses. Body length 4.94 (3.30-4.94). Carapace 1.02/0.94 (0.95-1.14/0.83-0.97); ocular breadth 0.91 (0.81-0.93). Chelicera 0.62/0.36 (0.56-0.62/0.31-0.37); movable finger 0.44 (0.43-0.50). Pedipalp: trochanter 0.67/0.34 (0.58-0.72/0.32-0.37); femur 01.30/0.33 (1.06-1.30/0.29-0.34); patella 1.04/0.46 (0.93-1.08/0.39-0.46); chela 1.93/0.65 (1.71-2.02/0.55-0.66); chela depth 0.61 (0.52-0.65); chela hand 0.91 (0.82-0.99); movable finger 0.99 (0.86/1.04). Leg I: femur 0.55/0.14 (0.49-0.58/0.13/0.14); patella 0.41/0.16 (0.34-0.41/0.14-0.17); tibia 0.57/0.11 (0.50-0.60/0.10-0.11); metatarsus 0.24/0.09 (0.21-0.28/0.09-0.10); tarsus 0.39/0.08 (0.35-0.39/0.08-0.09). Leg IV: femur 0.50/0.29 (0.44-0.71/0.26/0.29); patella 0.62/0.29 (0.51-0.62/0.26-0.29); tibia 0.98/0.14 (0.86-1.01/0.14-0.16); metatarsus 0.31/0.12 (0.29-0.35/0.11-0.14); tarsus 0.54/0.10 (0.45-0.54/0.10-0.13).

Comments

All other species have been assigned to *Globocreagris* on the basis of the lateral genital sac morphology of the male. Although no males were collected from this species, the molecular phylogeny clearly indicates that these are congeneric with the other Sky Island species.

ACKNOWLEDGMENTS

We are deeply grateful to Mark Harvey for his mentoring GBH in pseudoscorpion curation and identification during the early stages of this project. We thank the following

for collecting and donating specimens: Marshal Hedin and his lab, Alan Yanahan, Angela Hoover, Jeff Eble, Jillian Cowles, Tim Cota, and Niel Marchington. We thank the following curators for lending specimens from their collections for the duration of this study: Gonzalo Giribet (Harvard Museum of Comparative Zoology), Lorenzo Prendini (American Museum of Natural History), Raymond J. Pupedis (Peabody Museum of Natural History), Charles Griswold (California Academy of Sciences), We thank the following for additional assistance in lab and field work: Reilly McManus, Jason Schaller, Antonio Gomez, James Robertson, Paul Marek, Marty Meyer, and other members of the Moore lab. This work is in partial fulfillment of GBH's PhD degree in the Graduate Interdisciplinary Program in Entomology and Insect Science at the University of Arizona and is a product of the Arizona Sky Island Arthropod Project (ASAP) based in WM's laboratory at the University of Arizona. This project received funding support from the following grants and institutions: East Asia and Pacific Summer Institute (EAPSI) award 1209343 from the National Science Foundation; Ernst Mayr Travel Grant in Animal Systematics from the Harvard Museum of Comparative Zoology; Entomology and Insect Science Graduate Student Research Support Award from the University of Arizona Center for Insect Science; National Science Foundation award 1206382 to WM.

LITERATURE CITED

Ayoub, N.A. & S.E. Riechert. 2004. Molecular evidence for Pleistocene glacial cycles driving diversification of a North American desert spider, *Agelenopsis aperta*. *Molecular Ecology*, 13: 3453–3465.

Andújar, C., J. Serrano, & J. Gómez-Zurita. 2012. Winding up the molecular clock in the genus *Carabus* (Coleoptera: Carabidae): assessment of methodological decisions on rate and node age estimation. *BMC Evolutionary Biology*, 12: 40.

Bidegaray-Batista L & M.A. Arnedo. 2011. Gone with the plate: the opening of the Western Mediterranean basin drove the diversification of ground-dweller spiders. *BMC Evolutionary Biology*, 11(317):1–15.

Bouckaert, R., J. Heled, D. Kühnert, T. Vaughan, C-H. Wu, D. Xie, MA. Suchard, A. Rambaut, &, A.J. Drummond. 2014. BEAST 2: A Software Platform for Bayesian Evolutionary Analysis. *PLoS Computational Biology*, 10(4), e1003537. doi:10.1371/journal.pcbi.1003537

Broecker, W.S. & G.H. Denton. 1990. What drives glacial cycles? *Scientific American*, 262(1): 49–56.

Brower, A.V.Z. 1994. Rapid morphological radiation and convergence among races of the butterfly *Heliconius erato* inferred from patterns of mitochondrial DNA evolution. *Proceedings of the National Academy of Sciences*, 91: 6491–6495.

Brusca, R.C., J.F. Wiens, W.M. Meyer, J. Eble , K. Franklin, J.T. Overpeck and W. Moore. 2013. Dramatic response to climate change in the Southwest: Robert Whittaker's 1963 Arizona Mountain plant transect revisited. Ecology and Evolution DOI: 10.1002/ece3.720

Bryson, R.W., R.W. Murphy, A. Lathrop, & D. Lazcano-Villareal. 2011. Evolutionary drivers of phylogeographical diversity in the highlands of Mexico: a case study of the *Crotalus triseriatus* species group of montane rattlesnakes. *Journal of Biogeography*, 38: 697–710.

Bryson, R.W., B.R. Riddle, M.R. Graham, B.T. Smith, & L. Prendini. 2013. As old as the hills: montane scorpions in southwestern North America reveal ancient associations between biotic diversification and landscape history. *PLoS ONE* 8(1): e52822. DOI:10.1371/journal.pone.0052822.

Buddle, C.M. (2010). Photographic key to the Pseudoscorpions of Canada and the adjacent USA. Canadian Journal of Arthropod Identification No. 10, 03 February 2010, available online at http://www.biology.ualberta.ca/bsc/ejournal/b_10/b_10.html, doi:10.3752/cjai.2010.10.

Chamberlin, J.C. 1952. New and little-known false scorpions (Arachnida, Chelonethida) from Monterey County, California. *Bulletin of the American Museum of Natural History*, 99(4): 259–312.

Clouse, R.M. & W.C. Wheeler. 2014. Descriptions of two new, cryptic species of *Metasiro* (Arachnida: Opiliones: Cyphophthalmi: Neogoveidae) from South Carolina, USA, including a discussion of mitochondrial mutation rates. *Zootaxa*, 3814(2): 177–201.

Colgan, J.P., T.A. Dumitru, M. McWilliams & E.L. Miller. 2006. Timing of Cenozoic volcanism and Basin and Range extension in northwestern Nevada: New constraints from the northern Pine Forest Range. *Geological Society of America Bulletin*, 118(1): 126–139.

Ćurčić, B.P.M. 1984. A revision of some North American species of *Microcreagris* Balzan, 1982, (Arachnida: Pseudoscorpiones: Neobisiidae). *Bulletin of the British Arachnological* Society 6(4): 149–166.

Darriba D., G.L. Taboada, R. Doallo & D. Posada. 2012. jModelTest 2: more models, new heuristics and parallel computing. *Nature Methods*, 9(8): 772.

De Andrade, R. & P. Gnaspini. 2002. Feeding *in Maxchernes iporangae* (Pseudoscorpiones, Chernetidae) in captivity. *Journal of Arachnology* 30: 613–617.

DiDominico, A. & M. Hedin. 2016. New species in the *Sitalcina sura* species group (Opiliones, Laniatores, Phalangodidae), with evidence for a biogeographic link between California desert canyons and Arizona sky islands. *ZooKeys*, 586: 1–36.

Ferrari, L., M. López-Martínez, T. Orozco-Esquivel, S.E. Bryan, J. Duque-Trujillo, P. Lonsdale and L. Solari. 2013. Late Oligocene to Middle Miocene rifting and synextensional magmatism in the southwestern Sierra Madre Occidental, Mexico: The beginning of the Gulf of California rift. Geosphere 9: 1161-1200.

Francke, O.F. & Villegas-Guzmán, G.A. 2006. Symbiotic relationships between pseudoscorpions (Arachnida) and packrats (Rodentia). *The Journal of Arachnology* 34: 289–298.

Gantenbein, B. & C.R. Largiadèr. 2003. The phylogeographic importance of the Strait of Gibraltar as a gene flow barrier in terrestrial arthropods: a case study with the scorpion *Buthus occitanus* as a model organism. *Molecular Phylogenetics and Evolution*, 28: 119–130.

Griffin, J.R. 1990. Flora of Hastings Reservation. Hastings Natural History Reservation, Carmel Valley, California.

Guindon, S. and O. Gascuel 2003). A simple, fast and accurate method to estimate large phylogenies by maximum-likelihood. *Systematic Biology*, 52: 696–704.

Harvey, M.S. & W.B. Muchmore. 2010. Two new cavernicolous species of the pseudoscorpion genus *Cryptocreagris* from Colorado (Pseudoscorpiones: Neobisiidae). *Subterranean Biology*, 7: 55–64.

Harvey, M.S. (2013). Pseudoscorpions of the World, version 3.0. Western Australian Museum, Perth. http://www.museum.wa.gov.au/catalogues/pseudoscorpions

Harvey, M.S. 1992. The phylogeny and classification of the Pseudoscorpionida (Chelicerata: Arachnida). *Invertebrate Taxonomy*, 6: 1373–1435.

Hasegawa, M., H. Kishino, & T. Yano. 1985. Dating of the human-ape splitting by a molecular clock of mitochondrial DNA. *Journal of Molecular Evolution*, 22: 160–174.

Lanfear R, Calcott B, Ho SYW, Guindon S. 2012. PartitionFinder: combined selection of partitioning schemes and substitution models for phylogenetic analyses.
Molecular Biology and Evolution 29(6):1695–1701.

Maddison, W. P. and D.R. Maddison. 2016. Mesquite: a modular system for evolutionary analysis. Version 3.10 http://mesquiteproject.org

McCormack, J.E., B.S. Bowen, & T.B. Smith. 2008. Integrating paleoecology and genetics of bird populations in two sky island archipelagos. BMC Biology, 6:28. Doi:10.1186/1741-7007-6-28.

Meyer W.M., III, J.A. Eble, K. Franklin, R.B. McManus, S.L. Brantley, J. Henkel, P.E. Marek , W. E. Hall, C.A. Olson, R.McInroy, E.M. Bernal Loaiza, R.C. Brusca, W. Moore. (2015) Ground-Dwelling Arthropod Communities of a Sky Island Mountain Range in Southeastern Arizona, USA: Obtaining a Baseline for Assessing the Effects of Climate Change. *PLoS ONE* 10(9): e0135210. doi:10.1371/journal.pone.0135210

Mishler, B.D. & R.N. Brandon. 1987. Individuality, pluralism, and the phylogenetic species concept. *Biology and Philosophy*, 2: 397–414.

Muchmore, W.B. 1971. Phoresy by North and Central American pseudoscorpions. *Proceedings of the Rochester Academy of Sciences* 12(2): 79–97.

Muchmore, W.B. 1994. On four species of pseudoscorpions from California described by E. Simon in 1878 (Pseudoscorpionida: Neobisiidae, Chernetidae, Cheliferidae). *The Journal of Arachnology*, 22: 60–69.

Papadopoulou A., I. Anastasiou, A.P. Vogler. 2010. Revisiting the insect mitochondrial molecular clock: the mid-Aegean trench calibration. *Molecular Biology and Evolution*. 27(7):1659–72.

Pons, J., I. Ribera, J. Bertranpetit, & M. Balke. 2010. Nucleotide substitution rates for the full set of mitochondrial protein-coding genes in Coleoptera. *Molecular Phylogenetics and Evolution*, 56: 796–807.

Rambaut A., M.A. Suchard, D. Xie & A.J. Drummond 2014. Tracer v1.6, Available from http://beast.bio.ed.ac.uk/Tracer

Stamatakis, A. 2014. RAxML Version 8: A tool for phylogenetic analysis and post-analysis of large phylogenies. *Bioinformatics*, 30(9): 1312–1313.

Weygoldt, P. 1969. *The biology of pseudoscorpions*. Harvard University Press: Cambridge, Massachusetts.

Wheeler, Q.D. & N.I. Platnick. 2000. The Phylogenetic Species Concept (*sensu* Wheeler and Platnick) *in* Species Concepts and Phylogenetic Theory: A Debate. Q.D. Wheeler & R. Meier, eds. Columbia University Press. Pp. 55–69.

Wheeler, T. J., & Kececioglu, J. D. 2007. Multiple alignments by aligning alignments. *Bioinformatics*, 23: i559–i568.

Wheeler, T. J., & D.R. Maddison. 2012. Opalescent: A Mesquite package providing access to Opal within Mesquite. Version 2.10.

Wood, D.A., A.G. Vandergast, J.A., Lemos Espinal, R.n. Fisher, & A.T. Holycross. 2011. Refugial isolation and divergence in the Narrowheaded Gartersnake species complex (*Thamnophis rufipunctatus*) as revealed by multilocus DNA sequence data. *Molecular Ecology*, 20: 3856–3878.

Worth, C.B. (1971). Pseudoscorpions on a Dark-Eyed Junco, *Junco hyemalis*. *Bird-Banding*, 46(1): 76.

Young, M.R., & P.D.N. Hebert. 2015. Patterns of protein evolution in cytochrome oxidase 1 (COI) from the class Arachnida. *PLOS ONE*, 10(8): e0135053.

Figure 1. Dorsal habitus of *Globocreagris pinalenoensis* sp. nov. from the Pinaleño Mountains in Arizona.

Figure 2. Maximum likelihood tree of two genes (COI and 28S) from 500 independent starting trees. Bootstrap support from 500 bootstrap replicates is indicated to the left of nodes. *Globocreagris nigrescens* nests within the Arizona Sky Island clade, together forming strong support for a monophyletic *Globocreagris*. Specimens from each

mountain range form endemic clades with bootstrap support values of 70 or greater. Holotype specimens are indicated by bold type and an (H). COI sequences from the Huachuca Mountains and *G. nigrescens* are numts (nuclear mitochondrial sequences).

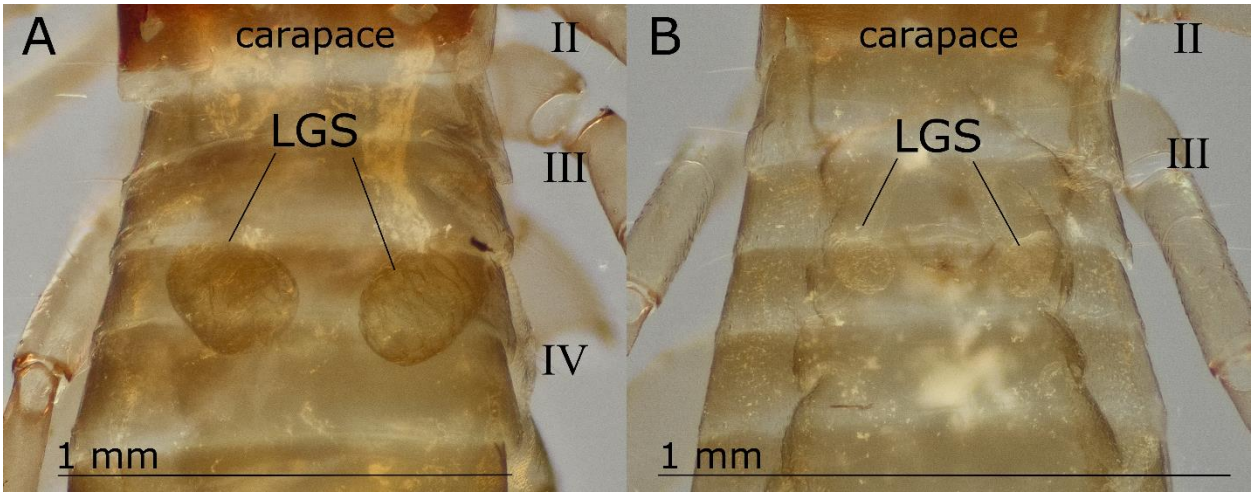

Figure 3. Dorsal views of the first four abdomenal segments. Lateral genital sacs (LGS) are visible through the tergites of cleared specimens. (A) *Globocreagris huachucaensis* (UAIC 1113087) and (B) a microcreagrine from Mt. Union (UAIC 1113079). Roman numerals indicate leg numbers.

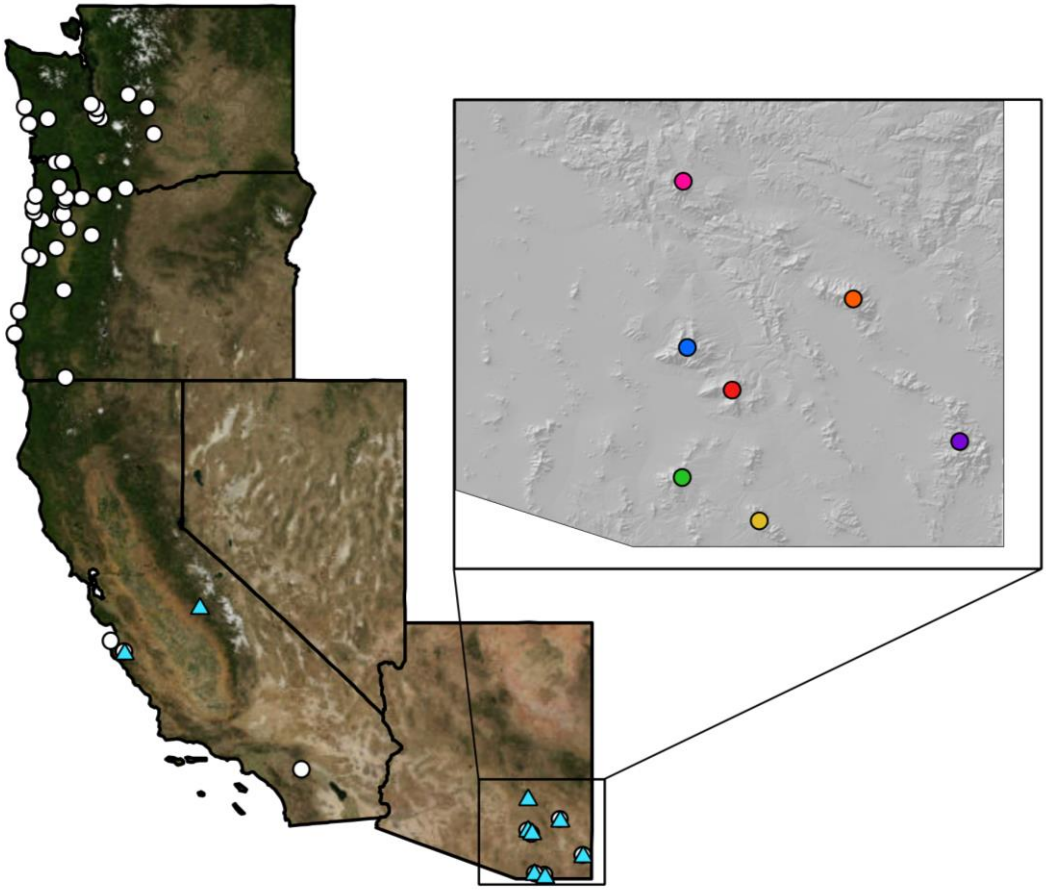

Figure 4. Updated distribution of the genus *Globocreagris*. White circles indicate localities from which male specimens have been collected. Blue triangles indicate the type localities of each described species. Callout shows localities of the 7 new species in southern Arizona. Pink = *G. pinalensis*, orange = *G. pinalenoensis*, blue = *G. santacatalinaensis*, red = *G. rinconensis*, purple = *G. chiricahuaensis*, green = *G. santaritaensis*, yellow = *G. huachucaensis*.

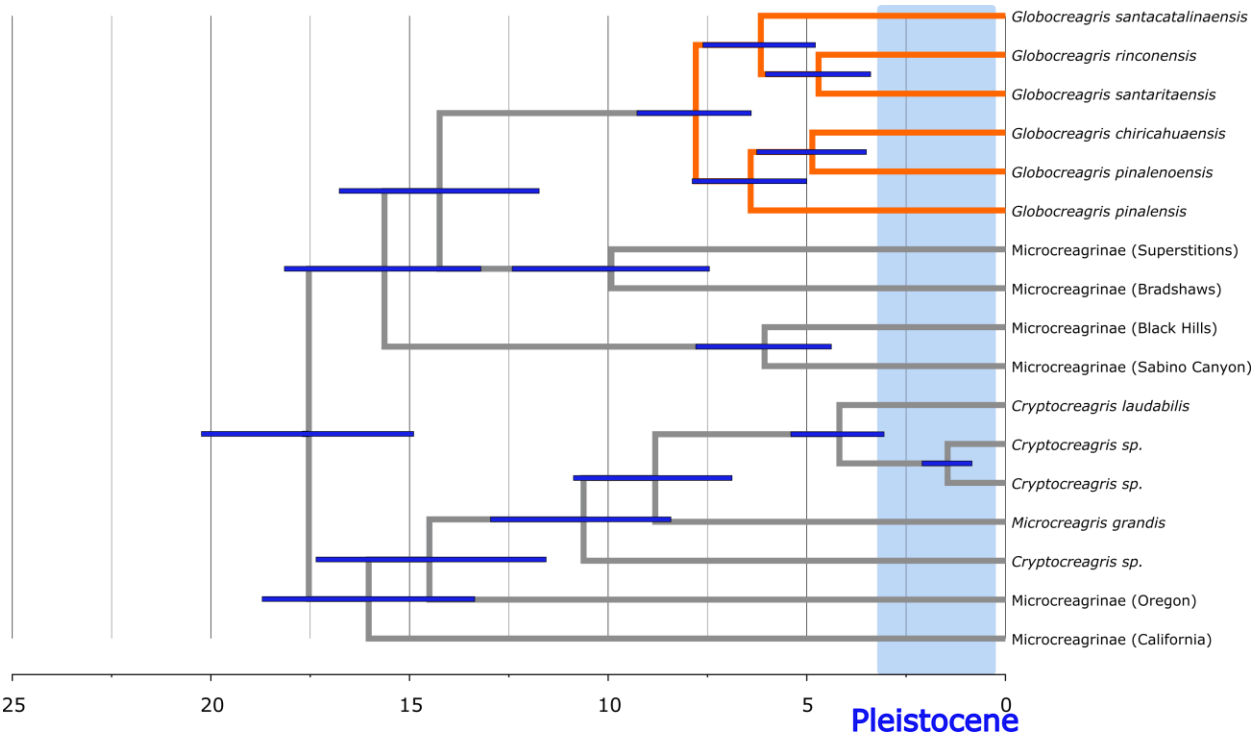

Figure 5. Chronogram indicating ages of nodes of select neobisiids in units of millions of years. All of the *Globocreagris* species included in the analysis diverged before the Pleistocene, which began about 2.6 mya.

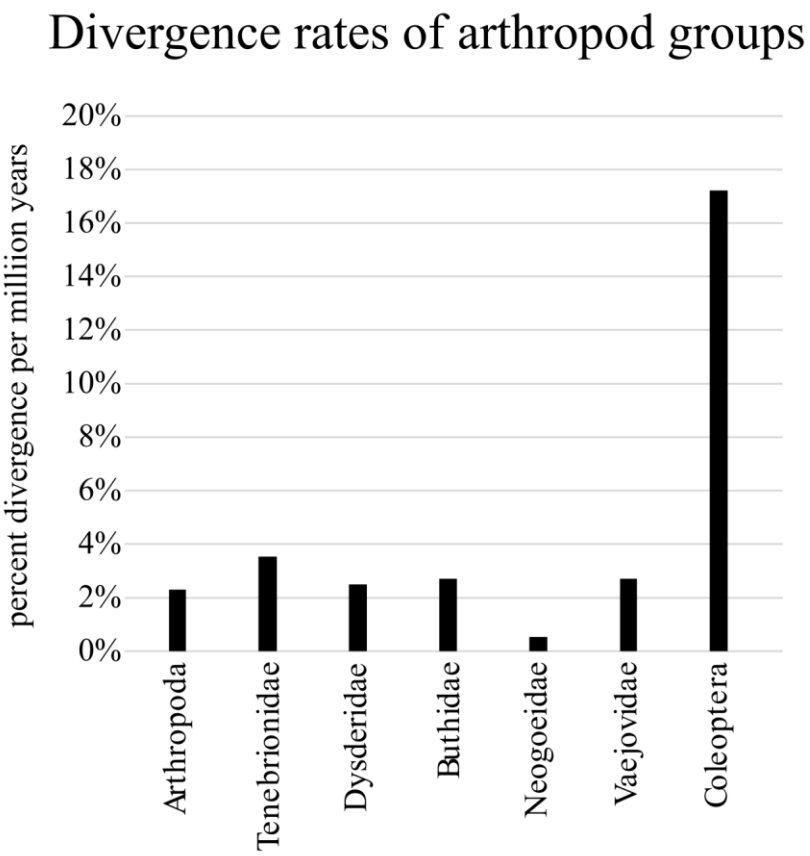

Figure 6. Graph of divergence rates of COI found in the literature in units of percent divergence per million years. Arthropoda is an exception as it is the most cited mitochondrial divergence rate, included because it is used so frequently in divergence time estimation. Arthropoda 2.3% (Brower 1994); Tenebrionidae 3.54% (Papadopoulou et al. 2010); Dysderidae 2.5% (Bidegaray Batista & Arnedo 2011); Buthidae 2.7% (Gantenbein & Largiadaèr 2003); Neogoeidae 0.53% (Clouse & Wheeler 2014); Vaejovidae 2.7% (Bryson et al. 2013); Coleoptera 17.21% (Pons et al. 2010).

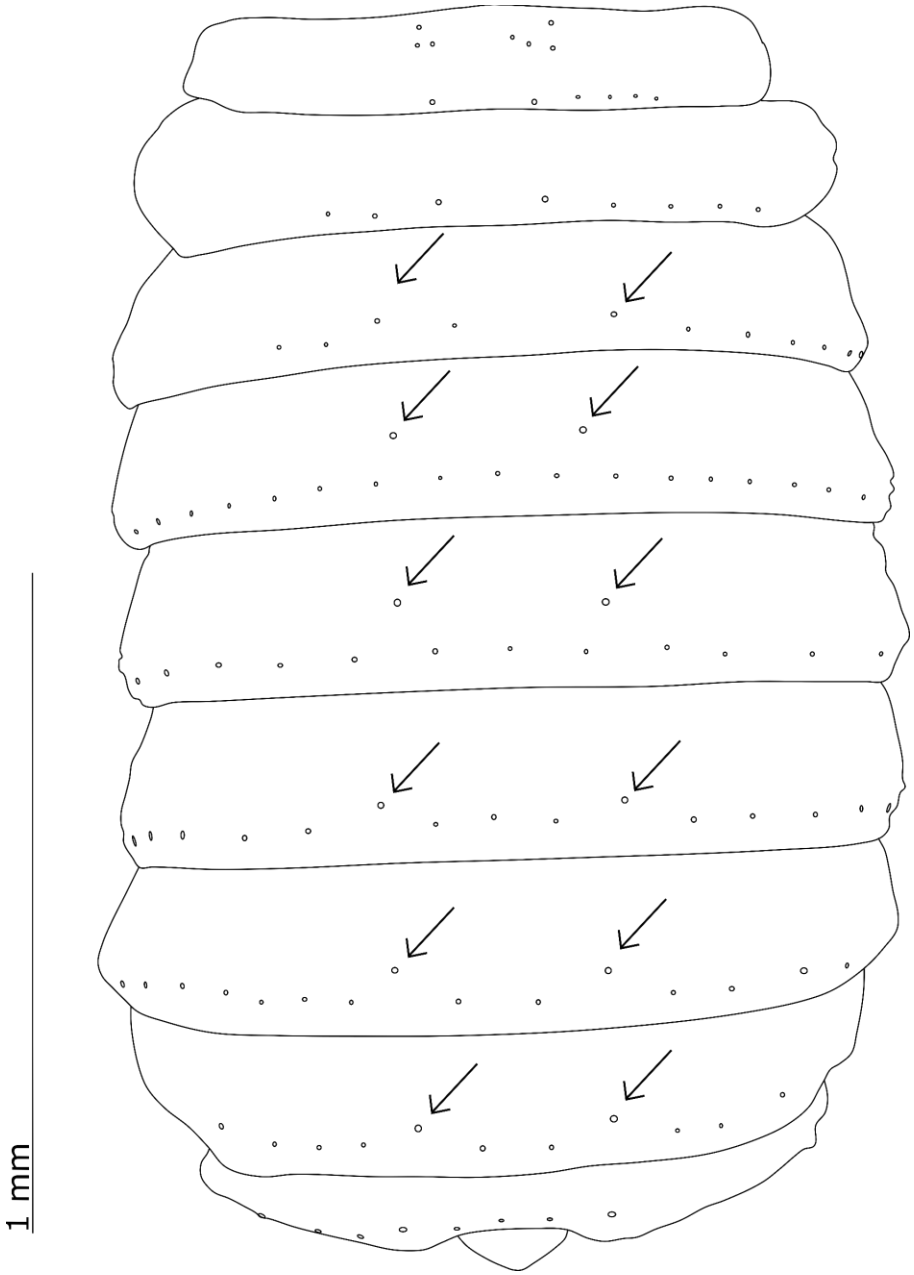

Figure 7. Ventral aspect of a female of *G. huachucaensis*, showing placement of setae. Arrows indicate the paired discal setae that are offset from the posterior row of setae on nearly all sternites.

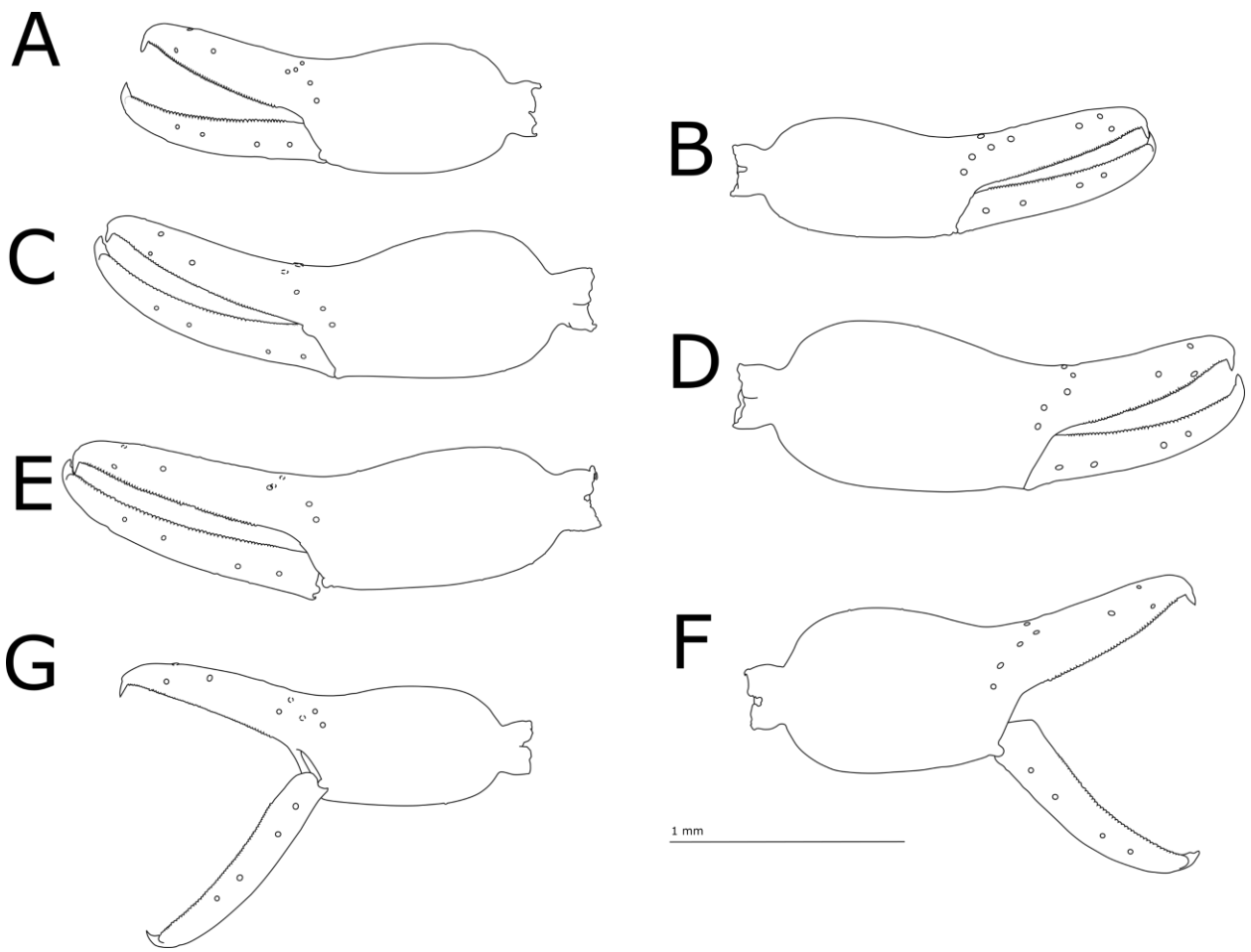

Figure 8. External view of pedipalpal chelae. A) *G. chiricahuaensis*, B) *G. santacatalinaensis*, C) *G. rinconensis*, D) *G. pinalensis*, E) *G. santaritaensis*, F) *G. pinalenoensis*, G) *G. huachucaensis*. D is female; the rest are males.

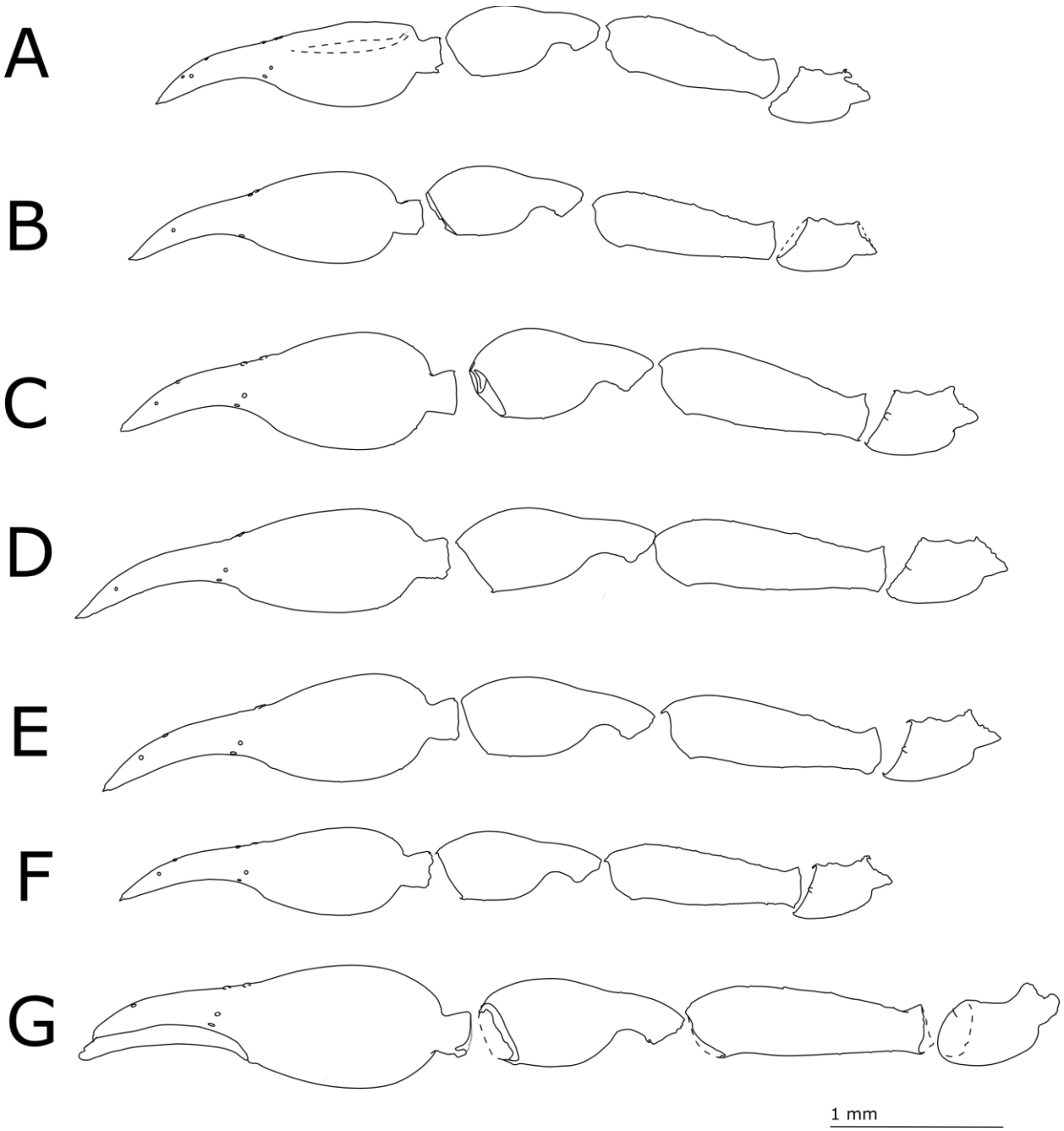

Figure 9. Dorsal view of pedipalps, showing relative proportions of each segment. A) *G. chiricahuaensis*, B) *G. huachucaensis*, C) *G. pinalenoensis*, D) *G. santaritaensis*, E) *G. rinconensis*, F) *G. santacatalinaensis*, G) *G. pinalensis*. Note that A has an unnatural depression in the external aspect of the chela, indicated here by dashed lines. All pedipalps pictured are from the right pedipalp except for F and G which are left pedipalps, but have been digitally reversed for ease of comparison. A – F are males; G is female.

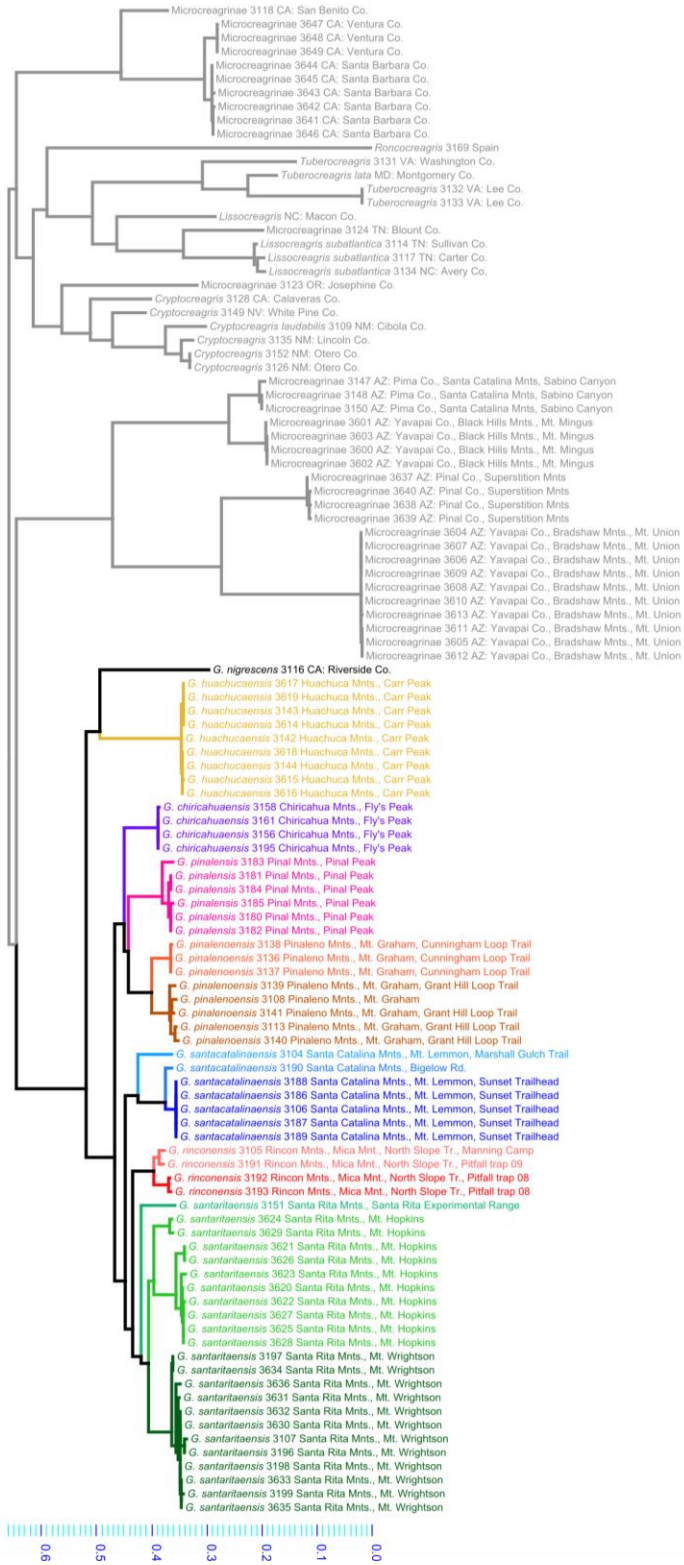

Figure S1. Complete tree from Figure 2 showing detail of collapsed branches. Branch lengths proportional to sequence evolution.

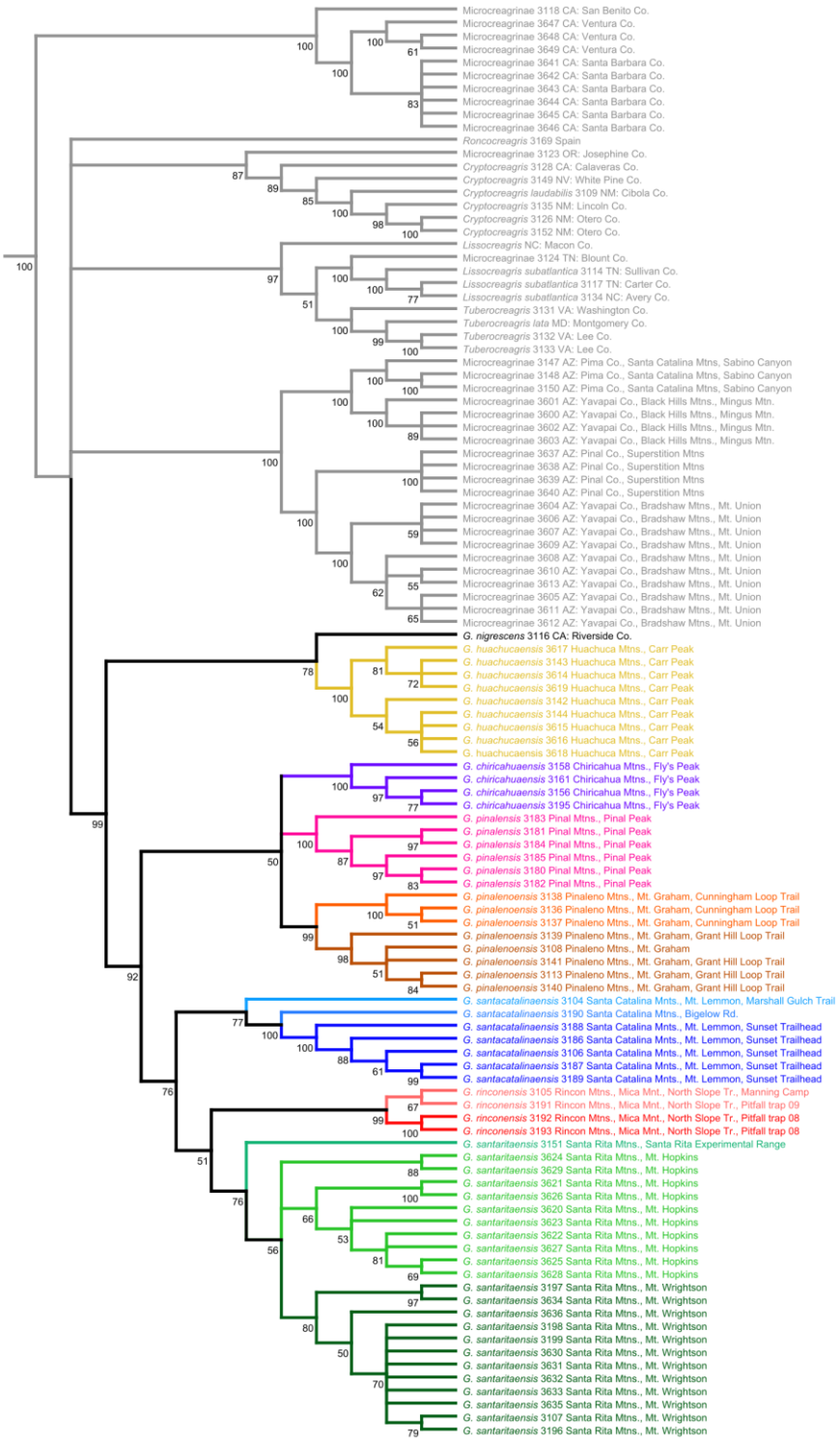

Figure S2. Complete combined COI and 28S tree from figure 2 showing bootstrap support for all branches that had bootstrap support greater than 50.

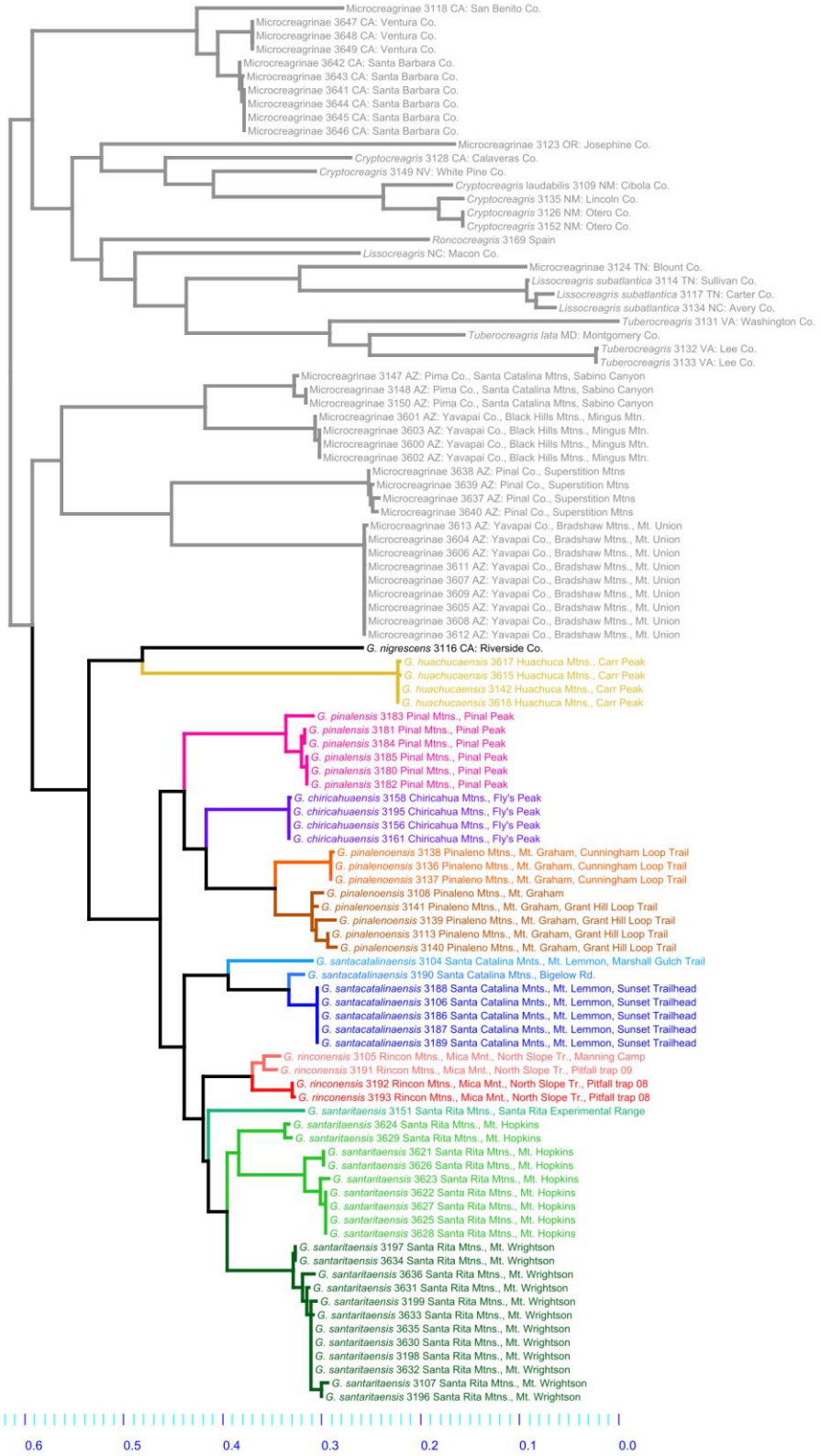

Figure S3. A RAxML phylogeny using only COI sequences. Tree found through ML search with 500 starting trees and 500 bootstrap replicates.

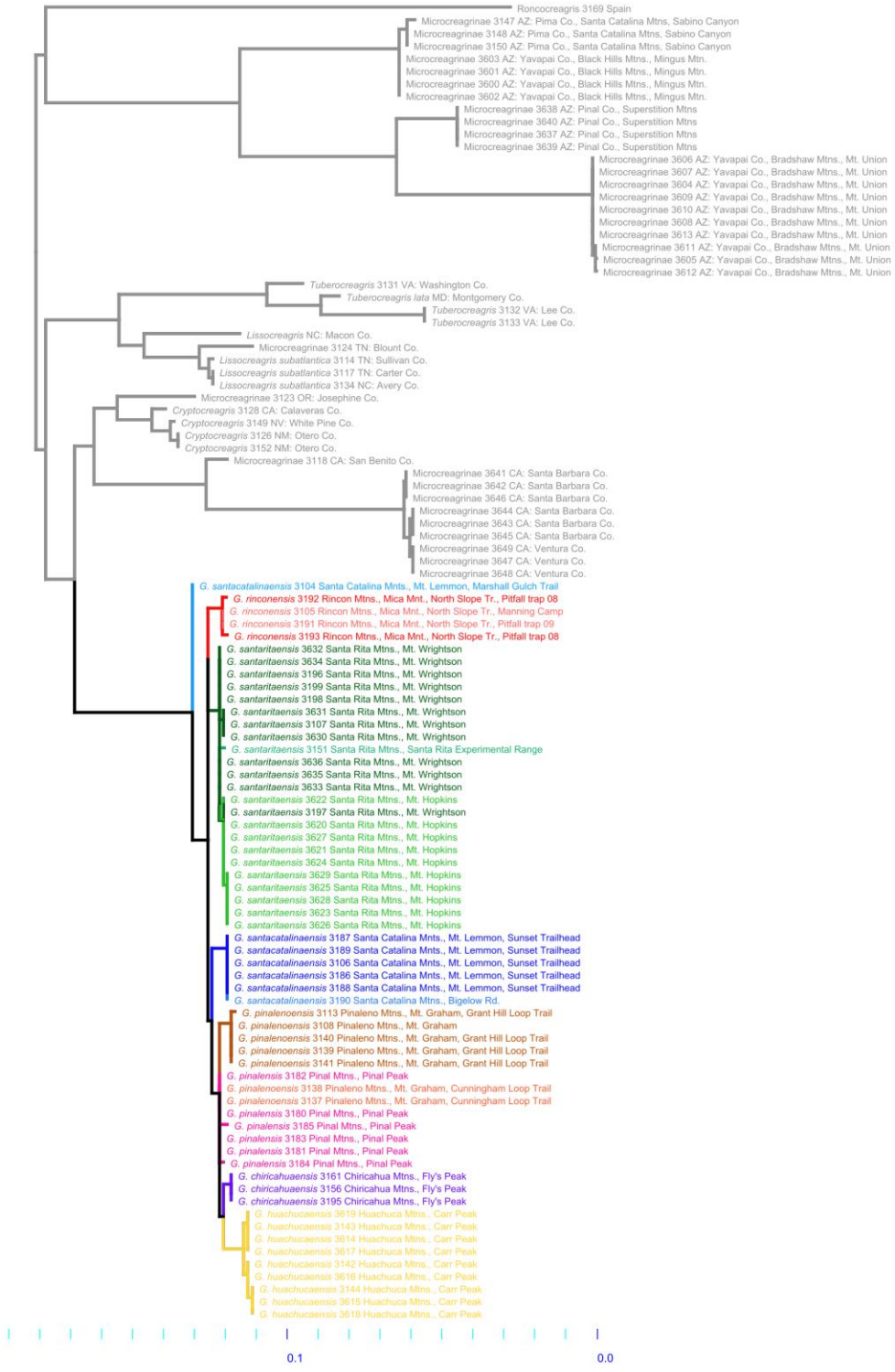

Figure S4. A RAxML phylogeny using only 28S sequences. Tree found through ML search with 500 starting trees and 500 bootstrap replicates.

Table 1. Taxon sampling table for the molecular phylogeny. Primers are as follows: COHua2R (CGATCTGTTAATAATATAGTGATGGC), HCO2198 (TAAACTTCAGGGTGACCAAAAAATCA), LCO1490 (GCATAGTTCACCATCTTTC), LS30F (ACCCCCTRAATTTAAGCATAT), LS1066R (CGACCGATTTGCACGTCAG), LS1126R (TCGGAAGGAACCAGCTACTA).

DNA Number	Body Part	Taxon/ geographic origin	Depository number	Genbank accession number COI	Genbank accession number 28S	COI Forward Primer	COI Reverse Primer	28S Forward Primer	28S Reverse Primer
3104	Whole body	*Globocreagris santacalinaensis* 3104	UAIC 1113000	MF124474	MF124336	HCO1490	HCO2198	LS30F	LS1126R
3105	Whole body	*Globocreagris rinconensis* 3105	UAIC 1113001	MF124475	MF124337	HCO1490	HCO2198	LS30F	LS1126R
3106	Whole body	*Globocreagris santacatalinaensis* 3106	UAIC 1113002	MF124476	MF124338	HCO1490	HCO2198	LS30F	LS1126R
3107	Whole body	*Globocreagris santaritaensis* 3107	UAIC 1113003	MF124477	MF124339	HCO1490	HCO2198	LS30F	LS1126R
3108	Whole body	*Globocreagris pinalenoensis* 3108	UAIC 1113004	MF124478	MF124340	HCO1490	HCO2198	LS30F	LS1126R
3109	Whole body	*Cryptocreagris laudabilis* USA: NM 3109	UAIC 1113005	MF124479	MF124341	HCO1490	HCO2198	NA	NA
3110	Whole body	Microcreagrinae USA: CA 3110	UAIC 1113006	MF124480	MF124342	HCO1490	HCO2198	LS30F	LS1066R
3112	Whole body	*Microbisium parvulum* USA: UT 3112	UAIC 1113008	MF124482	MF124343	HCO1490	HCO2198	LS30F	LS1126R
3113	Whole body	*Globocreagris pinalenoensis* 3113	UAIC 1113009	MF124483	MF124344	HCO1490	HCO2198	LS30F	LS1126R
3114	Whole body	*Lissocreagris subatlantica* USA: TN 3114	UAIC 1113010	MF124484	MF124345	HCO1490	HCO2198	LS30F	LS1126R
3115	Whole body	Neobisiinae, USA: TN 3115	UAIC 1113011	MF124485	MF124346	HCO1490	HCO2198	LS30F	LS1066R
3116	Whole body	*Globocreagris nigrescens* USA: Riverside, CA 3116	UAIC 1113012	MF124600	NA	HCO1490	HCO2198	LS30F	LS1126R
3117	Whole body	*Lissocreagris subatlantica* 3117	UAIC 1113013	MF124486	MF124347	HCO1490	HCO2198	LS30F	LS1126R
3118	Whole body	Microcreagrinae USA: San Benito, CA 3118	UAIC 1113014	MF124487	MF124348	HCO1490	HCO2198	LS30F	LS1126R
3119	Whole body	Microcreagrinae USA: San Mateo, CA 3119	UAIC 1113015	MF124488	MF124349	HCO1490	HCO2198	LS30F	LS1066R
3120	Whole body	*Parobisium charlotteae* USA: OR 3120	UAIC 1113016	MF124489	MF124350	HCO1490	HCO2198	LS30F	LS1066R
3121	Whole body	*Parobisium charlotteae* USA: OR 3121	UAIC 1113017	MF124490	MF124351	HCO1490	HCO2198	LS30F	LS1066R
3122	Whole body	*Neobisium sp.* USA: NC 3122	UAIC 1113018	MF124491	MF124352	HCO1490	HCO2198	LS30F	LS1066R
3123	Whole body	*Parobisium charlotteae* USA: OR 3123	UAIC 1113019	MF124492	MF124353	HCO1490	HCO2198	LS30F	LS1126R
3124	Whole body	Microcreagrinae USA: TN 3124	UAIC 1113020	MF124493	MF124354	HCO1490	HCO2198	LS30F	LS1126R
3125	Whole body	Neobisiinae USA: VA 3125	UAIC 1113021	MF124494	MF124355	HCO1490	HCO2198	LS30F	LS1066R
3126	Whole body	*Cryptocreagris sp.* USA: NM 3126	UAIC 1113022	MF124495	MF124356	HCO1490	HCO2198	LS30F	LS1126R
3127	Whole body	Neobisiinae USA: TN 3127	UAIC 1113023	MF124496	MF124357	HCO1490	HCO2198	LS30F	LS1126R
3128	Whole body	Microcreagrinae USA: Calaveras Co., CA 3128	UAIC 1113024	MF124497	MF124358	HCO1490	HCO2198	LS30F	LS1066R
3129	Whole body	*Fissilicreagris sp.* USA: Humboldt Co., CA 3129	UAIC 1113025	MF124498	MF124359	HCO1490	HCO2198	LS30F	LS1066R
3130	Whole body	Microcreagrinae USA: Calaveras Co., CA 3130	UAIC 1113026	MF124499	MF124360	HCO1490	HCO2198	LS30F	LS1126R
3131	Whole body	*Tuberocreagris sp.* USA: Washington Co., VA 3131	UAIC 1113027	MF124500	MF124361	HCO1490	HCO2198	LS30F	LS1126R
3132	Whole body	*Tuberocreagris sp.* USA: Lee Co., VA 3132	UAIC 1113028	MF124501	MF124362	HCO1490	HCO2198	LS30F	LS1126R
3133	Whole body	*Tuberocreagris sp.* USA: Lee Co., VA 3133	UAIC 1113029	MF124502	MF124363	HCO1490	HCO2198	LS30F	LS1126R
3134	Whole body	*Lissocreagris subatlantica* USA: NC 3134	UAIC 1113030	MF124503	MF124364	HCO1490	HCO2198	LS30F	LS1126R
3135	Whole body	*Cryptocreagris sp.* USA: NM 3135	UAIC 1113031	MF124504	NA	HCO1490	HCO2198	NA	NA
3136	Whole body	*Globocreagris pinalenoensis* 3136	UAIC 1113032	MF124505	NA	HCO1490	HCO2198	NA	NA
3137	Whole body	*Globocreagris pinalenoensis* 3137	UAIC 1113033	MF124506	MF124365	HCO1490	HCO2198	LS30F	LS1126R
3138	Whole body	*Globocreagris pinalenoensis* 3138	UAIC 1113034	MF124507	MF124366	HCO1490	HCO2198	LS30F	LS1126R

3139	Whole body	*Globocreagris pinalenoensis* 3139	UAIC 1113035	MF124508	MF124367	HCO1490	HCO2198	LS30F	LS1126R
3140	Whole body	*Globocreagris pinalenoensis* 3140	UAIC 1113036	MF124509	MF124368	HCO1490	HCO2198	LS30F	LS1126R
3141	Whole body	*Globocreagris pinalenoensis* 3141	UAIC 1113037	MF124510	MF124369	HCO1490	HCO2198	LS30F	LS1126R
3142	Whole body	*Globocreagris huachucaensis* 3142	UAIC 1113038	MF124601	MF124370	HCO1490	COHua2R	LS30F	LS1126R
3143	Whole body	*Globocreagris huachucaensis* 3143	UAIC 1113039	NA	MF124371	HCO1490	COHua2R	LS30F	LS1126R
3144	Whole body	*Globocreagris huachucaensis* 3144	UAIC 1113040	NA	MF124372	HCO1490	COHua2R	LS30F	LS1126R
3145	Whole body	*Globocreagris huachucaensis* 3145	UAIC 1113041	NA	NA	HCO1490	COHua2R	NA	NA
3146	Whole body	*Globocreagris huachucaensis* 3146	UAIC 1113042	NA	NA	HCO1490	COHua2R	NA	NA
3147	Whole body	Microcreagrinae Sabino Canyon 3147	UAIC 1113043	MF124511	MF124373	HCO1490	COHua2R	LS30F	LS1126R
3148	Whole body	Microcreagrinae Sabino Canyon 3148	UAIC 1113044	MF124512	MF124374	HCO1490	HCO2198	LS30F	LS1126R
3149	Whole body	*Microcreagris grandis* USA: NV 3149	UAIC 1113045	MF124513	MF124375	HCO1490	HCO2198	LS30F	LS1126R
3150	Whole body	Microcreagrinae Sabino Canyon 3150	UAIC 1113046	MF124514	MF124376	HCO1490	HCO2198	LS30F	LS1126R
3151	Whole body	*Globocreagris santaritaensis* 3151	UAIC 1113047	MF124515	MF124377	HCO1490	HCO2198	LS30F	LS1126R
3152	Whole body	*Cryptocreagris sp.* USA: NM 3152	UAIC 1113048	MF124516	MF124378	HCO1490	HCO2198	LS30F	LS1126R
3153	Whole body	*Parobisium charlotteae* USA: OR 3153	UAIC 1113049	MF124517	MF124379	HCO1490	HCO2198	LS30F	LS1126R
3156	Whole body	*Globocreagris chiricahuaensis* 3156	UAIC 113050	MF124519	NA	HCO1490	HCO2198	LS30F	LS1126R
3157	Chela	*Microbisium parvulum* USA: MD 3157	MCZ 130502	MF124520	MF124383	HCO1490	HCO2198	LS30F	LS1126R
3158	Whole body	*Globocreagris chiricahuaensis* 3158	UAIC 1113051	MF124521	NA	HCO1490	HCO2198	NA	NA
3159	Chela	*Novobisium tenue* 3159	MCZ 130504	MF124522	MF124384	HCO1490	HCO2198	LS30F	LS1126R
3160	Chela	*Roncus Transilvanicus* Slovakia 3160	MCZ 130505	MF124523	MF124385	HCO1490	HCO2198	LS30F	LS1126R
3161	Whole body	*Globocreagris chiricahuaensis* 3161	UAIC 1113052	MF124524	MF124386	HCO1490	HCO2198	LS30F	LS1126R
3163	Chela	*Tuberocreagris lata* 3163	MCZ 130508	MF124526	MF124388	HCO1490	HCO2198	LS30F	LS1126R
3173	Whole body	*Microbisium parvulum* Mexico 3173	MCZ 37164	NA	MF124396	HCO1490	HCO2198	LS30F	LS1126R
3174	Whole body	*Microbisium parvulum* Mexico 3174	MCZ 37883	NA	MF124397	HCO1490	HCO2198	LS30F	LS1126R
3175	Whole body	*Microbisium parvulum* Mexico 3175	MCZ 37879	MF124533	MF124398	HCO1490	HCO2198	LS30F	LS1126R
3176	Chela	*Microbisium parvulum* Mexico 3176	MCZ 37883	MF124534	MF124399	HCO1490	HCO2198	LS30F	LS1126R
3177	Whole body	*Microbisium parvulum* Mexico 3177	MCZ 37886	MF124535	MF124400	HCO1490	HCO2198	LS30F	LS1126R
3180	Chelae	*Globocreagirs pinalensis* 3180	UAIC 1113053	MF124538	MF124402	HCO1490	HCO2198	LS30F	LS1126R
3181	Chelae	*Globocreagris pinalensis* 3181	UAIC 1113054	MF124539	MF124403	HCO1490	HCO2198	LS30F	LS1126R
3182	Chelae	*Globocreagris pinalensis* 3182	UAIC 1113055	MF124540	MF124404	HCO1490	HCO2198	LS30F	LS1126R
3183	Chelae	*Globocreagris pinalensis* 3183	UAIC 1113056	MF124541	MF124405	HCO1490	HCO2198	LS30F	LS1126R
3184	Chelae	*Globocreagris pinalensis* 3184	UAIC 1113057	MF124542	MF124406	HCO1490	HCO2198	LS30F	LS1126R
3185	Whole body	*Globocreagris pinalensis* 3185	UAIC 1113058	MF124543	MF124407	HCO1490	HCO2198	LS30F	LS1126R
3186	Whole body	*Globocreagris santacatalinaensis* 3186	UAIC 1113059	MF124544	MF124408	HCO1490	HCO2198	LS30F	LS1126R
3187	Whole body	*Globocreagris santacatalinaensis* 3187	UAIC 1113060	MF124545	MF124409	HCO1490	HCO2198	LS30F	LS1126R
3188	Whole body	*Globocreagris santacatalinaensis* 3188	UAIC 1113061	MF124546	MF124410	HCO1490	HCO2198	LS30F	LS1126R
3189	Whole body	*Globocreagris santacatalinaensis* 3189	UAIC 1113062	MF124547	MF124411	HCO1490	HCO2198	LS30F	LS1126R
3190	Whole body	*Globocreagris santacatalinaensis* 3190	UAIC 1113063	MF124548	MF124412	HCO1490	HCO2198	LS30F	LS1126R

3191	Whole body	*Globocreagris rinconensis* 3191	UAIC 1113064	MF124549	MF124413	HCO1490	HCO2198	LS30F	LS1126R
3192	Whole body	*Globocreagris rinconensis* 3192	UAIC 1113065	MF124550	MF124414	HCO1490	HCO2198	LS30F	LS1126R
3193	Whole body	*Globocreagris rinconensis* 3193	UAIC 1113066	MF124551	MF124415	HCO1490	HCO2198	LS30F	LS1126R
3195	Whole body	*Globocreagris chiricahuaensis* 3195	UAIC 1113068	MF124553	MF124416	HCO1490	HCO2198	LS30F	LS1126R
3196	Whole body	*Globocreagris santaritaensis* 3196	UAIC 1113069	MF124554	MF124417	NA	NA	LS30F	LS1126R
3197	Whole body	*Globocreagris santaritaensis* 3197	UAIC 1113070	MF124555	MF124418	HCO1490	HCO2198	LS30F	LS1126R
3198	Whole body	*Globocreagris santaritaensis* 3198	UAIC 1113071	MF124556	MF124419	HCO1490	HCO2198	LS30F	LS1126R
3199	Whole body	*Globocreagris santaritaensis* 3199	UAIC 1113072	MF124557	MF124420	HCO1490	HCO2198	LS30F	LS1126R
3600	Whole body	Microcregrinae Black Hills 3600	UAIC 1113073	MF124558	MF124421	HCO1490	HCO2198	LS30F	LS1126R
3601	Whole body	Microcregrinae Black Hills 3601	UAIC 1113074	MF124559	MF124422	HCO1490	HCO2198	LS30F	LS1126R
3602	Whole body	Microcregrinae Black Hills 3602	UAIC 1113075	MF124560	MF124423	HCO1490	HCO2198	LS30F	LS1126R
3603	Whole body	Microcregrinae Black Hills 3603	UAIC 1113076	MF124561	MF124424	HCO1490	HCO2198	LS30F	LS1126R
3604	Whole body	Microcreagrinae Bradshaw Mts. 3604	UAIC 1113077	MF124562	MF124425	HCO1490	HCO2198	LS30F	LS1126R
3605	Whole body	Microcreagrinae Bradshaw Mts. 3605	UAIC 1113078	MF124563	MF124426	HCO1490	HCO2198	LS30F	LS1126R
3606	Whole body	Microcreagrinae Bradshaw Mts. 3606	UAIC 1113079	MF124564	MF124427	HCO1490	HCO2198	LS30F	LS1126R
3607	Whole body	Microcreagrinae Bradshaw Mts. 3607	UAIC 1113080	MF124565	MF124428	HCO1490	HCO2198	LS30F	LS1126R
3608	Whole body	Microcreagrinae Bradshaw Mts. 3608	UAIC 1113081	MF124566	MF124429	HCO1490	HCO2198	LS30F	LS1126R
3609	Whole body	Microcreagrinae Bradshaw Mts. 3609	UAIC 1113082	MF124567	MF124430	HCO1490	HCO2198	LS30F	LS1126R
3610	Whole body	Microcreagrinae Bradshaw Mts. 3610	UAIC 1113083	NA	MF124431	NA	NA	LS30F	LS1126R
3611	Whole body	Microcreagrinae Bradshaw Mts. 3611	UAIC 1113084	MF124568	MF124432	HCO1490	HCO2198	LS30F	LS1126R
3612	Whole body	Microcreagrinae Bradshaw Mts. 3612	UAIC 1113085	MF124569	MF124433	HCO1490	HCO2198	LS30F	LS1126R
3613	Whole body	Microcreagrinae Bradshaw Mts. 3613	UAIC 1113086	MF124570	MF124434	HCO1490	HCO2198	LS30F	LS1126R
3614	Whole body	*Globocreagris huachucaensis* 3614	UAIC 1113087	NA	MF124435	HCO1490	COHua2R	LS30F	LS1126R
3615	Whole body	*Globocreagris huachucaensis* 3615	UAIC 1113088	MF124602	MF124436	HCO1490	COHua2R	LS30F	LS1126R
3616	Whole body	*Globocreagris huachucaensis* 3616	UAIC 1113089	NA	MF124437	HCO1490	COHua2R	LS30F	LS1126R
3617	Whole body	*Globocreagris huachucaensis* 3617	UAIC 1113090	MF124603	MF124438	HCO1490	COHua2R	LS30F	LS1126R
3618	Whole body	*Globocreagris huachucaensis* 3618	UAIC 1113091	MF124604	MF124439	HCO1490	COHua2R	LS30F	LS1126R
3619	Whole body	*Globocreagris huachucaensis* 3619	UAIC 1113092	NA	MF124440	HCO1490	COHua2R	LS30F	LS1126R
3620	Whole Body	*Globocreagris santaritaensis* 3620	UAIC 1113093	NA	MF124441	NA	NA	LS30F	LS1126R
3621	Whole Body	*Globocreagris santaritaensis* 3621	UAIC 1113094	MF124571	MF124442	HCO1490	HCO2198	LS30F	LS1126R
3622	Whole Body	*Globocreagris santaritaensis* 3622	UAIC 1113095	MF124572	MF124443	HCO1490	HCO2198	LS30F	LS1126R
3623	Whole Body	*Globocreagris santaritaensis* 3623	UAIC 1113096	MF124573	MF124444	HCO1490	HCO2198	LS30F	LS1126R
3624	Whole Body	*Globocreagris santaritaensis* 3624	UAIC 1113097	MF124574	MF124445	HCO1490	HCO2198	LS30F	LS1126R
3625	Whole Body	*Globocreagris santaritaensis* 3625	UAIC 1113098	MF124575	MF124446	HCO1490	HCO2198	LS30F	LS1126R
3626	Whole Body	*Globocreagris santaritaensis* 3626	UAIC 1113099	MF124576	MF124447	HCO1490	HCO2198	LS30F	LS1126R
3627	Whole Body	*Globocreagris santaritaensis* 3627	UAIC 1113100	MF124577	MF124448	HCO1490	HCO2198	LS30F	LS1126R
3628	Whole Body	*Globocreagris santaritaensis* 3628	UAIC 1113101	MF124578	MF124449	HCO1490	HCO2198	LS30F	LS1126R
3629	Whole Body	*Globocreagris santaritaensis* 3629	UAIC 1113102	MF124579	MF124450	HCO1490	HCO2198	LS30F	LS1126R
3630	Whole Body	*Globocreagris santaritaensis* 3630	UAIC 1113103	MF124580	MF124451	HCO1490	HCO2198	LS30F	LS1126R
3631	Whole Body	*Globocreagris santaritaensis* 3631	UAIC 1113104	MF124581	MF124452	HCO1490	HCO2198	LS30F	LS1126R
3632	Whole Body	*Globocreagris santaritaensis* 3632	UAIC 1113105	MF124582	MF124453	HCO1490	HCO2198	LS30F	LS1126R
3633	Whole Body	*Globocreagris santaritaensis* 3633	UAIC 1113106	MF124583	MF124454	HCO1490	HCO2198	LS30F	LS1126R
3634	Whole Body	*Globocreagris santaritaensis* 3634	UAIC 1113107	MF124584	MF124455	HCO1490	HCO2198	LS30F	LS1126R
3635	Whole Body	*Globocreagris santaritaensis* 3635	UAIC 1113108	MF124585	MF124456	HCO1490	HCO2198	LS30F	LS1126R
3636	Whole Body	*Globocreagris santaritaensis* 3636	UAIC 1113109	MF124586	MF124457	HCO1490	HCO2198	LS30F	LS1126R

3637	Whole Body	Microcreagrinae Superstition Mts. 3637	UAIC 1113110	MF124587	MF124458	HCO1490	HCO2198	LS30F	LS1126R
3638	Whole Body	Microcreagrinae Superstition Mts. 3638	UAIC 1113111	MF124588	MF124459	HCO1490	HCO2198	LS30F	LS1126R
3639	Whole Body	Microcreagrinae Superstition Mts. 3639	UAIC 1113112	MF124589	MF124460	HCO1490	HCO2198	LS30F	LS1126R
3640	Whole Body	Microcreagrinae Superstition Mts. 3640	UAIC 1113113	MF124590	MF124461	HCO1490	HCO2198	LS30F	LS1126R
NA	**NA**	*Neobisium sp.* 3 JA-2011 voucher MNHN-JAC15	MNHN-JAC15	JN018209.1	NA	NA	NA	NA	NA
NA	**NA**	*Neobisium sp.* 2 JA-2011 voucher MNHN-JAC14	MNHN-JAC-14	JN018208.1	NA	NA	NA	NA	NA
NA	**NA**	*Roncus sp.* JA-2011 voucher MNHN-JAC28	MNHN-JAC28	JN018186.1	JN018400.1	NA	NA	NA	NA
NA	**NA**	*Neobisium sp.* 1 JA-2011 voucher MNHN-JAA9	MNHN-JAA9	NA	NA	NA	NA	NA	NA
NA	**NA**	*Neobisium geronenses* voucher MNHN-JAC22	MNHN-JAC22	JN018184.1	JN018398.1	NA	NA	NA	NA
NA	**NA**	*Bisetocreagris sp.* 2 JA-2011 voucher MNHN-JAD69	MNHN-JAD69	JN018182.1	JN018396.1	NA	NA	NA	NA
NA	**NA**	*Bisetocreagris sp.* 1 JA-2011 voucher MNHN-JAC35	MNHN-JAC35	JN018181.1	JN018395.1	NA	NA	NA	NA
NA	**NA**	*Roncus transsilvanicus* voucher DNA102454		NA	EU559477.1	NA	NA	NA	NA
NA	**NA**	*Microbisium parvulum* voucher DNA102453		NA	EU559476.1	NA	NA	NA	NA
NA	**NA**	*Neobisium polonicum* voucher DNA102432		NA	EU559457.1	NA	NA	NA	NA
NA	**NA**	*Novobisium tenue* voucher DNA102420		NA	EU559452.1	NA	NA	NA	NA
NA	**NA**	*Tuberocreagris lata* voucher DNA102419		NA	EU559451.1	NA	NA	NA	NA
NA	**NA**	*Lissocreagris sp.* JM-2008 voucher DNA102417		NA	EU559450.1	NA	NA	NA	NA

Table S1. Localities and specimen numbers for new specimens added to the genus *Globocreagris*.

Sex	Specimen	Institution	Locality	Latitude	Longitude
M	DM.6.01001	CAS	USA: Oregon: Coos Co., Charleston, Institute of Marine Biology, 18 January 1957, D. McKey Fender	43.34	-124.44
M	DM.6.01002	CAS	USA: Oregon: Coos Co., Charleston, Institute of Marine Biology, 18 January 1957, D. McKey Fender	43.34	-124.44
M	DM-1 1.01004	CAS	USA: Oregon: Coos Co., Charleston, forrest litter, 13 August 1956, K.M. Fender	43.34	-124.44
M	DM-10.01001	CAS	USA: Oregon: Tillamook Co., Tierra del Mar, litter 15, 6 March 1955, K.M. Fender	45.25	-123.96
M	DM-122.01004	CAS	USA: Oregon: Benton Co., 5 mi N.W. of Corvallis, forest litter, February 1962, D.L. Mays	44.56	-123.37
M	DM-13.01001	CAS	USA: Oregon: Multnomah Co., Oneonta Gorge, on the Columbia River highway, 16 October 1955, K.M. Fender	45.58	-122.07
M	DM-14.01003	CAS	USA: Oregon: Yamhill Co., Peavine Ridge (near Mt. Minnville), from alder duff, September 1955, K.W. Fender	45.2	-123.28
M	DM-15.01004	CAS	USA: Oregon: Tillamook Co., Cape Lookout, 17 March 1957, K.M. Fender	45.35	-123.97
M	DM-16.01001	CAS	USA: Oregon: Yamhill Co., Peavine Ridge (near Mt. Minnville), 27 March 1957, K.M Fender	45.2	-123.28
M	DM-16.01002	CAS	USA: Oregon: Yamhill Co., Peavine Ridge (near Mt. Minnville), 27 March 1957, K.M Fender	45.2	-123.28
M	DM-16.02001	CAS	USA: Oregon: Yamhill Co., Peavine Ridge (near Mt. Minnville), 27 March 1957, K.M Fender	45.2	-123.28
M	DM-17.01003	CAS	USA: Oregon: Yamhill Co., Peavine Ridge (near Mt. Minnville), 27 March 1957, K.M Fender	45.2	-123.28
M	DM-2.01006	CAS	USA: Oregon: Lincoln Co., Tierra del Mar, rotten spruce log mature sand dune, 25 September 1955, K.M. Fender	45.25	-123.96
M	DM-22.01004	CAS	USA: Oregon: Tillamook Co., Tierra del Mar, 28 April 1957, D. McKey Fender	45.25	-123.96

M	DM-25.01001	CAS	USA: Oregon: Yamhill Co., McMinneville, in a house, 15 May 1957, D. McKey Fender	45.21	-123.18
M	DM-28.01003	CAS	USA: Oregon: Curry Co., Floras Creek, 30 November 1957, D. McKey Fender	42.91	-124.48
M	DM-3.01001	CAS	USA: Oregon: Curry Co., 3 miles south of Langlois, D. McKey Fender J. Asburry	42.88	-124.46
M	DM-3.01005	CAS	USA: Oregon: Curry Co., 3 miles south of Langlois, D. McKey Fender J. Asburry	42.88	-124.46
M	DM-58.01003	CAS	USA: Oregon: Lincoln Co., Waldport, from spruce cones, 26 December 1951, John E. Davis	44.42	-124.06
M	DM-59.01001	CAS	USA: Oregon: Marion Co., Salem, near Brush College, in fir cones, 19 November 1947	44.94	-123.03
M	DM-59.01002	CAS	USA: Oregon: Marion Co., Salem, near Brush College, in fir cones, 19 November 1948	44.94	-123.03
M	DM-8.01001	CAS	USA: Oregon: Yamhill Co., Sourgrass Creek, alder-fern debris, 2 October 1955, K.M. Fender	45.1	-123.77
M	DM-9.01001	CAS	USA: Oregon: Tillamook Co., Tierra del Mar, spruce forest floor debris in mature sand dune, 25 September 1955, K.M. Fender	45.25	-123.96
M	DM-9.01002	CAS	USA: Oregon: Tillamook Co., Tierra del Mar, spruce forest floor debris in mature sand dune, 25 September 1955, K.M. Fender	45.25	-123.96
M	EB-137.01001		USA: Oregon: Jackson Co., approx. 15 milies southwest of Ruch, upper applegate, mossy bark, rotted log, 1800 feet, 13 November 1972, E.M. Benedict	42.05	-123.12
M	JC-1060.02001	CAS	USA: Oregon: Washington Co., Forest Grove, 22 February 1941, J.C. and Anne Chamberlin	45.52	-123.11
M	JC-1060.02002	CAS	USA: Oregon: Washington Co., Forest Grove, 22 February 1941, J.C. and Anne Chamberlin	45.52	-123.11
M	JC-1136.01001	CAS	USA: Washington: Peirce Co., Puyallup, beat from dead alder, 9 March 1938, Wm. W. Baker	47.18	-122.29
M	JC-1150.02003	CAS	USA: Oregon: Multnomah Co., Portland, Glen Harbor, leaf mould, 28 January 1940, Post	45.51	-122.68
M	JC-1150.02005	CAS	USA: Oregon: Multnomah Co., Portland, Glen Harbor, leaf mould, 28 January 1940, Post	45.51	-122.68
M	JC-1150.02006	CAS	USA: Oregon: Multnomah Co., Portland, Glen Harbor, leaf mould, 28 January 1940, Post	45.51	-122.68
M	JC-1243.01001	CAS	USA: Washington: Grays Harbor Co., Westport, in moss, 26 Februrary 1933, Wm. W. Baker	46.89	-124.1
M	JC-1245.01001	CAS	USA: Washington: Pierce Co., Puyallup, in moss, 24 January 1932, Wm. W. Baker	47.18	-122.29
M	JC-1248.02001	CAS	USA: Oregon: Lincoln Co., 2 mi north of Waldport, duff conifer forest, 14 March 1937, J.C. Chamberlin	44.42	-124.06
M	JC-1248.02002	CAS	USA: Oregon: Lincoln Co., 2 mi north of Waldport, duff conifer forest, 14 March 1937, J.C. Chamberlin	44.42	-124.06
M	JC-1411.01001	CAS	USA: Oregon: Multnomah Co., 5-6 miles west of Portland, Berlese funnel, 1941, C.L Ritchie	45.51	-122.78
M	JC-1577.01001	CAS	USA: Washington: King Co., Snoqualmie Pass, Denny Creek Camp, 16 September 1935, R.V. Chamberlin and W. Ivie	47.41	-121.44
M	JC-1577.01002	CAS	USA: Washington: King Co., Snoqualmie Pass, Denny Creek Camp, 16 September 1935, R.V. Chamberlin and W. Ivie	47.41	-121.44
M	JC-1654.01001	CAS	USA: Oregon: Douglas Co., 1.5 miles S. of Lane Co., on Eugene-Roseberg highway, leaf mould, 18 November 1937, J.C. Chamberlin	43.75	-123.17
M	JC-1777.02001	CAS	USA: California: Pacific Grove, 15 August 1931, W. Ivie	36.61	-121.91
M	JC-1800.01001	CAS	USA: Washington: Pierce Co., Puyallup, 23 February 1932, Wm. W. Baker	47.18	-122.29
M	JC-1807.01001	CAS	USA: Washington: Pierce Co., Graham, 2 October 1932, Wm. W. Baker	47.05	-122.3
M	JC-1810.01001	CAS	USA: Oregon: Washington Co., 5 miles south of Forest Grove, 18 November 1940, W. Ivie	45.45	-123.14
M	JC-1869.02001	CAS	USA: Oregon: near Clatskanie, Locoda Station, needles of pine and cedar, 31 March 1937, J. Schuh	46.16	-123.15
M	JC-1902.01001	CAS	USA: Washington: Pierce Co., Electron, 25 March 1947, S.E. Crumb and Wm. W. Baker	46.99	-122.19
M	JC-1904.01002	CAS	USA: Washington: Grays Harbor Co., Westport, Joe Wilcox	46.89	-124.1
M	JC-1904.02001	CAS	USA: Washington: Grays Harbor Co., Westport, Joe Wilcox	46.89	-124.1
M	JC-1935.01001	CAS	USA: Washington: Pierce Co., Puyallup, 24 December 1934, Wm. W. Baker	47.18	-122.29
M	JC-1940.01001	CAS	USA: Washington: Pierce Co., Electron, 7 April 1937, Wm. W. Baker	46.99	-122.19
M	JC-1946.02001	CAS	USA: Washingotn: Grays Harbor Co., Montesano, 25 February 1933, Wm. W. Baker	46.98	-123.6
M	JC-1947.01001	CAS	USA: Washington: Pierce Co., Puyallup, in moss, 16 January 1932, Wm. W. Baker	47.18	-122.29
M	JC-1951.01001	CAS	USA: Washington: Cowlitz Co., Oak Point, 11 October 1933, Wm. W. Baker	46.19	-123.19
M	JC-1957.01001	CAS	USA: Washington: Grays Harbor Co., Westport, 9 April 1933, Wm. W. Baker	46.89	-124.1
M	JC-1958.02001	CAS	USA: Washington: Grays Harbor Co., Montesano, 14 April 1933, Joe Wilcox	46.98	-123.6
M	JC-1961.01001	CAS	USA: Washington: Kittitas Co., Cle Elum, 4 April 1933, Wm. W. Baker	47.19	-120.94
M	JC-1961.01003	CAS	USA: Washington: Kittitas Co., Cle Elum, 4 April 1933, Wm. W. Baker	47.19	-120.94
M	JC-1962.01001	CAS	USA: Washington: Yakima Co., Tieton, 2 April 1933, Wm. W. Baker	46.7	-120.75
M	JC-1963.01001	CAS	USA: Washington: Grays Harbor Co., Pacific Beach, 14 May 1932, Joe Wilcox	47.2	-124.2
M	JC-1964.01001	CAS	USA: Washington: Grays Harbor Co., Montesano, 20 February 1932, Joe Wilcox	46.98	-123.6

M	JC-1965.01001	CAS	USA: Washington: Pierce Co., Puyallup, in moss, January-February 1932, Wm. W. Baker	47.18	-122.29
M	JC-1967.01001	CAS	USA: Washington: Wahkiakum Co., Puget, in moss, 14 February 1932, Wm. W. Baker	46.17	-123.38
M	JC-1968.02001	CAS	USA: Washington: Grays Harbor Co., Montesano, in moss, 20 March 1932, Wm. W. Baker	46.98	-123.6
M	JC-1970.01001	CAS	USA: Washington: Pierce Co., Puyallup, in moss, 6 March 1932, Wm. W. Baker	47.18	-122.29
M	JC-1971.01001	CAS	USA: Washington: Pierce Co., Tacoma, in moss, 29 January 1932, Wm. W. Baker	47.25	-122.44
M	JC-1972.01001	CAS	USA: Washington: Kittitas Co., Cle Elum, in debris, 21 April 1935, Wm. W. Baker	47.19	-120.94
M	JC-1982.01001	CAS	USA: Oregon: Washington Co., Timber, dead leaves, 19 April 1941, J.C. Chamberlin	45.72	-123.295
M	JC-2061.01001	EMEC	USA: California: Monterey Co., Monterey, Francis Simes Hastings Natural History Reservation, Neotona [sic.] house, 646 LPT, 24 January 1946, Microcreagris nigrescens paratype	36.38	-121.56
M	JC-2099.01001	EMEC	USA: California: Monterey Co., Monterey, Francis Simes Hastings Natural History Reservation, Roberstson Creek, 26 March 1946, J.M. Linsdale, Globocreagris nigrescens holotype	36.38	-121.56
M	JC-706.02001	CAS	USA: Washington: Pierce Co., Puyallup, needles of Douglas fir on ground, 27 February 1929, Wm. W. Baker	47.18	-122.29
M	JC-895.02003	CAS	USA: Oregon: Benton Co., 5-6 mi W of Greenbury, Leaf mould in foothills, 3 March 1937, J.C. Chamberlin and J. Schugh	44.44	-123.38
M	JC-896.03001	CAS	USA: Oregon: Lincoln Co., junction of Alsea and Five Rivers, leaf mould, alder and maple, 13 March 1937, Joe Schuh	44.36	-123.83
M	S-3397.6	AMNH	USA: Oregon: Tillamook Co., Garibaldi, 2 miles north of Duff, 15 March 1955, V. Roth	45.56	-123.91
M	S-3401.5	AMNH	USA: Oregon: Hood River Co., Hood River, 4 February 1955, V. Roth	45.7	-121.52
M	S-3402.7	AMNH	USA: Oregon: Marion Co., 4 miles north of Gates, 23 January 1955, V. Roth	44.81	-122.42

APPENDIX C.

THE FIRST PUTATIVE VENOM SEQUENCES FROM A PSEUDOSCORPION (PSEUDOSCORPIONES: NEOBISIIDAE)

Garrett B. Hughes and Wendy Moore

Department of Entomology, University of Arizona, Tucson, AZ, 85721, USA; Email: gbhughes@email.arizona.edu

ABSTRACT

There are many organisms that produce venom secretions. In recent years, next-generation sequencing has allowed researchers to quickly investigate the composition of venom proteins relatively quickly, even for under-studied organisms. Pseudoscorpions are venomous arachnids whose venom components have not yet been investigated. Here we present the first transcriptome of pseudoscorpion venom glands. By comparing the transcriptomes of the venom bearing chelae and non-venom bearing patella-femur of the neobissine, *Globocreagris pinalenoensis* Hughes and Moore, we identify key components of their venom including astacin-like metalloproteases, chitinases, cysteine-rich secretory proteins, Kunitz-type serine protease inhibitors, phospholipase A2, and scorpion La1-like peptides. We briefly review these proteins and discuss possible functions in light of what is known of pseudoscorpion behavior.

INTRODUCTION

Venoms are complex mixtures of proteins, salts, and other biosynthesized products used for subduing prey and defending against enemies. Venoms are found in a diverse array of animals, from insects and mollusks, to reptiles and mammals. The proteinaceous components of venom appear to have been recruited to venom glands over evolutionary time from non-toxic proteins that have other functions in the body (Fry et al. 2009, Reyes-Velasco et al. 2014). Venoms are involved in disrupting ion channels, blocking other proteins, lysing tissues, and many other functions (Fry et al. 2009). Venoms are frequently surveyed for use in medicine, both to understand the effects of venom on humans and for development of drugs to treat other ailments (Lewis & Garcia 2003).

Spiders and scorpions are well-known venomous animals that often inspire fear in humans because of a few medically significant taxa. Spiders and scorpions belong to the order Arachnida. This order consists of 11 extant orders, 3 of which possess distinct venom glands and associated venom-delivery apparatuses: Scorpiones, Araneae, and Pseudoscorpiones. Although the ordinal relationships within the Arachnida are not clear (Sharma et al. 2014), one consistent trend across the majority of phylogenetic hypotheses is that scorpions, spiders, and pseudoscorpions are never each other's sister group, suggesting that each order has derived its venom systems independently (Fig. 1). This hypothesis is supported morphologically by the different locations of the venom glands and venom-delivery systems in these orders. Spiders possess venom glands in their cephalothorax and inject venom using the chelicerae. Scorpions possess venom glands in the post-anal telson at the end of the metasoma and deliver venom through the aculeus at the tip of the telson. Pseudoscorpions possess venom in the pedipalp chelae and deliver venom through the venedens – a tooth at the tip of one or both of the fingers of the chelae. Additionally, these orders are each extremely old. Geologic evidence suggests that the first appearance of each of these orders was the Silurian (428 ma) for scorpions, Devonian (392 ma) for pseudoscorpions, and Carboniferous (312 ma) for spiders (Dunlop 2010). Spider and scorpion venoms are relatively well-studied, but little is known of pseudoscorpion venom.

All species classified in the pseudoscorpion suborder Iocheirata possess venom glands in the chelate pincers of the pedipalps (Harvey 1991) (Fig. 2). Pedipalps are sensory pre-oral appendages in arachnids that are used to manipulate food and other items. Pseudoscorpions, like their cousins, the scorpions, use their pedipalp chelae to grasp prey items. Those that possess venom glands will often subdue their prey with venom before transferring them to the chelicerae for maceration and ingestion (Gilbert 1951). The pseudoscorpion venom apparatus consists of a large venom sac lined with glandular cells which leads to a small venom duct and exits out the terminal tooth called a venedens (Fig. 3A). In between the venom duct and venom sac is an enigmatic structure called the nodus ramosus. Its function is not known, currently, but it is a sclerotized structure that is visible in specimens cleared with KOH. Pseudoscorpions can have venom glands in the fixed finger, the movable finger, or both fingers of the pedipalp chelae. The size and shape of the venom sac varies among taxa; it may be short and fully contained within the finger or may extend into the chela hand.

Although pseudoscorpions have long been known to possess venom based on morphological investigations (Croneberg 1888, Chamberlin 1924) and observations of prey behavior after being attacked (Gilbert 1951), little is known of the function and nothing is known of the composition of their venom. To date, only one study has investigated the venom of pseudoscorpions by introducing crude venom extract to artificial nerve cells (dos Santos & Coutinho-Netto 2006), but this study did not identify any components of the venom.

Transcriptomics is a rapidly growing field that allows researchers to investigate venoms without purifying and sequencing each protein. Hidden Markov models and gene ontology predictors can give insights into the components of animal venoms and their various functions. Such approaches have been used to explore the toxins of a variety of animals, from relatively understudied animals like bloodworms (von Reumont et al. 2014), to well-known animals like scorpions (Santibáñez-López et al. 2016). Transcriptomic approaches may be particularly well-suited to preliminary investigations of understudied organisms by helping researchers identify a broad array of putative proteins relatively inexpensively. These proteins can then be targeted for subsequent protein-sequencing and assays of protein function.

In this study, we present the first transcriptomic investigation of pseudoscorpion venom glands using the species *Globocreagris pinalenoensis* Hughes and Moore 2017 (Neobisiidae). We predict that pseudoscorpion venom will have many functions similar to spiders and scorpions despite the venom apparatuses having evolved anciently and independently in these three groups. We make this prediction on the basis of prey similarity. That is, pseudoscorpions, spiders, and scorpions all prey frequently upon other arthropods, so we expect the venom components to converge toward similar functions.

METHODS

We obtained 50 specimens of *Globocreagris pinalenoensis* (Neobisiidae) from the Pinaleño Mountains, Graham Co., Arizona. Before extracting the venom glands for RNA sequencing, we attempted to milk the pseudoscorpions using a protocol adapted from Murali and Chandrashekara (2013). By forcing the pseudoscorpions to expend their venom, we hoped to be able to capture more venom transcripts as the venom system

attempted to replenish the venom proteins stored in the venom sac. A sterilized agar gel was cut into small pieces, held in sterilized forceps, and presented to pseudoscorpions in a threatening manner to induce pinching. When presented with the gel, pseudoscorpions spread their pedipalps, opened their chelae, and retreated. When cornered, pseudoscorpions attacked the gel with their chelae, presumably utilizing their venom defensively.

Two days after milking, we extracted the venom glands from the pseudoscorpions for RNA sequencing. Although nothing is known about how fast venom protein transcription is initiated after expending venom, we hoped that 2 days would be sufficient time for upregulation without being so long that the venom gland returned to its resting state. Each specimen was placed into a dish with RNA*later*. The pedipalps were removed from the live pseudoscorpions. The patellae and femora (Fig. 2B) of each specimen were detached from the chelae and combined into a single vial of RNA*later*. To extract the venom glands from the chelae, an incision was made along the ventral surface of the chela from the joint between the chela and patella to the joint of the movable finger. The two condyles of the movable finger were also clipped, using dissecting scissors. These incisions allowed us to pull the vast chelal musculature from the chela by grabbing each finger with forceps and pulling them apart; the muscle tissue remained attached to the movable finger and separated from the venom gland which was attached to the fixed finger. We then removed excess cuticle from the chela so that only the fixed finger with the attached venom gland remained and we placed these into a combined vial of RNA*later*. The chela musculature and excess cuticle were discarded. In total, 100 venom glands were obtained from 50 specimens.

RNA samples were homogenized and RNA extracted using Qiagen RNeasy Mini Kit. DNA was removed during extraction. Libraries were built using Illumina TruSeq RNA kit. RNA sequencing was carried at the University of Arizona Genetics Core facility on an Illumina HiSeq2500 machine with the Illumina Rapid-Run SBS chemistry. Our 2 samples were among 6 samples run on a single lane.

We used Trinity (Grabherr et al. 2011) on the University of Arizona high performance computer to assemble the RNA-seq files with a default k-mer size and word size of 25. In total 192,076 transcripts were assembled with a median contig length of 361 and a mean contig length of 654.94. We combined the Illumina data for assembly so that we could directly compare contigs between the two samples and see how many reads from each sample made up each contig.

After assembly, sequences were passed through the Trinotate pipeline, consisting of Trinity (Grabherr et al. 2011), HMMER (Finn et al. 2011), Pfam (Punta et al. 2012), SignalP (Petersen et al. 2011), tmHMM (Krogh et al. 2001), BLASTX and BLASTP (Altschul et al. 1990), KEGG (Kanehisa et al. 2011), GO (The Gene Ontology Consortium 2000), eggnog (Powell et al. 2011), and RNAmmer (Lagesen et al. 2007). We used FileMaker Pro (10.0v1 FileMaker, Inc.) to organize and explore the Trinotate data.

Because we pooled our specimens together, we did not have bioreplicates, and therefore had no measure of statistical significance of expression. As a surrogate, we tracked the number of reads from the chela and from the patella-femur samples separately. We filtered all contigs by selecting those that had at least 100 reads from the chela map back to the contig and selecting contigs with at least five times as many chela

reads that mapped back to the contig as reads from the patella-femur. We manually examined the Pfam, GO terms, and BLAST hits of these sequences and identified those that had putative venom function.

We checked each putative venom sequence for whether SignalP detected signal peptides. Signal peptides are found in transmembrane proteins and in secreted proteins. Because venom peptides are expected to be produced within gland cells and secreted into the storage reservoir, we would predict venom proteins to have signal peptides. SignalP 4.0 has an improved ability to distinguish signal peptides from transmembrane regions (Petersen et al. 2011).

RESULTS AND DISCUSSION

Trinity assembled 160,838 gene groups with 192,076 transcripts. We removed all contigs that had 0 reads matching from the chelae for a total of 179,266 transcripts of which, 34,231 were unique to the chelae.

In total, we found 887 gene isoforms that met our conditions of having at least 100 reads from the chelae transcriptome and at least 5 times more reads from the chelae transcriptome than from the patella-femur transcriptome. Of these, 497 did not match any sequences in the BLAST databases. Including alternate open reading frames, there were 564 putative sequences. We found open reading frames in 262 of these sequences, all of which had signal peptides detected with SignalP.

The remaining 390 gene isoforms had hits to known proteins in BLASTX or BLASTP searches. Including alternate open reading frames, there were 773 putative sequences. Of these, 214 were unique to the chelae. SignalP detected signal peptides on 374 of these gene isoforms. We manually examined the BLAST hits, Pfam families, and GO terms and found 41 sequences that seemed likely to be venom proteins (Table 1). Below, we briefly discuss the function of the most notable putative venom toxins in light of what is known of pseudoscorpions and their kin. These putative venoms are presented in order of decreasing likelihood of being venom proteins.

Scorpion La1-like peptides – These toxins have been found in the venoms of many scorpions (Schwartz et al. 2007, Silva et al., 2009, Ma et al. 2009, Ma et al. 2010, Diego-García et al. 2012, He et al. 2013, Luna-Ramírez et al. 2013, Santibáñez-López et al. 2016). These toxins possess a single von Willebrand Factor (VWF) Type C domain. Proteins with this domain appear to be involved in hemostasis (Peyvandi et al. 2011), bone morphogenesis (Zhang et al. 2002), protein transport, apoptosis, and inflammation (Lenting et al. 2012), but its function in scorpion venom is currently unknown. We found 3 open reading frames that matched the conserved 6-cysteine motif of VWF type C domain and had BLAST matches to La1-like peptides. La1-like peptides do not seem to be important to toxicity toward humans because they are present even in harmless scorpions like *Hadrurus gertschi* (Schwartz et al. 2007) and *Urodacus yaschenkoi* (Luna-Ramírez et al. 2013). Thus, they are likely to be involved in prey-capture. Since scorpions are primarily predators of arthropods, this venom toxin probably targets insect systems. Since pseudoscorpions also prey upon arthropods, it is not surprising that such a toxin would be present in their venom. What *is* surprising is that La1-like peptides are only

known from scorpions, making the discovery of La1-like peptide in a pseudoscorpion quite notable.

Phospholipase A2 – Phospholipase A2 (PLA2) is found in the venom of many organisms, including cephalopods, cnidarians, insects, scorpions, snakes, and ticks (Fry et al. 2009). PLA2 typically cleaves fatty acids from glycerol (Finn et al. 2017), but it can assume a variety of other roles, including neurotoxin (Menashé et al. 1980), myotoxin (Guiterrez & Lomonte 1995), cytotoxin (Ownby et al. 1997), and lipid signal (Burke & Dennis 2009). An aspartate residue and two glycine residues are important for coordinating the calcium ion ligand in the venom PLA2 of a viper (van den Bergh et al. 1988). Two of our transcripts had PLA2 domains as indicated by Pfam and appear to have the conserved glycine and aspartate residues necessary for the functional protein. These sequences had highest similarity to phospholipase A2 from honey bees of the genus *Apis*. PLA2 from *Apis* has been demonstrated to be cytotoxic to skeletal muscle cells in rats (Ownby et al. 1997). PLA2, when purified from cobra venom, was found to have high toxicity in arthropods (Menashé et al. 1980). It's possible that pseudoscorpion phospholipase A2 from venom also has cytotoxic properties that help it subdue prey, which consists of arthropods like springtails, small flies, larvae, and various other small arthropods (Weygoldt 1969). However, given the diversity of phospholipase A2 functions – even within venoms – it is impossible to say for sure until the proteins are isolated and characterized.

Astacin-like Metalloprotease – Astacin-like proteases are a subfamily of zinc-metalloproteases with the designation peptidase M12A. The first member described from this subfamily was astacin, a digestive enzyme of crayfish (Titani et al. 1987). Astacin-like metalloproteases share the common motif of HEXXHXXGFXHEXXRXDR followed by a subsequent MXY domain. The histidines of the HEXXH region and the tyrosine of the MXY coordinate the zinc ion (Bond & Beynon 1995). Astacin-like metalloproteases often break down structural proteins such as gelatin, casein, insulin B chain, and bradykinin (Bond & Beynon 1995). The first astacin-like metalloprotease venom toxin was found in the venoms of brown spiders (da Silveira et al. 2007), but they have also been found recently in sea anemone venom (Macrander et al. 2015). We found a total of 20 transcript isoforms with 28 open reading frames that hit astacin-like metalloprotease toxins from *Loxosceles*. Trevisan-Silva and others (2010) propose that metalloproteases in venoms may explain why *Loxosceles* wounds don't heal well because the proteases may break down platelets and other structural proteins near the bite site. When rabbit subendothelial cells are exposed to *Loxosceles* astacin-like protease, they are lysed and lose adhesion to their substrate (da Silveira et al. 2007). This may help with the spread of other toxin compounds as cell barriers are broken up. It has also been suggested that metalloproteases may be involved with pre-digestion of proteins in the prey (Trevisan-Silva et al. 2010). Gilbert (1951) described the feeding behaviors of some British pseudoscorpions. He observed that species that possess venom glands hold their prey in their pedipalps after capture for up to 20 minutes. While this certainly allows time for the venom to disable the prey item, it is also possible that this time allows for digestive venom proteins to begin preparing the prey for ingestion. Venom proteases may also be involved in post-translationally modifying other venom proteins before, during, or after injection into the victim (Fox & Serrano 2008).

Kunitz-type toxins –Kunitz-type serine protease inhibitors are found in the venoms of a variety of taxa, including snakes, spiders, scorpions, insects, mollusks, and cnidarians (Fry et al. 2009). They primarily belong to the bovine pancreatic trypsin inhibitor group. These proteins have a 50-residue-long domain that contains 6 cysteines involved in disulfide bonds (Punta et al. 2012, Finn et al. 2017). Five of the astacin-like protease toxins we found in the transcriptome had both kunitz-type serine protease inhibitor domains and astacin-like domains, indicating these transcripts may have dual protease and protease-inhibition activity. Kunitz-type serine protease inhibitors often inhibit enzymes like trypsin, chymotryipsin, plasmin, and elastase (Chaim et al. 2011). The presence of plasmin inhibition is thought to prevent wounds from closing and is thought to be important in the salivary secretions of haematophagous insects, which are now considered to be venoms (Fry et al. 2009). For non-haematophagous insects, the benefit of inhibiting proteases in the victim seems less clear, though it may retard immune responses (Choo et al. 2012). Kunitz-type serine protease inhibitors can also exhibit potassium channel blocking activity, as found in the tarantula *Ornithoctonus huwena* (Yuan et al. 2008) and several species of scorpions (Chen et al. 2012). In these cases, they are referred to as Kunitz-type toxins (Ranashinghe & McManus 2013). The Kunitz-type serine protease inhibitors found in *Globocreagris pinalenoensis* may possess potassium channel blocking activity like other Kunitz-type toxins, allowing it to paralyze prey.

Chitinase – Chitinases are found in the venoms of centipedes (Undheim et al. 2014), spiders (Yan & Wang 2015), cephalopods and insects (Fry et al. 2009). The chitinases in the pseudoscorpion transcriptome are most similar to chitinase 3. Chitinase 3 proteins belong to the glycoside hydrolase family 18 which bind chitin and usually hydrolyze it. There are four major domains in insect chitinases. Despite the evolutionary distance between insects and pseudoscorpions, one of those domains is mostly conserved in the pseudoscorpion: FDGLDLDWEYP. This is the active catalytic site for chitin hydrolysis, following the generic motif of DXXDXDXE, with the glutamic acid residue being the most critical for catalytic function (Tsujibo et al. 2003, Arakane & Muthukrishnan 2010). The other three domains are also present, although much more divergent from the insect motifs. Despite these small differences, these chitinases appear to be functional, with both chitin-binding and chitinase catalytic domains. There is still some question, however, over whether chitinases found in venom proteins are serving primarily to break down cellulose. The parasitic wasp, *Chelonus*, also has chitinases in its venom that maintain the critical glutamic acid residue, yet the eggs it parasitizes are devoid of chitin (Kirshanan et al. 1994). Furthermore, it is unclear how the chitinase can be utilized in the venom without it acting upon the chitin of the animal producing the venom (Kirshanan et al. 1994). More investigation is needed into the role of chitinases in venom.

Cysteine-rich secretory proteins – Cysteine-rich secretory proteins, also known as CRiSPs, are small-molecular-weight proteins with many disulfide bonds that belong to the CAP (cysteine-rich secretory proteins, antigen-5, and pathogenesis-related 1 proteins) superfamily. They are common in venoms from a variety of venomous animals, including spiders, scorpions, snakes, and insects (Fry et al. 2009). CRiSPs found in snake venom and mammalian reproductive systems can inhibit ion channels (Gibbs & O'Bryan 2007). We found 4 gene isoforms that Pfam identified as CRiSPs. BLAST searches matched

these most closely to a family of CAP proteins called peptidase inhibitor 16 (PI16) instead of the CRiSP family. It's unclear whether these proteins are acting as peptidase inhibitors, ion channel inhibitors, or both.

CONCLUSION

We have presented the first transcriptome of a pseudoscorpion venom gland and identified putative toxins used by these predators. One notable limitation to our study is that we had no method of assessing whether transcripts were statistically significantly more highly expressed in the chelae than in the patellae and femora. We used the number of reads mapping back to each contig as a rough estimate of expression, but our inability to normalize the reads across samples means that our determination of whether a transcript was more highly expressed in the chela than the pedipalps is uncertain. It's possible that some sequences appeared to be more highly expressed in the chelae that really were not, or that we may not have detected sequences that were more highly expressed in the chelae. We had attempted to mitigate the effects of this shortcoming by applying stringent filtering conditions on the transcripts. Our findings present a solid starting point for future explorations of the venom content of pseudoscorpions.

Remarkably, we found 262 open reading frames from the transcriptome of the chelal venom sacs that had no BLAST hits. These could represent novel proteins with new function, since very few of them had domains recognized by Pfam and each possessed a signal peptide. There is potentially a rich source of bioactive proteins to be characterized from the venom of pseudoscorpions, especially considering the ancient divergence between venomous arachnids.

As we predicted, we found prominent spider and scorpion toxins in the venom of the pseudoscorpion (*Loxosceles* PLA2 and *Mesobuthus* La1-like peptide). We also found putative venom proteins that may be involved in ion-channel inhibition, which would explain the paralysis induced by pseudoscorpions on their prey (Gilbert 1951, de Andrade & Gnaspini 2002).

Future work should include extraction and purification of pseudoscorpion venom to verify that the putative proteins found in this transcriptome are found as mature peptides in the venom. We have also identified a dire need for functional assays of common venom components to determine their function for subduing prey and or defending against would-be predators. In particular, we need to know how chitinases, astacin-like metalloproteases, and La1-like peptides from venom act to disable other organisms.

ACKNOWLEDGEMENTS

We are deeply grateful to Reilly McManus and Tanya Renner for their assistance with the computational aspects of transcriptome assembly and sequence searches. This work is in partial fulfillment of GBH's PhD degree in the Graduate Interdisciplinary Program in Entomology and Insect Science at the University of Arizona.

LITERATURE CITED

Altschul, S.F., W. Gish, W. Miller, E.W. Myers, DJ.J. Lipman. 1990. Basic local alignment search tool. *Molecular Biology*, 215:403–410.

Arakane, Y., & S. Muthukrishnan. 2010. Insect chitinase and chitinase-like proteins. *Cellular and Molecular Life Sciences*, 67: 201–216.

Bond, J.S. & R.J. Beynon. 1995. The astacin family of metalloendopeptidases. *Protein Science*, 4: 1247–1261.

Burke, J.E. & E.A. Dennis. 2009. Phospholipase A2 structure/function, mechanism, and signaling. *Journal of Lipid Research*, April Supplement, S237–S242.

Chaim, O.M., D. Trevisan-Silva, D. Chaves-Moreira, A.C.M. Wille, V.P. Ferrer, F.H. Matsuara, O.C. Mangili, R.B. da Silveira, L.H. Grmski, W. Gremski, A. Senff-Ribeiro, & S.S. Veiga. 2011. Brown spider (*Loxoscelese* genus) venom toxins: tools for biological purposes. *Toxins*, 3: 309–344, doi:10.3390/toxins3030309.

Chamberlin, J.C. 1924. Preliminary note on the pseudoscorpions as a venomous order of the Arachnida. *Entomological news, and proceedings of the Entomological Section of the Academy of Natural Sciences of Philadelphia*, 35:205–209.

Chen, Z., Y. Hu, W. Yang, Y. He, J. Feng, B. Wang, R. Zhao, J. Ding, Z. Cao, W. Li, & Y. Wu. 2012. Hg1, novel peptide inhibitor specific for Kv1.3 channels from first scorpion Kunitz-type potassium channel toxin family. *The Journal of Biological Chemistry*, 287(17): 13813–13821.

Choo, Y.M., K.S. Lee, H.J. Yoon, Y. Qiu, H. Wan, M.R. Sohn, H.D. Sohn, & B.R. Jin. 2012. Antifibrinolytic role of a bee venom serine protease inhibitor that acts as a plasmin inhibitor. *PLoS One*, 7(2): e32269; doi: 10.1371/journal.pone.0032269.

Croneberg, A. 1888. Beitrag zur kenntniss des baues der pseudoscorpione. *Bulletin de la Société impériale des naturalistes de Moscou*, 2:416–461.

da Silveira, R.B., A.C.M. Wille, O.M. Chaim, M.H. Appel, D.T. Silva, C.R.C. Franco, L. Toma, O.C. Mangili, W. Gremski, C.P. Dietrich, H.B. Nader, & S.S. Veiga. 2007. Identification, cloning, expression, and functional characterization of an astacin-like metalloprotease toxin from *Loxosceles intermedia* (brown spider) venom. *Journal of Biochemistry*, 406: 355–363.

de Andrade, R. & P. Gnaspini. (2002). Feeding in *Maxchernes iporangae* (Pseudoscorpiones, Chernetidae) in captivity. The Journal of Arachnology, 30: 613-617.

Diego-García, E., S. Peigneur, E. Clynen, T. Marien, L. Czech, L. Schoofs, & J. Tytgat. 2012. Molecular diversity of the telson and venom compononts from *Pandinus cavimanus* (Scorpionidae Latreille 1802): transcriptome, venomics and function. *Proteomics*, 12: 313–328.

dos Santos, W.F. & J. Coutinho-Netto. 2006. Effects of the *Paratemnus elongates* pseudoscorpion venom in the uptake and binding of the L-glutamate and GABA from rat cerebral cortex. *Journal of Biochemistry and Molecular Toxicology*, 20(1): 27–34.

Dunlop, J.A. 2010. Geological history and phylogeny of Chelicerata. *Arthropod Structure & Development*, 39: 124–142.

Finn, R.D., T.K. Attwood, P.C. Babbitt, A. Bateman, P. Bork, A.J. Bridge, H. Chang, Z. Dosztányi, S. El-Gebali, M. Fraser, J. Gough, D. Haft, G.L. Holliday, H. Huang, X. Huang, I. Letunic, R. Lopez, S. Lu, A. Marchler-Bauer, H. Mi, J. Mistry, D.A. Natale, M. Necci, G. Nuka, Christine A. Orengo, Youngmi Park, Sebastien Pesseat, Damiano Piovesan, Simon C. Potter, N.D. Rawlings, N. Redaschi, L. Richardson, C. Rivoire, A. Sangrador-Vegas, C. Sigrist, I. Sillitoe, B. Smithers, S. Squizzato, G. Sutton, N. Thanki, P.D. Thomas, S.C.E. Tosatto, C.H. Wu,

Fox, J.W. & S.M.T. Serrano. 2008. Insights into and speculations about snake venom metalloproteinase (SVMP) synthesis, folding and disulfide bond formation and their contribution to venom complexity. *FEBS Journal*, 275: 3016–3030.

Gibbs, G.M. & M.K. O'Bryan. 2007. Cysteine rich secretory proteins in reproduction and venom. *Society for Reproduction and Fertility Supplement*, 65: 261–267.

I. Xenarios, L. Yeh, S. Young & A.L. Mitchell. 2017. InterPro in 2017 — beyond protein family and domain annotations. *Nucleic Acids Research*, Jan 2017; doi: 10.1093/nar/gkw1107

Finn, R.D., J. Clements, & S.R. Eddy. 2011. HMMER web server: interactive sequence similarity searching Nucleic Acids Research. Web Server Issue 39: W29–W37.

Fry, B.G., K. Roelants, D.E. Champagne, H. Scheib, J.D.A. Tyndall, G.F. King, T.J. Nevalainen, J.A. Norman, R.J. Lewis, R.S. Norton, C. Renjifo, & R.C. Rodríguez de la Vega. 2009. The toxicogenomic multiverse: convergent recruitment of proteins into animal venoms. *Annual Review of Genomics and Human Genetics*, 10: 483–511.

Gilbert, O. 1951. Observations on the feeding of some British false scorpions. *Proceedings of the Zoological Society of London*, 121(3): 547–555.

Grabherr, M.G., B.J. Haas, M. Yassour, J.Z. Levin, D.A. Thompson, I. Amit, X. Adiconis, L. Fan, R. Raychowdhury, Q. Zeng, Z. Chen, E. Mauceli, N. Hacohen, A. Gnirke, N. Rhind, F. di Palma, B.W. Birren, C. Nusbaum, K. Lindblad-Toh, N.

Friedman, A. Regev. 2011. Full-length transcriptome assembly from RNA-Seq data without a reference genome. *Nature Biotechnology* 29: 644–652.

Guiterrez, J. & B. Lomonte. 1995. Phospholipase A2 from *Bothrops* snake venom. *Toxicon*, 33(11): 1405–1424.

Harvey, M.S. 1992. The phylogeny and classification of the Pseudoscorpionida (Chelicerata: Arachnida). *Invertebrate Taxonomy*, 6: 1373–1435.

He, Y., R. Zhao, Z. Di, Z. Li, X. Xu, W. Hong, Y. Wu, H. Zhao, W. Li, & Z. Cao. 2013. Molecular diversity of Chaerilidae venom peptides reveals the dynamic evolution of scorpion venom components from Buthidae to non-Buthidae. *Journal of Proteomics*, 89: 1–14.

Kanehisa, M., S. Goto, Y. Sato, M. Furumichi, & M. Tanabe. 2012. KEGG for integration and interpretation of large-scale molecular datasets. *Nucleic Acids Research*, 40: D109–D114.

Krogh, A., B. Larsson, G. von Heijne, E.L. Sonnhammer. 2001. Predicting transmembrane protein topology with a hidden Markov model: application to complete genomes. *Journal of Molecular Biology*, 305(3):567–80.

Lagesen, K., P.F. Hallin, E. Rodland, H.H. Staerfeldt, T. Rognes, D.W. Ussery. 2007. RNammer: consistent annotation of rRNA genes in genomic sequences *Nucleic Acids Research*, 35(9): 3100-3108.

Lenting, P.J., C. Casari, O.D. Christophe, & C.V. Denis. 2012. von Willebrand factor: the old, the new and the unknown. *Journal of Thrombosis and Haemostasis*, 10: 2428–2437.

Lewis, R.J. & M.L. Garcia. 2003. Therapeutic potential of venoms. *Nature Reviews Drug Discovery*, 2: 790–802.

Luna-Ramírez, K., V. Quintero-Hernández, L. Vargas-Jaimes, C.V.F. Batista, K.D. Winkel, & L.D. Possani. Characterization of the venom from the Australian scorpion *Urodacus yaschenkoi*: molecular mass analysis of components, cDNA sequences and peptides with antimicrobial activity. *Toxicons*, 63: 44–45.

Ma, Y., R. Zhao, Y. He, S. Li, J. Liu, Y. Wu, Z. Cao & W. Li. 2009. Transcriptome analysis of the venom gland of the scorpion *Scorpiops jendeki*: implication for the evolution of the scorpion venom arsenal. *BMC Genomics*, 10: 290; DOI:10.1186/1471-2164-10-290.

Ma, Y., Y. He, R. Zhao, Y. Wu, W. Li, Z. Cao. 2012. Extreme diversity of scorpion venom peptides and proteins revealed by transcriptomic analysis: implication for

proteome evolution of scorpion venom arsenal. *Journal of Proteomics*, 75(5): 1563–1576.

Macrander, J., M.R. Brugler, & M. Daly. 2015. A RNA-seq approach to identify putative toxins from acrorhagi in aggressive and non-aggressive *Anthopleura elegantissima* polyps. *BMC Genomics*, 16: 221.

Menashé, M., H. Rochat, & E. Zlotkin. 1980. Cobra venom phospholipase highly toxic to arthropods—I. Purification and characterization. *Insect Biochemistry*, 10: 621–630.

Murali, S. & K. Chandrashekara. 2013. Milking method' – novel technology for venom collection from aculate Hymenoptera and used for screening of *in-vitro* antimicrobial activity against pathogens. *International Journal of Agriculture, Environment & Biotechnology*, 6(3): 551–555.

Ownby, C.L., J.R. Powell, M. Jiang, J.E. Fletcher. 1997. Mellitin and phospholipase A2, from bee (*Apis mellifera*) venom causes necrosis of murine skeletal muscle *in vivo*. *Toxicon*, 35(1): 67–80.

Petersen, T.N., S. Brunak, G. von Heijne, & H. Nielsen. 2011. SignalP 4.0: discriminating signal peptides from transmembrane regions *Nature Methods*, 8: 785–786.

Peyvandi, F., I. Garaiola, & L. Baronciani. 2011. Role of von Willebrand factor in the haemostasis. *Blood Transfusion*, 9 Suppl 2: s3-s8 DOI 10.2350/2011.0028S

Powell, S., D. Szklarczyk, K. Trachana, A. Roth, M. Kuhn, J. Muller, R. Arnold, T. Rattei, I. Letunic, T. Doerks, L.J. Jensen, C. von Mering, P. Bork. 2011. eggNOG v3.0: orthologous groups covering 1133 organisms at 41 different taxonomic ranges. *Nucleic Acids Research*, 40(Database issue): D284–D289.

Punta, P.C. Coggill, R.Y. Eberhardt, J. Mistry, J. Tate, C. Boursnell, N. Pang, K. Forslund, Ceric, J. Clements, A. Heger, L. Holm, E.L.L. Sonnhammer, S.R. Eddy, A. Bateman, R.D. Finn. 2012. The Pfam protein families database. *Nucleic Acids Research*, Database Issue 40:D290–D301.

Ranashinghe, S. & D.P. McManus. 2013. Structure and function of invertebrate Kunitz serine protease inhibitors. *Developmental and Comparative Immunology*, 39: 219–277.

Reyes-Velasco, J., D.C. Card, A.L. Andrew, K.J. Shaney, R.H. Adams, D.R. Schield, N.R. Casewell, S.P. MAckessy, & T.A. Castoe. Expression of venom gene homologs in diverse python tissues suggests a new model for the evolution of snake venom. *Molecular Biology and Evolution*, 32(1): 173–183.

Santibáñez-López, C.E., J.E. Cid-Uribe, C.V.F. Batista, E. Ortiz, & L.D. Possani. Venom gland transcriptomic and proteomic analyses of the enigmatic scorpion *Superstitionia*

donensis (Scorpiones: Superstitioniidae), with insights on the evolution of its venom components. *Toxins,* 8(12): 367; doi:10.3390/toxins8120367.

Schwartz, E.F., E. Diego-García, R.C. Rodríguez de la Vega, & L.D. Possani. Transcriptome analysis of the venom gland of the Mexican scorpion *Hadrurus gertschi* (Arachnida: Scorpiones). *BMC Genomics,* 8: 119.

Sharma, P.P., S.T. Kaluziak, A.R. Pérez-Porro, V.L. Gonzaléz, G. Hormiga, W.C. Wheeler, & G. Giribet. 2014. Phylogenomic interrogation of Arachnida reveals systemic conflicts in phylogenetic signal. *Molecular Biology and Evolution,* 31(11): 2963–2984.

Silva, E.C.N., T.S. CAmargos, A.Q. Maranhão, I. Silva-Pereira, L.P. Silva, L.D. Possani, & E.F. Schwartz. 2009. Cloning and characterization of cDNA sequences encoding for new venom peptides of the Brazilian scorpion *Opisthacanthus cayaporum*. *Toxicon,* 54: 252–261.

Titani, K., H.J. Torff, S. Hormel, S. Kumar, K.A. Walsh, J. Rodl, H. Neurath, & R. Zwilling. 1987. Amino acid sequence of a unique protease from the crayfish *Astacus fluviatilis*. *Biochemistry*, 26: 222–226.

The Gene Ontology Consortium. 2000. Gene Ontology: tool for the unification of biology. *Nature Genetics*, 25: 25–29.

Trevisan-Silva, D., L.H. Gremski, O.M. Chaim, R.B. da Silviera, G.O. Meissner, O.C. Mangili, K.C. Barbaaro, W. Gremski, S.S. Veiga, & A. Senff-Ribeiro. 2010. Astacin-like metalloproteases are a gene family of toxins present in the venom of different species of the brown spider (genus *Loxosceles*). *Biochime,* 92: 21–32.

Tsujibo, H., T. Kubota, M. Yamamoto, K. Miyamoto, & Y. Inamori. Characteriziation of chitinase genes from an alkaliphilic actinomycete, *Nocardiopsis prasina* oPC-131. *Applied and Environmental Microbiology,* 69(2): 894–900.

Undheim, E.A.B., A. Jones, K.R. Clauser, J.W. Hollna,d S.S. Pineda, G.F. King, & B.G. Fry. 2014. Clawing through evolution: toxin diversification and convergence in the ancient lineage Chilopoda (centipedes). *Molecular Biology and Evolution*, 32(8): 2124–2148.

van den Bergh, C.J., A.J. Slotboom, H.M. Verheij, & G.H. de Haas. 1988. The role of aspartic acid-49 in the active site of phospholipase A2. *European Journal of Biochemistry,* 176: 353–357.

von Reumont, B.M., L.I. Campbell, S. Richter, L. Hering, D. Sykes, J. Hetmank, R.A. Jenner, & C. Bleidorn. 2014. A polychaete's powerful punch: venom gland transcriptomics of *Glycera* reveals a complex cocktail of toxin homologs. *Genome Biology and Evolution,* 6(9): 2406–2423.

Weygoldt, P. 1969. The Biology of Pseudoscorpions. Harvard University Press, Cambridge, Massachusetts.

Yan, S. & X. Wang. 2015. Recent advances in research on widow spider venoms and toxins. *Toxins*, 7: 5055–5067.

Yuan, C-H., Q-Y. He, K. Peng, J-B. Diao, L-P. Jiang, X. Tang, & S. Liang. 2008. Discovery of a distinct superfamily of kunitz-type toxin (KTT) from tarantulas. *PLoS One*, 3(10): e3414, doi:10.1371/journal.pone.0003414.

Zhang, J., Y. Huang, L. Q., J. Nickel, & W. Sebald. 2002. von Willebrand factor type C domain-containing proteins regulate bone morphogenetic protein signaling through different recognition mechanisms. *The Journal of Biological Chemistry*, 282: 20002–20014.

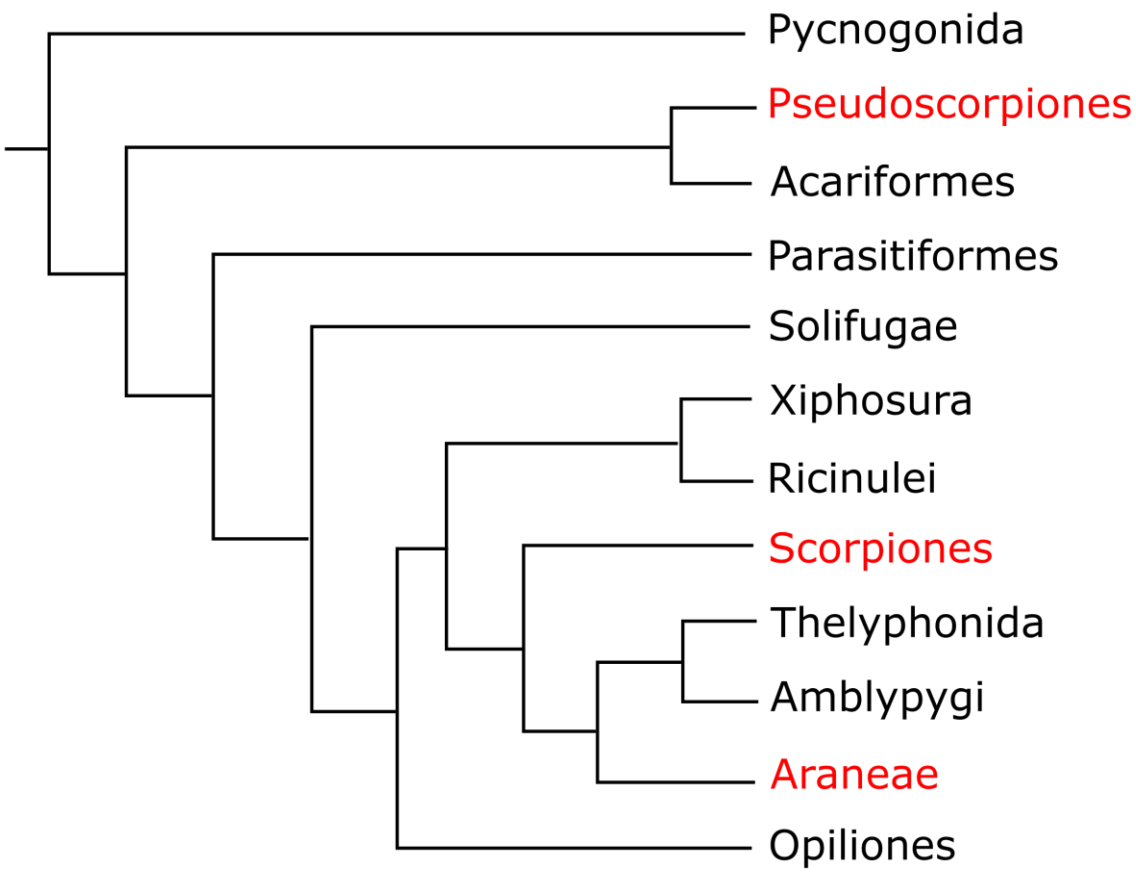

Figure 1. The most recent molecular phylogeny of the Arachnida, including chelicerate outgroups of Pycnogonida and Xiphosura, which appeared within Arachnida (adapted from Sharma et al. 2014). Red names indicate orders whose members secrete venom from non-salivary glands.

Figure 2. Dorsal habitus of *Globocreagris pinalenoensis* Hughes & Moore from the Pinaleño Mountains in Arizona.

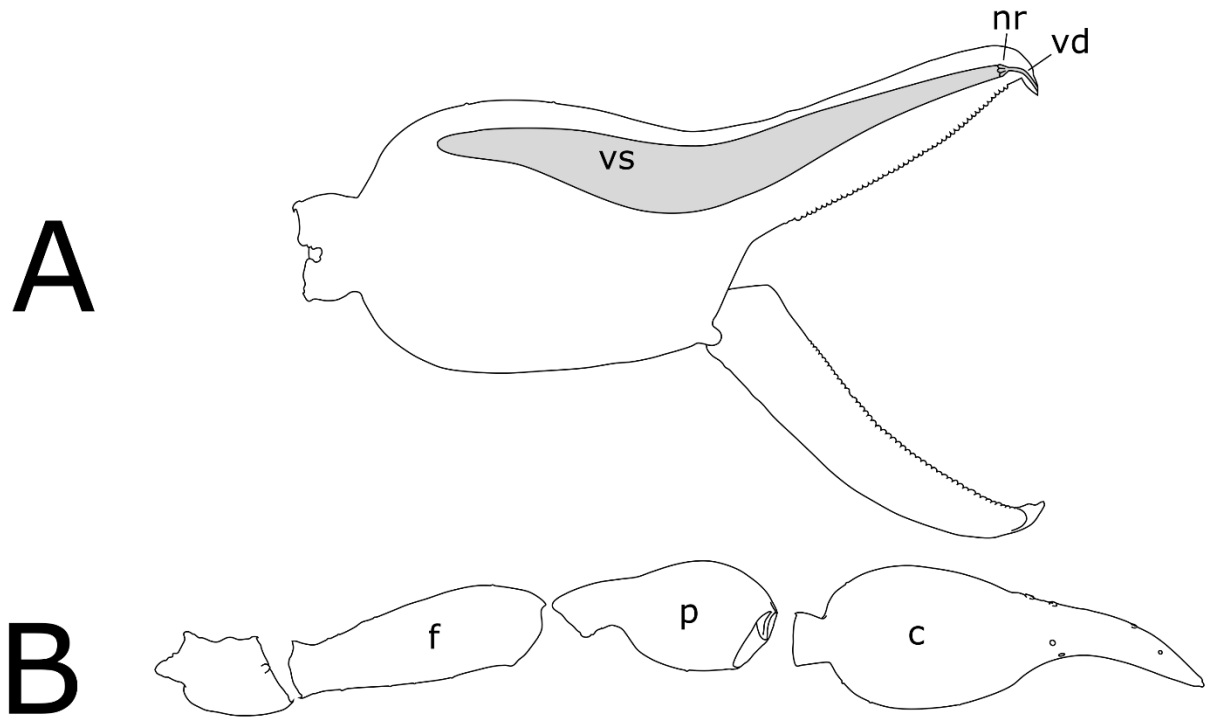

Figure 3. Pedipalp of *G. pinalenoensis*. A) External view of chela showing venom apparatus in gray. The venom sac (vs) feeds into the sclerotized nodus ramosus (nr) and into the venom duct (vd) which exits out the terminal tooth, or venedens. B) Dosal view of pedipalp showing the segments dissected and sequenced for this study: femur (f), patella (p), and chela (c).

Table 1. This table lists the gene isoforms we selected that 1) had at least 100 reads from the chela, 2) had at least 5 times as many chela reads as femur-patella reads, and 3) had BLAST or Pfam results that indicated putative venom function. Transcript isoforms that are reported twice had different open reading frames.

transcript ID	BLAST	Pfam	chela reads	pedipalp reads
TRINITY_DN66200_c0_g1_i1	Probable chitinase 3	PF01607.23^CBM_14^Chitin binding Peritrophin-A domain^23-72^E:1.8e-15`PF00704.27^Glyco_hydro_18^Glycosyl hydrolases family 18^102-448^E:1.8e-95	988.17	183.27
TRINITY_DN66200_c0_g1_i3	Probable chitinase 3	PF00704.27^Glyco_hydro_18^Glycosyl hydrolases family 18^33-362^E:1.9e-86	207.08	24.79
TRINITY_DN66455_c0_g1_i1	Probable chitinase 3	PF01607.23^CBM_14^Chitin binding Peritrophin-A domain^29-78^E:3.3e-15`PF00704.27^Glyco_hydro_18^Glycosyl hydrolases family 18^108-454^E:3.3e-95	1147.83	199.37
TRINITY_DN65843_c0_g2_i1	Zinc metalloproteinase nas-15; Zinc metalloproteinase nas-13; Astacin-like metalloprotease toxin 1	PF01400.23^Astacin^Astacin (Peptidase family M12A)^2-172^E:9.3e-38	156.86	2.13
TRINITY_DN66298_c0_g2_i4	Zinc metalloproteinase nas-4; Astacin-like metalloprotease toxin 2; Astacin-like metalloprotease toxin 3	PF01400.23^Astacin^Astacin (Peptidase family M12A)^2-157^E:3.8e-29	196.95	34.65
TRINITY_DN65843_c0_g2_i3	Zinc metalloproteinase nas-13; Zinc metalloproteinase nas-15	PF01400.23^Astacin^Astacin (Peptidase family M12A)^2-172^E:7.8e-38	118.61	7.94
TRINITY_DN64977_c1_g1_i2	Astacin (Peptidase family M12A)	PF01400.23^Astacin^Astacin (Peptidase family M12A)^57-250^E:3.7e-42	217.71	0
TRINITY_DN65843_c0_g2_i1	Zinc metalloproteinase nas-15; Zinc metalloproteinase nas-13; Astacin-like metalloprotease toxin 1	PF01400.23^Astacin^Astacin (Peptidase family M12A)^2-172^E:9.3e-38	156.86	2.13
TRINITY_DN66298_c0_g2_i4	Zinc metalloproteinase nas-4; Astacin-like metalloprotease toxin 2; Astacin-like metalloprotease toxin 3	PF01400.23^Astacin^Astacin (Peptidase family M12A)^2-157^E:3.8e-29	196.95	34.65
TRINITY_DN65843_c0_g2_i3	Zinc metalloproteinase nas-13; Zinc metalloproteinase nas-15	PF01400.23^Astacin^Astacin (Peptidase family M12A)^2-172^E:7.8e-38	118.61	7.94
TRINITY_DN64977_c1_g1_i2	Astacin-like metalloprotease toxin 1, 5; Zinc metalloproteinase nas-13	PF01400.23^Astacin^Astacin (Peptidase family M12A)^57-250^E:3.7e-42	217.71	0
TRINITY_DN56247_c0_g1_i2	Astacin-like metalloprotease toxin 3, 2, 4	PF01400.23^Astacin^Astacin (Peptidase family M12A)^2-110^E:8.4e-22	219	20
TRINITY_DN61466_c0_g2_i1	Astacin-like metalloprotease toxin 1; Zinc metalloproteinase nas-7; Astacin-like metalloprotease toxin 5	PF01400.23^Astacin^Astacin (Peptidase family M12A)^57-244^E:9e-56	1558.25	198
TRINITY_DN62300_c0_g1_i2	Astacin-like metalloprotease toxin 3, 2, 1	PF01400.23^Astacin^Astacin (Peptidase family M12A)^48-242^E:8.4e-48	29017.33	3227.13
TRINITY_DN62786_c0_g1_i1	Astacin-like metalloprotease toxin 1, 5; Zinc metalloproteinase nas-7	PF01400.23^Astacin^Astacin (Peptidase family M12A)^57-239^E:2.7e-52	1319.65	148.69
TRINITY_DN63482_c0_g1_i1	Astacin-like metalloprotease toxin 1, 2, 5	PF01400.23^Astacin^Astacin (Peptidase family M12A)^17-206^E:4.5e-50	230	36
TRINITY_DN63951_c0_g1_i1	Astacin-like metalloprotease toxin 1, 2, 3	PF01400.23^Astacin^Astacin (Peptidase family M12A)^46-235^E:7.1e-50	248	43
TRINITY_DN64977_c0_g2_i1	Astacin-like metalloprotease toxin 1, 3, 2	PF01400.23^Astacin^Astacin (Peptidase family M12A)^1-111^E:6.4e-22	310.55	34.94
TRINITY_DN64977_c1_g1_i3	Astacin-like metalloprotease toxin 1, 5; Zinc metalloproteinase nas-13	PF01400.23^Astacin^Astacin (Peptidase family M12A)^57-250^E:3.7e-42	249.5	21.58
TRINITY_DN65671_c0_g1_i1	Astacin-like metalloprotease toxin 2, 3, 1	PF01400.23^Astacin^Astacin (Peptidase family M12A)^50-244^E:4.9e-48	26775	3135
TRINITY_DN65843_c0_g2_i2	Astacin-like metalloprotease toxin 1; zinc metalloprotease nas-13, 15	PF01400.23^Astacin^Astacin (Peptidase family M12A)^2-172^E:4.8e-38	175.53	11.93
TRINITY_DN66298_c0_g2_i1	Astacin-like metalloprotease toxin 1; Bone morphogenic protein 1; Astacin-like metalloprotease toxin 5	PF01400.23^Astacin^Astacin (Peptidase family M12A)^38-228^E:2.6e-40	645.11	56.15
TRINITY_DN66298_c0_g2_i5	Astacin-like metalloprotease toxin 1, 5	PF01400.23^Astacin^Astacin (Peptidase family M12A)^3-188^E:1.1e-38	208.89	21.18
TRINITY_DN66833_c0_g2_i1	Astacin-like metalloprotease toxin 1; Bone morphogenic protein 1; Astacin-like metalloprotease toxin 5	PF01400.23^Astacin^Astacin (Peptidase family M12A)^38-228^E:2.6e-40	621.93	47.28
TRINITY_DN66833_c0_g2_i2	Astacin-like metalloprotease toxin 5, 1	PF01400.23^Astacin^Astacin (Peptidase family M12A)^2-128^E:1.8e-31	123.63	10
TRINITY_DN66833_c0_g2_i4	Astacin-like metalloprotease toxin 5, 1; Zinc metalloproteinase nas-39	PF01400.23^Astacin^Astacin (Peptidase family M12A)^2-125^E:1e-29	724.94	40.98
TRINITY_DN67625_c0_g2_i3	Astacin-like metalloprotease toxin 1, 5, 3	PF00014.22^Kunitz_BPTI^Kunitz/Bovine pancreatic trypsin inhibitor domain^67-117^E:6.2e-14`PF01400.23^Astacin^Astacin (Peptidase family M12A)^116-297^E:3e-35	425.86	34.18
TRINITY_DN67562_c0_g1_i4	Astacin-like metalloprotease toxin 1, 5, 4	PF00014.22^Kunitz_BPTI^Kunitz/Bovine pancreatic trypsin inhibitor domain^67-117^E:6.2e-14`PF01400.23^Astacin^Astacin (Peptidase family M12A)^116-297^E:1.1e-35	498.42	36.96
TRINITY_DN67625_c0_g1_i2	Astacin-like metalloprotease toxin 1, Zinc metalloproteinase nas-13, Astacin-like metalloprotease toxin 5	PF00014.22^Kunitz_BPTI^Kunitz/Bovine pancreatic trypsin inhibitor domain^76-127^E:5.5e-11`PF01400.23^Astacin^Astacin (Peptidase family M12A)^123-221^E:2.9e-24	540.97	39

TRINITY_DN67625_c0_g2_i2	Astacin-like metalloprotease toxin 1, 4, 5	PF00014.22^Kunitz_BPTI^Kunitz/Bovine pancreatic trypsin inhibitor domain^4-54^E:3.6e-14`PF01400.23^Astacin^Astacin (Peptidase family M12A)^53-234^E:2e-35	202.64	13.64
TRINITY_DN67562_c0_g1_i3	Astacin-like metalloprotease toxin 1; Kunitz-type serine protease inhibitor C; Kunitz-type serine protease inhibitor taicotoxin	PF00014.22^Kunitz_BPTI^Kunitz/Bovine pancreatic trypsin inhibitor domain^76-127^E:1.8e-14`PF01400.23^Astacin^Astacin (Peptidase family M12A)^122-211^E:1.1e-18	990.62	95.02
TRINITY_DN67562_c0_g1_i1	Kunitz-type serine protease inhibitor C	PF00014.22^Kunitz_BPTI^Kunitz/Bovine pancreatic trypsin inhibitor domain^76-127^E:3.2e-11	176.01	6.89
TRINITY_DN65231_c0_g3_i4	Phospholipase A2	PF05826.11^Phospholip_A2_2^Phospholipase A2^193-287^E:8e-35	452.51	54.12
TRINITY_DN66872_c0_g1_i1	Phospholipase A2	PF05826.11^Phospholip_A2_2^Phospholipase A2^159-253^E:6.5e-35	519.92	45.65
TRINITY_DN56168_c0_g1_i2	Venom peptide MmKTx1	PF15430.5^SVWC^Single domain von Willebrand factor type C^35-102^E:2.7e-10	5194.58	40
TRINITY_DN57574_c0_g1_i1	Venom peptide MmKTx1; Toxin-like protein 1	PF15430.5^SVWC^Single domain von Willebrand factor type C^37-104^E:3.1e-10	2028.29	5.38
TRINITY_DN57574_c0_g1_i3	Venom peptide MmKTx1; Toxin-like protein 1	PF15430.5^SVWC^Single domain von Willebrand factor type C^37-104^E:2e-10	2634.57	14.62
TRINITY_DN65554_c0_g3_i2	Peptidase inhibitor 16	PF00188.25^CAP^Cysteine-rich secretory protein family^20-142^E:1.2e-20	1031.29	60.21
TRINITY_DN65554_c0_g3_i1	Peptidase inhibitor 16	PF00188.25^CAP^Cysteine-rich secretory protein family^20-142^E:1.4e-20	777.71	123.79
TRINITY_DN64861_c0_g1_i2	Peptidase inhibitor 16	PF00188.25^CAP^Cysteine-rich secretory protein family^65-187^E:2e-20	778.57	108.35
TRINITY_DN64861_c0_g1_i1	Peptidase inhibitor 16	PF00188.25^CAP^Cysteine-rich secretory protein family^65-187^E:2.2e-20	1449.43	154.65